Four Essays on the Economics of Energy and Resource Markets

Inauguraldissertation
zur
Erlangung des Doktorgrades
der
Wirtschafts- und Sozialwissenschaftlichen Fakultät
der
Universität zu Köln

2014

vorgelegt
von

Diplom-Volkswirt, Diplom-Geoinformatiker Harald Hecking

aus

Vreden

Referent:	Prof. Dr. Felix Höffler
Korreferent:	PD Dr. Christian Growitsch
Tag der Promotion:	16.01.2015

Acknowledgements

First, I would like to express my gratitude to my supervisor Prof. Dr. Felix Höffler. Through his constructive feedback and thought-provoking ideas, he provided inspiration for my research throughout the last three years. I would also like to thank PD Dr. Christian Growitsch for co-refereeing my thesis and for his helpful comments and advice. Furthermore, I am thankful to Prof. Dr. Johannes Münster for agreeing to be the chair of the examination committee for this thesis.

I am very grateful to Prof. Dr. Marc Oliver Bettzüge and the Institute of Energy Economics at the University of Cologne for providing a motivating research environment. In addition, I would like to thank Monika Deckers as well as the whole administration, communication and IT team for their support. I would also like to extend my gratitude to Robert Germeshausen and Laura Hersing who provided excellent research assistance as well as to Broghan Helgeson for proofreading my thesis.

A special thanks goes to my fellow research associates for the great times we had together at the institute. The fruitful discussions, stimulating ideas and feedback in our team interactions as well as the lessons in applied game theory made the last years very special. In particular, I would like to thank Timo Panke for the professional, productive and cordial work on our research projects on resource markets. Additionally, I am thankful to Dr. Caroline Dieckhöner for her great collaboration in our joint research.

And finally, I would like to express my deepest appreciation to Miriam and my family for their invaluable and endless support. In particular, I feel indebted to my parents, to whom I wish to dedicate this thesis.

Harald Hecking October 2014

Contents

List of Figures

List of Tables

Abbreviations

AE	United Arab Emirates
bcm	billion cubic metres
BDH	Verband für Effizienz und erneuerbare Energien
BEI	Bremer Energie Institut
BF	blast furnace
BGR	Bundesanstalt für Geowissenschaften und Rohstoffe (Federal Institute for Geoscience and Natural Resources)
BHP	Broken Hill Proprietary Company
BHPB	BHP Billiton
BOF	basic oxygen furnace
BPIE	Buildings Performance Institute Europe
BREE	Bureau of Resources and Energy Economics
CGE	computed general equilibrium models
CIEP	Clingendael International Energy Programme
CO_2	carbon dioxide
CSN	Companhia Siderúrgica Nacional
DIscrHeat	DIscrete choice HEat market simulation model
DRI	direct reduced iron
EAF	electric arc furnace
ENTSOG	European Network of Transmission System Operators for Gas
EU	European Union
EU-ETS	European Union Emission Trading System
EWI	Institute of Energy Economics at the University of Cologne
Fe	Ferrum (chemical element)
FGE	Facts Global Energy
FMG	Fortescue Metal Group

FOB	free on board
FOC	first order condition
GAMS	General Algebraic Modeling System
GDP	gross domestic product
GHG	greenhouse gas
GIIGNL	The International Group of Liquefied Natural Gas Importer
IEA	International Energy Agency
IPCC	Intergovernmental Panel on Climate Change
IWU	Institut Wohnung und Umwelt
JP	Japan
kcm	Thousand cubic metres
KKT	Karush-Kuhn-Tucker (conditions)
kWh	kilowatt hour
LKAB	Luossavaara-Kiirunavaara Aktiebolag
LNG	Liquefied Natural Gas
LP	linear program
LTC	long term contract
mcm	million cubic metres
MCP	mixed complementarity problem
Mt	million tonnes
MWh_{el}	electrical megawatt hour
MWh_{th}	thermal megawatt hour
NBP	National Balancing Point
OECD	Organisation for Economic Co-operation and Development
OLS	ordinary least squares
OME	Observatoire Méditerranéen de l'Energie
PV	photovoltaics
PVI	parallel vertically integration
QA	Qatar
RES	Renewable energies
SNIM	Société Nationale Industrielle et Minière
TTF	Title Transfer Facility
UK	United Kingdom

UNCED	United Nations Conference on Environment and Development
USA	United States of America
WSA	World Steel Association

Dedicated to my parents

Chapter 1

Introduction

1.1 Motivation

The development of the world's economies has relied and will continue to rely on natural resources. Phosphor, for example, is needed to produce fertilizers, bauxite is used for aluminium production, copper is essential for electrical wires, iron ore is an input to steel production, crude oil fuels global transport and natural gas heats people's homes and is, just like coal, burned to generate electricity. From a microeconomic perspective, resource and energy markets, including the markets for power and heat, exhibit a variety of characteristics that motivate the research questions investigated in the thesis at hand.

First, resource markets, including the markets for energy resources, are usually spatial markets. Since resources are distributed unevenly over the world, there may be great distances between supply and demand. Thus, the location of supply and demand and, hence, transport costs play a crucial role. Second, many resource markets, such as the European natural gas market or global seaborne trade of iron ore or coking coal, are characterized by supply oligopolies. With regard to, for example, the European gas market, governments of exporting countries (such as Russia, Norway, Algeria or the Netherlands) enable an oligopoly by licensing a major part of the national exports to solely one (state-owned) company.

Third, resource and energy supply is often capital intensive and requires investments with long amortization times, such as conventional or renewable power plants for electricity supply or, from a household perspective, technologies for heat provision (e.g., gas heaters). The investment decisions are driven by a variety of aspects such as future energy prices, technological development or energy policy: Policy instruments often aim at influencing the investment decisions, since, fourth, production and transport of energy and resources may cause negative environmental externalities. One important externality in energy markets is the emission of carbon dioxide (CO_2). It is emitted by burning fossil fuels, e.g., in the power sector or for the heating of private households. Classical policy instruments to tackle CO_2 emissions are subsidies for renewable energy, CO_2 taxes or emission quotas such as the European Union Emissions Trading System (EU-ETS).

Many resource and energy markets are interdependent. Natural gas, for example, is an input to the power market. Another type of interdependency is two natural resources being substitutes. Coal and gas, for example, are substitutable inputs in power generation and compete both in the long-term (concerning power plant investment) and in short-term (concerning power plant dispatch). A third possible interdependency of two resource markets is both goods being complementary inputs, such as iron ore and coking coal, both being indispensable inputs for steel production.

This thesis seeks to improve the understanding of resource and energy markets, their specific characteristics and their interaction with each other. Therefore, the thesis includes four research papers on the markets for natural gas, coking coal, iron ore, electricity and heat. Each paper, representing one chapter of this thesis, addresses one or more of the specific characteristics outlined above.

Chapter 2 assesses the effects of a supply shock on the world market for natural gas. Motivated by the modeling of gas supply as a spatial Cournot oligopoly, the paper investigate the vulnerability of different gas importing countries to price increases during a supply shock. It seeks to evaluate the countries' strategic positions during a crisis, which are mainly influenced by their access to gas infrastructure and resource endowment.

Chapter 3 deals again with supply-side oligopolies. However, the paper presented here does not account only for one market but rather for two interacting markets. The research is motivated by the need for complementary inputs in steel production, namely iron ore and coking coal. Interestingly, some of the biggest mining companies play a major role in both markets. Therefore, it assesses the optimal business strategy for these oligopolists: to optimize the iron ore and the coking coal division on a firm-level or on a division-level?

Chapter 4 also investigates the interaction between two different markets: here, the European markets for gas and power. The research is motivated by the hypothesis that CO_2 reduction policies in the power sector, such as the EU-ETS, subsidies for renewables or a coal tax, do not only influence the power market but also have feedback effects on the oligopolistic gas market. The analysis is driven by the question on how climate policies affect the price elasticity of the power sector's gas demand and, therefore, gas prices. If climate policies would, for example, decrease the gas price then they may even be able to decrease the overall power system costs.

Chapter 5 assesses the CO_2 abatement costs of the German heat market for private households. The research is motivated by households making long-term investment decisions about heating technologies. However, these decisions are not solely based on monetary criteria, but also on household preferences. Accounting for both preferences and expenditures of private households, welfare-based CO_2 abatement costs of climate policies are derived.

1.2 Methodology

Each of the four analyses is conducted using different numerical simulation models, which are developed and presented in the thesis at hand. The research in Chapters 2 to 4 is based on spatial Cournot oligopoly models of different resource markets, namely natural gas, iron ore and coking coal (see Section 1.2.1). In Chapter 5, a dynamic bottom-up model of the German heat market is developed, which simulates the investment decisions of households in new heaters (see Section 1.2.2).

1.2.1 Modeling Resource Markets as Spatial Cournot Oligopolies

As stated before, many resource markets are spatial markets, such as the markets for natural gas, iron ore or coking coal. Hitchcock (1941) or Kantorovich (1942) have contributed seminal research papers on spatial market equilibria. In the focus of their research is the so-called transportation problem, i.e. to satisfy a fixed demand of a good produced in spatially separated production regions at minimal transport costs. The transportation problem can be solved with standard linear programming algorithms (see Samuelson, 1952) and can be scaled to model more complex systems such as the European natural gas market (see, for instance, Lochner and Dieckhöner, 2011). However, the approach of minimizing supply costs implies that suppliers are price-takers.

As outlined above, a perfectly competitive supply-side appears to be a strong assumption for many resource markets. In this light, Takayama and Judge (1971) were the first to develop a spatial monopoly model. Beckmann (1972, 1973) and Harker (1984, 1986) extended this approach in their research on spatial Cournot oligopolies. Unlike the classical transportation problem, a Cournot oligopoly model is a non-linear problem: since an oligopolist influences the price by its output quantity, the profit function (price times output) is not linear.

Mixed complementarity problems (MCP) are a common approach to simulate (larger scale and spatial) Cournot oligopoly problems numerically. A variety of research has been made in modeling energy and resource markets in an MCP such as Boots et al. (2004), Gabriel et al. (2005), Paulus and Trüby (2011) or Trüby (2013).

The main idea of MCP models is to derive an equilibrium for the individual optimization problems of different players in a market. Using the example of a gas exporter e_i who wants to produce and sell gas x_i to a demand region d, the functioning of MCP models is demonstrated in the following.

The exporter e_i has only one competitor e_j, produces at marginal costs c_i and is subject to a demand function, which is assumed to be linear in this example. Thus, the exporter is faced with the following optimization problem:

$$\max_{x_i} \Pi_{e_i} = (p_d(x_i + x_j) - c_i) * x_i \quad \text{with} \quad p_d(x_i + x_j) = a - b * (x_i + x_j). \tag{1.1}$$

This yields the following first-order condition:

$$\frac{\partial \Pi_{e_i}}{\partial x_i} = p_d - c_i + \frac{\partial p_d}{\partial x_i} * x_i. \tag{1.2}$$

The respective complementary slackness condition, when assuming a linear demand function, is:

$$0 \leq x_i \perp - p_d + c_i + b * x_i \geq 0 \Leftrightarrow x_i * (p_d - c_i - b * x_i) = 0. \tag{1.3}$$

This condition formalizes the economic rationale of the exporter e_i: If the price p_d covers the costs c_i plus the oligopoly markup $b * x_i$, then the exporter is willing to produce a positive output x_i. If, in contrast, costs and markup exceed the price, the output is zero.

The same principle is applied when developing more complex models, including, e.g., transport decisions, capacity constraints or investment decisions in infrastructure, such as the resource market models in the Chapters 2 to 4. Although being more complex, each of the developed resource market models basically represents a spatial Cournot oligopoly. More details will be discussed in the following:

The analysis in Chapter 2 is conducted using a spatial Cournot oligopoly model of the global gas market, named COLUMBUS (see Hecking and Panke, 2012). The simulation model has been developed in a joint work with Timo Panke and is formulated as a MCP. In COLUMBUS, we aim to find a spatial equilibrium for gas suppliers, infrastructure operators and the demand side of the market. We include the most relevant players active in the global gas market, i.e., pipeline operators, liquefied natural gas (LNG) facilities, storage operators and gas producers as well as their trading branches, the so-called "gas exporters". Since COLUMBUS also includes the decisions on future infrastructure investment and the operation of gas storage, the model is intertemporal. Nonetheless, it is a one-shot Cournot game, since all players make all decisions at once for the entire time horizon of the model. Concerning the analysis in Chapter 2, the model enables to derive the fundamental price effects of a supply shock and to disentangle these price effects into factors which increase or decrease prices.

Although the MCP approach is useful to model a spatial Cournot oligopoly, some simplifying assumptions limit the exact representation of the real-world gas market. First of all, we assume perfect information of all players: That is, every player has full knowledge about future market developments such as future costs, production and demand. In particular, each player has perfect information about the costs, the capacities and the transport options of every other player in the market. Thus, all players share the same information set, or, in other words, the model assumes symmetric information. Additionally, players have perfect foresight, i.e., they can anticipate shocks like a supply disruption and their duration (as discussed in more detail in Section 2.3.3).

Another caveat is the modeling of the demand side of a market. Modeling a Cournot oligopoly in a MCP requires a price-sensitive demand function. This demand function has to be specified exogenously and has to be represented in an analytical form. Obviously, the assumed demand elasticity is a major driver of the equilibrium price and demand.

Furthermore, data requirements of a global gas market model such as COLUMBUS are very high: The model requires data on country-wise, sector-wise and seasonal gas demand, on production costs and capacities as well as on infrastructure. Although data has been collected thoroughly, reasonable assumptions, e.g., on the demand elasticity have to be made. To cope with this problem, this thesis includes a detailed sensitivity analysis on the COLUMBUS assumptions in Sections A.3 and A.4.

The research in Chapter 3 is again based on MCP simulation modeling. In a joint work with Timo Panke, we develop two spatial and interacting Cournot oligopoly models: one simulating the seaborne iron ore trade, the other simulating the coking coal trade. Since both goods are complementary inputs in pig iron production (which is then processed to steel), we, in a next step, model the interaction between both markets. Our approach to integrate two Cournot oligopolies into one model is based on two conditions. First, since both products are complementary, the market output of iron ore X_i has to equal that of coking coal X_c in each demand market. Second, the price of the final product (pig iron) p_{pi} has to equal the price of iron ore p_i plus that of coking coal p_c, thereby neglecting the other costs of pig iron production and assuming perfect competition in the pig iron ore market. These conditions are common knowledge to all Cournot players in both markets and are included in the players' optimization rationale. The integrated simulation model enables us to investigate whether mining companies that are integrated in the production of both coking coal and iron ore, should optimize the output of both goods on a firm-level or a division-level.

Besides the drawbacks that generally apply to MCP simulation models (as discussed above), our integrated model of complementary inputs requires two strong assumptions: first, that players active in one input market regard the price of the other complement as given and second, that the output of both complements has to be equal. These assumptions have the following effect: Iron ore producers, for example, optimize their output with respect to the pig iron demand function given a certain coking coal price. This coking coal price and the resulting iron ore price induce a certain market output of both goods. However, if the output of both goods is not equal, the overall market of iron ore and coking coal is not in equilibrium. The iron ore and coking coal producers therefore have to include this equilibrium condition into their optimal output decision. The strict equality of iron ore and coking coal output is a strong assumption which does not hold in reality as, for example, stocking of coal and iron ore is an opportunity to balance markets. In the literature on complementary goods, one can often find another extreme assumption: If the output of one good exceeds the output of the other good, then the price of the first good becomes zero. Obviously, this assumption is not more realistic. Therefore, the approach presented in this thesis enables to at all model two Cournot oligopolies of complementary goods. Nonetheless, other approaches for integrating two complementary market models are still open for further research.

For the analysis in Chapter 4, I develop another simulation model that integrates two markets: the global gas market and the European power market. The global gas market is simulated with COLUMBUS (see above), which is combined with a linear model of the European power market named DIMENSION (see, e.g., Richter, 2011). Both models are, standalone, tools for partial analyses of the respective markets. That is, the gas demand function in COLUMBUS is exogenous, whereas in DIMENSION, prices of gas supply for the power market are exogenous. However, both models being run standalone could yield inconsistent results. The procedure to integrate the models is as follows: First, n gas price samples are drawn, and for each sample one DIMENSION run is simulated to derive the gas demand from the power sector. Second, the derived price/demand samples are used to approximate annual inverse demand functions $p(x)$ in an analytical form. Third, these demand functions are used in COLUMBUS to derive the oligopolistic gas market equilibrium. Lastly, the gas market equilibrium prices are used as inputs of the DIMENSION model in order to derive the power market outcome which is consistent with the gas market outcome. Applying the simulation approach enables, e.g., the analysis of climate policies in the power market, thereby accounting for the feedback effects on the oligopolistic gas market.

This approach tackles one major disadvantage of common MCP models. Instead of using an exogenous demand function in COLUMBUS, the demand function (for the power sector) is endogenous. However, the integrated simulation model has other caveats. Deriving an analytical representation of gas price/demand samples can be challenging. If the approximation does not fit the point cloud well, the gas demand of the power market model and the gas market model may not converge. Additionally, deriving numerous runs of the DIMENSION model is computationally expensive.

1.2.2 Combining a Dynamic Bottom-up Model with a Discrete Choice Model

Whereas in Chapters 2 to 4 MCP models of spatial Cournot oligopolies play a fundamental role, the simulation model developed and applied in Chapter 5 follows a different approach. The development of the German heat market, which is in the center of the research of Chapter 5, is influenced by millions of private households' investment decisions in new heating systems. Therefore, in a joint work with Caroline Dieckhöner, we develop DIscrHEat (DIscrete choice HEat market simulation model), which is a dynamic bottom-up simulation of the German heat market of private households. DIscrHEat derives the development of installed heating systems of German private households up to 2030. The simulation, inspired by an earlier approach of Stadler et al. (2007), combines a dynamic bottom-up model with a discrete choice model (see Train, 2003):

DIscrHEat includes a dataset on the entirety of German residential buildings, distinguished by age, size, insulation level, demand of heat energy and installed heating system. Let X_t represent the state (i.e., the heating system installed and the insulation level) of all German residential buildings in time period t. The main idea of DIscrHEat is that the state X_t evolves in time, mainly because of buildings changing the installed heating system. The state change, M_t, i.e., the households' decision about the investment in a certain heating technology, is derived using a discrete choice model, which was estimated using a unique dataset on historic technology choices and heating costs. The state change depends on the building characteristics and on the costs of the different heating system alternatives. This yields the following relation:

$$X_{t+1} = X_t + M_t \tag{1.4}$$

The detailed representation of the states of all residential buildings and their installed heating system enables us to derive, e.g., CO_2 emissions, energy consumption or total costs in each time period t. Additionally, we are able to simulate separate climate policies such as carbon taxes or subsidies for low-carbon technologies, which affect the costs of heating systems and therefore the state change M_t. This enables us to measure welfare costs of CO_2 abatement, e.g., the excess burden of these climate policies.

Clearly, the chosen approach has some caveats. First, we assume exogenous modernization rates of heating systems. This assumption reflects the observation that nowadays most of the households modernize the heating system when it breaks down. However, we do not know whether households might change their behavior in the future. Second, since we model the households' choices of a heating system using an estimation based on historical data from 2010, we implicitly assume that this behavior and, hence, household preferences will remain the same in the future. Third, our discrete choice estimation is based on historical observations of, e.g., heating system costs and technology choices for the year 2010. However, in our model, we vary the heating system costs in large ranges by simulating a variety of carbon tax levels and subsidy levels. Therefore, we extrapolate from our discrete choice estimation. Some of these caveats could be tackled in future research by estimating a discrete choice model with data from another year. As such, it could be investigated, whether preferences may have already changed during the last years.

1.3 Outline of the thesis

After having discussed the motivation and the methodology of the four research papers included in this thesis, the following section outlines the overall structure of the thesis.

Chapter 2, *Supply Disruptions and Regional Price Effects in a Spatial Oligopoly*, examines a supply shock on the global gas market, the output decisions of oligopolistic gas producers and the implications for the security of gas supply of importing countries. This essay is a joint work with Christian Growitsch and Timo Panke and was recently published in Growitsch, Hecking, and Panke (2014)[1]:

Supply shocks in the global gas market may affect countries differently as the market is regionally inter-linked but not perfectly integrated. Additionally, high supply-side market power may expose countries to market power in different ways. To evaluate the strategic position of importing countries with regard to gas supplies, we disentangle the import price into different components and characterize each component as price

[1] This article is copyrighted by John Wiley & Sons Ltd. and reprinted by permission. The presented article is forthcoming in *Review of International Economics* from Wiley Blackwell.

increasing or price decreasing. Because of the complexity of the interrelations in the global gas market, we use an equilibrium model programmed as a mixed complementarity problem (MCP) and simulate the blockage of liquefied natural gas (LNG) flows through the Strait of Hormuz. This enables us to account for the oligopolistic nature and the asymmetry of the gas supply. We find that Japan faces the most severe price increases as the Japanese gas demand completely relies on LNG supply. In contrast, European countries such as the UK benefit from good interconnection to the continental pipeline system and domestic price-taking production, both of which help to mitigate an increase in the physical costs of supply as well as in the exercise of market power.

Chapter 3, *Quantity-setting Oligopolies in Complementary Input Markets*, assesses the strategic behavior of mining companies integrated into the production of iron ore and coking coal, with both goods being complementary inputs in pig iron production. This paper was written in co-authorship with Timo Panke and was published in the EWI working paper series.

The global market for coking coal is linked to the global market for iron ore since both goods are complementary inputs in pig iron production. Moreover, international trade of both commodities is highly concentrated, with only a few large companies active om both input markets. Given this setting, the paper presented investigates the strategy of quantity-setting (Cournot) mining companies that own both a coking coal and an iron ore division. Do these firms optimize the divisions' output on a firm-level or by each division separately (division-by-division)? First, using a theoretical model of two Cournot duopolies of complementary goods, we find that there exists a critical capacity constraint below/above at which firm-level optimization results in identical/superior profits compared to division-level optimization. Second, by applying a spatial multi-input equilibrium simulation model of the coking coal and iron ore markets, we find that due to the limited capacity firms gain no (substantial) additional benefit from optimizing output on a firm-level.

Chapter 4, *CO_2 Abatement Policies in the Power Sector under an Oligopolistic Gas Market*, deals with the impact of climate policies on European power system costs, thereby accounting for the interaction of the power market and the oligopolistic gas market and therefore gas price changes. The paper was written by the author of this thesis and was published in the EWI working paper series.

The essay examines the power system costs when a coal tax or a fixed bonus for renewables is combined with CO_2 emissions trading. It explicitly accounts for the interaction between the power and the gas market and identifies three cost effects: First, a tax and a subsidy both cause deviations from the cost-efficient power market equilibrium. Second, these policies also impact the power sector's gas demand function as well as the gas market equilibrium and therefore have a feedback effect on power generation quantities indirectly via the gas price. Thirdly, by altering gas prices, a tax or a subsidy indirectly affects the total costs of gas purchased by the power sector. However, the direction of the change in the gas price, and therefore the overall effect on power system costs, remains ambiguous. In a numerical analysis of the European power and gas market, I find using a simulation model integrating both markets that a coal tax affects gas prices ambiguously, whereas a fixed bonus for renewables decreases gas prices. Furthermore, a coal tax increases power system costs, whereas a fixed bonus can decrease these costs due to the negative effect on the gas price. Lastly, the more market power that gas suppliers have, the stronger the outlined effects will be.

Chapter 5, *Greenhouse Gas Abatement Cost Curves of the Residential Heating Market*, investigates the effects of climate policies on the decision behavior of private households concerning heating system installations. The essay is a joint work with Caroline Dieckhöner and was published in the EWI working paper series.

In this paper, we develop a microeconomic approach to deduce greenhouse gas abatement cost curves of the residential heating sector. Our research is based on a dynamic bottom-up microsimulation of private households' investment decisions for heating systems up to 2030. By accounting for household-specific characteristics, we investigate the welfare costs of different abatement policies in terms of the compensating variation and the excess burden. We investigate two policies: i) a carbon tax and ii) subsidies on heating system investments. We deduce abatement cost curves for both policies by simulating welfare costs and greenhouse gas emissions up to 2030. We find that i) welfare-based abatement costs are generally higher than pure technical equipment costs, ii) given utility maximizing households a carbon tax is the welfare-efficient policy and iii) if households are not utility maximizing, a subsidy on investments may have lower marginal greenhouse gas abatement costs than a carbon tax.

Chapter 2

Supply Disruptions and Regional Price Effects in a Spatial Oligopoly – an Application to the Global Gas Market

2.1 Introduction

International resource markets link more and more of the world's economies. As interdependence increases, regional supply shocks, such as disruptions of trade flows caused by, e.g., geopolitical conflicts, may be of global relevance. The global oil market, for example, has seen several of such supply shocks in history, among the most prominent conflicts being the First Gulf War in 1991 as well as the Iraq War in 2003. As a result of the high level of integration within the global oil market, these regional conflicts caused global price shocks that affected countries all over the world.

A notable example of a resource market that is not highly integrated on a global scale is the natural gas market. Imperfect global integration is indicated by high regional price differences, e.g., between Asia and the United States. Various aspects may explain these regional price differences: First, transport of liquefied natural gas (LNG)[2], including liquefaction and regasification, is more complex and costly compared with that of crude oil. Second, the supply side of the global gas market is characterized by high market concentration, as large state-owned companies such as Gazprom (Russia), Sonatrach (Algeria), Statoil (Norway) or Qatargas (Qatar) control significant export

[2]LNG is natural gas that is liquefied by cooling it down to about $-162°$C. Thereby its volume is reduced by approximately 600 times.

volumes. Third, differences in flexibility of demand and, fourth, the degree of import diversification are further important aspects that have to be taken into account when investigating changes in prices due to supply shocks. Japan, for example, relies solely on LNG imports to meet its gas demand. Furthermore, following the catastrophic incident in Fukushima the country's natural gas demand has become more and more price inelastic owing to the reduction in nuclear power generation and the subsequent higher utilization of the remaining coal- and gas-fired power plants.

Since gas is sometimes transported thousands of kilometres, often crossing different countries or crucial waterways, trade flows are highly vulnerable to disruption. One example of such a supply shock was the Russian-Ukrainian gas crisis in 2008/2009. While European gas prices significantly increased during the crisis, US gas prices, for example, were hardly affected, thereby illustrating the low integration of the global gas market. Another prominent example of a neuralgic transport route is the Strait of Hormuz, a passage that is 21 nautical miles wide and connects the Persian Gulf with the Indian Ocean. The Strait of Hormuz is already today of eminent importance, as LNG exports from the Persian Gulf, i.e., from Qatar (77.4 billion cubic meters (bcm)) and the United Arab Emirates (7.8 bcm), accounted for 29% of worldwide LNG trades in 2010 (IEA, 2011c). Furthermore, there is no opportunity to bypass this crucial waterway by means of pipeline transport and its importance is likely to increase considerably in the upcoming years as gas demand in Asia is expected to strongly increase. In fact, the IEA projects a doubling of gas demand based on 2011 values in China and India by 2017. The world's two largest LNG importers are Korea and Japan both satisfying more than 95% of national gas demand with LNG – and will presumably continue to increase their gas consumption as well. Although demand is not predicted to rise in Europe, decreasing indigenous production will foster imports into the European market as well (ENTSOG, 2011).

In economic terms, given the regional differences in supply structure, demand flexibility and the supply-side concentration, a potential blockage of the Strait of Hormuz could therefore be interpreted as a supply shock in a spatial oligopoly with a competitive fringe and asymmetric players. Owing to the nature of this economic problem, the price effect of the supply shock in a gas importing country may differ depending on the (i) location of the disruption and (ii) the demand-supply situation in the country under consideration.

With respect to the supply shock caused by the blockage of the Strait of Hormuz, our paper aims at identifying and quantifying the major factors influencing the magnitude of price effects in globally disperse demand regions. We therefore develop a model to disentangle the import price into different components and characterize each component as price increasing or price decreasing (hereinafter referred to as price-increasing components or price-decreasing components, respectively), such as production and transport costs, scarcity rents of production and infrastructure, oligopoly mark-ups, supplies of competitive fringe and long-term contracts.

Our methodology to analyze regional price effects in a spatial oligopoly is structured in three steps. First, we illustrate the price formation in a simple asymmetric Cournot oligopoly. Second, since the interrelations of the global gas market are more complex owing to, e.g. seasonal demand patterns, capacity constraints and spatial supply cost differences, we use a global gas market simulation model (Hecking and Panke, 2012). The spatial partial equilibrium model accounts for 87 countries, comprising the major national producers and importers, as well as the relevant gas infrastructure such as pipelines, LNG terminals and storages. In order to accurately simulate the global gas market, i.e. incorporate demand reactions and the possibilities of strategic behavior, the model is programmed as a mixed complementarity problem (MCP). The flexibility and the high level of detail of the model allow us to simulate the interrelations of the global gas market within a consistent framework and to identify regional price and welfare effects. The third and central step of our approach to identify and quantify region-specific price drivers is to combine the price formation from the simple Cournot model with the gas market simulation model. By using the dual variables from the simulation, we are able to quantify to what extent marginal transport and production costs, scarcity rents of transport and production capacity as well as the exploitable oligopoly mark-up cause prices to increase. We are also able to identify factors that may result in decreasing prices such as trade relations to price-taking fringe suppliers and secured deliveries by long-term supply contracts.

Although a disruption of the Strait of Hormuz is fictitious, its consequences are interesting from an economic as well as a geopolitical point of view, especially since Qatar's LNG exports supply countries all over the world. We simulate a blockage lasting 6 months and focus on the USA, the UK and Japan, each serving as a prominent example of a distinct supply structure. We observe the strongest price reactions in Asia, with prices in Japan rising from an already high level (US\$505 per 1000 cubic metres (kcm)) by US\$171/kcm during the 6-month disruption. While US gas prices hardly change at all, European gas prices are significantly affected during the disruption, albeit to a lesser extent than in Japan, as, e.g., gas prices in UK increase by up to US\$79/kcm.

We identify and quantify three other factors to explain the difference in price changes between the UK and Japan. First, Japan is fully dependent on imports from the disturbed LNG market, whereas the UK has alternative supply opportunities from the European pipeline grid. Second, Japan's lower endowment of price-taking indigenous production and storage capacity explains its higher exposure to changes in supply costs as well as increased exertion of market power. Third, as Qatar is an important source of Japan's contracted LNG import volumes, the price decreasing effects of Japan's long-term contracts (LTCs) are reduced in comparison with the reference scenario. Consequently, Japan's gas price increase is US$92/kcm higher than any increase seen in the UK.

Thus, the spatial impact of the supply disruption becomes obvious with respect to different gas importing countries. However, the location of the supply shock matters as well. In another fictitious supply disruption scenario we assume a 6-month blockage of Ukrainian gas transits to Europe and contrast the results in this scenario with the scenario of the blockage of the Strait of Hormuz. We find that gas prices, for example, in Italy are affected most by the Ukraine blockage whereas Japanese gas prices, contrary to the disruption of the Strait of Hormuz, are hardly affected. Consequently, our analysis underlines that in a spatial oligopoly shocks will have a different impact depending on (i) where they occur and (ii) the importing country under consideration.

Our research is related to literature on quantitative analyses of security of gas supply with particular attention to numerical simulations of spatial Cournot oligopolies in resource markets. Building on the seminal paper by Takayama and Judge (1964), as well as on Harker (1986) and Yang et al. (2002), a variety of research has been made on spatial Cournot oligopolies and MCP models in resource markets (see, e.g., Haftendorn and Holz, 2010, Paulus and Trüby, 2011 or Trüby, 2013). Applications of MCP models to natural gas markets are, e.g., Boots et al. (2004), Gabriel et al. (2005), Holz et al. (2008) and Egging et al. (2010). Yet to our knowledge, none of the existing papers applying MCP models to natural gas markets tries to identify which factors influence price changes during a supply shock and to what extent prices may be affected.

Quantitative research on security of supply is rather scarce and solely concentrates on Europe. Three of the few examples are Lise and Hobbs (2008), Lise et al. (2008) and Dieckhöner (2012b), who measure the impacts of new pipeline corridors to Europe and of new LNG ports on security of supply. Papers on simulation-based analyses of the effects of (geo-) political conflicts on the natural gas market are also rare and concentrate on Europe only. Bettzüge and Lochner (2009) and Egging et al. (2008) analyze the impact of disruptions on Ukrainian gas flows and short-run marginal supply costs. Lochner and Dieckhöner (2011) analyze the effects of a civil unrest in North Africa on European security of natural gas supply.

We contribute to the existing literature on security of supply and spatial oligopolies in energy markets in three ways. First, we develop a framework for analyzing regional price reactions after a trade disruption in a spatial oligopoly by separating price components into increasing and decreasing factors. Second, we assess the strategic position of gas importing countries during a trade disruption by applying our methodology. Third, as opposed to most studies on security of gas supply, our model covers the global natural gas market, thus allowing us to analyze the consequences of a regional (geo-) political conflict across the world.

The remainder of this paper is structured as follows. The methodology is described in Section 2.2, in which we derive the spatial oligopoly simulation model and develop an approach to distinguish price components using the model results. Section 2.3 describes the data, main parameter assumptions and the scenario setting. The results are presented in Section 2.4, with particular focus on analyzing the price difference between Japan and the UK, identifying the major price drivers and providing an in-depth analysis of both countries' supply situations. Section 2.5 concludes.

2.2 Methodology

We argue that international gas trade is best represented by a Cournot oligopoly with a competitive fringe: on the one hand, large state-owned companies such as Gazprom, Sonatrach, Qatargas or Statoil account for a significant share of global export volumes. On the other hand, a large number of companies with little annual production operate on the supply side, most of them providing no significant export volumes – thus representing a competitive fringe.[3]

In order to separate natural gas import price into price-increasing and price-decreasing components, we first provide a theoretical foundation of how prices are determined in a Cournot oligopoly with a competitive fringe. However, the natural gas market is more complex than a simple Cournot oligopoly. Since international gas trade is characterized by spatially distributed demand and supply plus a complex network of pipelines and LNG infrastructure, it is necessary to develop a numerical spatial oligopoly model to simulate the market. Next, we apply the price formula from the simple Cournot oligopoly model to the numerical oligopoly model in order to identify factors that increase and decrease import prices.

[3]We provide model results for the international gas market in 2010 assuming perfect competition in Appendix A.3. We find that the model results do not match actual market results. Consequently, we choose to model the global gas market as a Cournot oligopoly with a competitive fringe. We model the eight most important LNG exporting countries and the three most important pipeline exporters as Cournot players. The countries able to exercise market power are Australia, Algeria, Egypt, Indonesia, Malaysia, Nigeria, The Netherlands, Norway, Qatar, Russia and Trinidad and Tobago. All countries have almost all of their exports coordinated by one firm or consortium. Appendix A.3 also contains the model results for our Cournot setting. By comparing these with actual market results, a better match is found than under the perfect competition setting.

2.2.1 Oligopoly Pricing

We start out by quickly recalling how the price in a Cournot oligopoly with a competitive fringe is determined (see also Tirole, 1988), which provides us with a theoretical foundation for our analysis. We begin by deriving the optimal supply Q^* in a Cournot oligopoly with N asymetric players, i.e., players having differing marginal cost functions. In a second step, we derive the resulting price formula in such a market and elaborate on how a competitive fringe changes the way prices are determined in an oligopoly.

Initially, we assume that N players maximize their profits by setting their optimal supply to a single end user market (q_i). Each player $i \in N$ has individual marginal costs of supply, msc_i, that are assumed to be constant and positive. Furthermore, we assume a linear inverse demand function, where the price $P(Q)$ decreases with the total quantity $Q = \sum_{i=1}^{N} q_i$ supplied to the market, i.e.,

$$P(Q) = A - BQ \quad \text{with } A, B > 0. \tag{2.1}$$

For a player i, the first order condition for sales is as follows:

$$\frac{\partial \pi_i}{\partial q_i} = P(Q) - Bq_i - msc_i = 0 \quad \forall i \tag{2.2}$$

with π_i representing the profit of player i. Substituting the wholesale price $P(Q)$ by the linear inverse demand function yields:

$$\frac{\partial \pi_i}{\partial q_i} = A - B\sum_{i=1}^{N} q_i - Bq_i - msc_i = 0 \quad \forall i. \tag{2.3}$$

Consequently, the profit-maximizing total supply to the wholesale market, Q^*, is determined by the following equation:

$$\sum_{i=1}^{N} \frac{\partial \pi_i}{\partial q_i} = N(A - BQ^*) - BQ^* - \sum_{i=1}^{N} msc_i = 0 \tag{2.4}$$

$$\Leftrightarrow Q^* = \frac{NA - \sum_{i=1}^{N} msc_i}{B(N+1)}. \tag{2.5}$$

Inserting Equation 2.4 into the linear inverse demand function yields:

$$P^*(Q^*) = A - BQ^* \tag{2.6}$$

$$= \frac{1}{N+1}A + \frac{1}{N+1}\sum_{i=1}^{N} msc_i \tag{2.7}$$

$$= \frac{BQ^*}{N} + \frac{\sum_{i=1}^{N} msc_i}{N}. \tag{2.8}$$

Consequently, in a Cournot oligopoly with asymetric players, the equilibrium price equals the average marginal supply costs plus an average mark-up that depends on the slope of the demand function and total supply to the market.

The existence of a zero-cost competitive fringe with a binding capacity constraint (q_{cf}^{max}) simply leads to a reduction of the mark-up by $\frac{Bq_{cf}^{max}}{N}$, as the competitive fringe produces its maximum capacity and the oligopolistic players maximize profit over the residual demand function.[4]

2.2.2 A Spatial Equilibrium Model of the Global Gas Market

Although we derive the formula for a simplified market, the method to determine the price is essentially the same as in a set-up with multiple interconnected markets and time periods (due to, e.g., the possibility of storing a commodity). The main difference between the simplified and complex formula is that scarcity rents of production and infrastructure capacity are affected by the interrelation of all markets and time periods. Because of the size of the problem at hand (high number of players, markets and time periods), deriving an equilibrium solution is challenging. Therefore, we develop a numerical spatial oligopoly model to simulate international gas trade.

The spatial equilibrium model is formulated as a mixed complementarity problem. This method allows us to make use of elastic demand functions as well as simulate strategic behavior in international gas trade. As we argue that the natural gas market is best represented by a Cournot oligopoly with a competitive fringe, both aspects (elastic demand and strategic behavior) are essential to accurately model the natural gas market.[5] Figure 2.1 illustrates the logical structure of our model.

Exporters are vertically integrated with one or more production nodes and trade gas with the buyers located at the demand nodes. We use a linear function to represent total demand at each of the demand nodes.[6] Exporters compete with each other in satisfying the demand, thereby acting as Cournot players or in a competitive manner. Therefore, at each demand node, all exporters form an oligopoly with a competitive fringe. The

[4] In the natural gas market, short-run marginal costs of price-taking fringe players are substantially lower than actual market prices. In addition, capacity of the competitive fringe is low compared with overall market size. This justifies why we focus on a zero-cost competitive fringe with a binding capacity constraint. Our application therefore follows the approach chosen in Borenstein and Bushnell (1999).

[5] Haftendorn (2012) stresses the point that when modeling a Cournot oligopoly with a competitive fringe with non-binding capacity constraints using conjectural variation models, the resulting market equilibrium may yield the oligopoly players lower profits compared with a setting in which they set prices equal to marginal supply costs, i.e., act as price takers. However, this objection is of no concern to our analyses since the competitive fringe in the reference scenario, and hence also in the scenario with a blockage of the Strait of Hormuz, faces binding capacity constraints.

[6] For more details on how the demand functions are determined, please refer to Section 2.3.1.

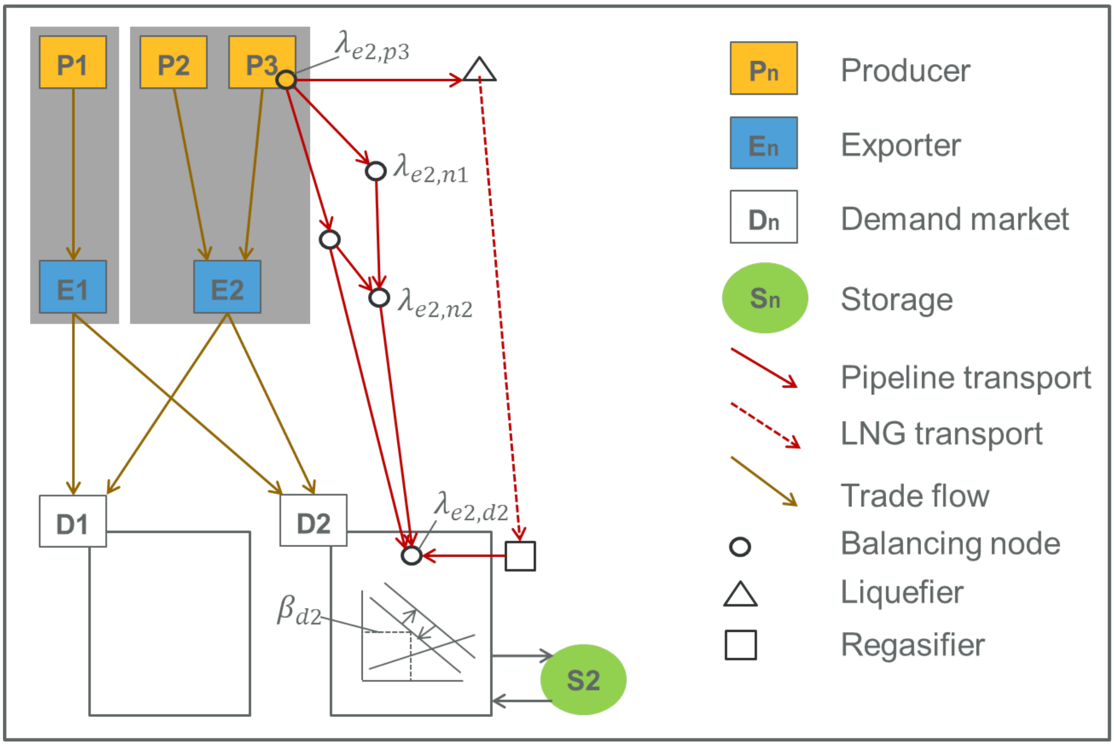

FIGURE 2.1: Logical Structure of the Gas Market Model

oligopoly is spatial and asymmetric, as each exporter's marginal supply costs ($\lambda_{e,d,t}$), i.e., the costs associated with the physical realization of the trades, vary depending on the location of production and demand nodes. Each exporter's marginal supply costs consist of marginal production and transport costs, including the scarcity rent for production and transport capacity. As different exporters compete for transport capacity, e.g., two exporters may want to use the same pipeline to deliver gas to a demand node, trades of one exporter influence the costs of another exporter's physical transports.

We start out by developing the optimization problems of the different players in our model and derive the corresponding first-order optimality conditions for one player. The first-order conditions combined with the market clearing conditions constitute our partial equilibrium model for the global gas market. The vector of variables in parentheses on the right-hand side of each constraint are the Lagrange multipliers used in developing the first-order (Karush-Kuhn-Tucker (KKT)) conditions. The complementary slackness condition is indicated by the perpendicular sign, $\perp$, with $0 \leq x \perp y \geq 0 \Leftrightarrow x^t y = 0$ for vectors x and y.

2.2.2.1 The Exporter's Problem

The exporter $e \in E$ is defined as a trading unit of a vertically integrated firm owning one or more production regions $p \in P_e$. The exporters earn revenues by selling gas ($tr_{e,d,t}$)

on the wholesale markets of the importing regions $d \in D$. Each exporter e maximizes its profits, i.e., revenues from sales minus costs of supply over all modeled time periods $t \in T$ and all importing regions d. Exporters may behave as price-takers in the market, but can alternatively be modeled as if able to exercise market power.

The profit function $\Pi_{eI}(tr_{e,d,t})$ is defined as[7]

$$\max_{tr_{e,d,t}} \Pi_{eI}(tr_{e,d,t}) = \sum_{t \in T} \sum_{d \in D} (\beta_{d,t} - \lambda_{e,d,t}) * tr_{e,d,t} \tag{2.9}$$

where $\beta_{d,t}$ is the market clearing price in importing region d, $tr_{e,d,t}$ is the quantity that trader e sold to region d at time t and $\lambda_{e,d,t}$ corresponds to the exporter's costs of physical gas delivered to demand node d. LTCs play a significant role in natural gas markets. Therefore, some of the trade flows between the exporters and importing regions have a lower bound, i.e., a minimal delivery obligation $mdo_{e,d,t}$.[8] Thus, LTCs are taken into account by incorporating the following constraint:

$$\sum_{t \in T} tr_{e,d,t} - mdo_{e,d,t} \geq 0 \quad \forall e, d, t \qquad (\chi_{e,d,t}). \tag{2.10}$$

The Lagrange of the exporter's optimization problem is defined by Inequality 2.10 and Equation 2.9. Taking its first partial derivative with respect to the decision variable $tr_{e,d,t}$ gives us the first-order condition (FOC) for trade between exporter e and demand node d:

$$\frac{\partial L_{eI}}{\partial tr_{e,d,t}} = -\beta_{d,t} + cv_e * slope_{d,t} * tr_{e,d,t} - \chi_{e,d,t} + \lambda_{e,d,t} \geq 0 \quad \perp \quad tr_{e,d,t} \geq 0 \qquad \forall e, d, t. \tag{2.11}$$

The parameter $slope_{d,t}$ is the slope of the linear demand function in node d. The term cv_e is the conjectural variation of exporter e and is a binary parameter indicating whether ($cv_e = 1$) or not ($cv_e = 0$) the trader is able to exercise market power.

In addition to the LTC constraint, each exporter also faces an individual market clearing condition that has to be fulfilled for every model node in which an exporter is active

$$pr_{e,p,t} - tr_{e,d,t} + \sum_{n1 \in A_{\cdot,n}} fl_{e,n1,n,t} - \sum_{n1 \in A_{n,\cdot}} fl_{e,n,n1,t} = 0 \quad \perp \quad \lambda_{e,n,t} \text{ free} \qquad \forall e, n, t \tag{2.12}$$

with $A_{\cdot,n}$ a set including all transport routes leading to node n. Variables $pr_{e,p,t}$ and $fl_{e,n,n1,t}$ denote produced gas volumes in production region $p(n) \in P_e$ and physical transport volumes between node n and $n1$, respectively. Therefore, the corresponding

[7] In order to keep the formulae as simple as possible, no discount factor is included.

[8] To limit complexity, we exclude the possibility of reshipping contracted LNG to other countries, as observed in 2011 and 2012 in the USA. Volumes however are rather small.

dual variable $\lambda_{e,n,t}$ equals the exporter's costs of physical supply to node n. If we consider a demand node $d(n) \in D_e$, market clearing condition 2.12 simplifies to[9]

$$\sum_{n1 \in A_{\cdot,d}} fl_{e,n1,d,t} - tr_{e,d,t} = 0 \quad \perp \quad \lambda_{e,d,t} \text{ free} \qquad \forall e, d, t. \tag{2.13}$$

Hence, Equation 2.12 ensures that the gas volumes, which exporter e sold on the wholesale market of demand node d, are actually physically transported to the node. If we consider a production node p, market clearing condition 2.12 collapses to:

$$pr_{e,p,t} - \sum_{n1 \in A_{p,\cdot}} fl_{e,p,n1,t} = 0 \quad \perp \quad \lambda_{e,p,t} \text{ free} \qquad \forall e, p, t. \tag{2.14}$$

Thus, the gas volumes produced have to match the physical flows out of node p. Production costs are represented by a production function, as used in Golombek et al. (1995, 1998). The corresponding marginal production cost function $mprc_{e,p,t}(pr_{e,p,t})$ takes the form: $mprc_{p,t}(pr_{e,p,t}) = a + b * pr_{e,p,t} - c * ln(1 - \frac{pr_{e,p,t}}{cap_{e,p,t}})$. Since trader e and its associated production regions P_e are considered to be part of a vertically integrated firm, profit maximization dictates that either the production entity or the trading entity sell their product at marginal costs, while the other entity exercises market power. In our setting, the trading units are modeled as oligopoly players while production is priced at marginal costs. Hence, the corresponding dual variable $\lambda_{e,p,t}$ to Equation 2.14 represents marginal production costs. Production in production region p is subject to a production constraint:

$$cap_{e,p,t} - pr_{e,p,t} \geq 0 \quad \forall e, p, t \qquad (\mu_{e,p,t}). \tag{2.15}$$

Equations 2.13 and 2.14 also ensure that $\sum_{p \in P_e} pr_{e,p,t} = \sum_{d \in D_e} tr_{e,d,t}$, i.e., total production equals total trade volume for every exporter e in each time period t. As trade flows are linked to physical flows, each exporter also faces the problem of how to minimize transport costs by choosing the cost-minimal transport flows $fl_{e,n,n1,t}$. In our model, this is implicitly accounted for by a separate optimization problem of the following form:

$$\max_{fl_{e,n,n1,t}} \Pi_{eII}(fl_{e,n,n1,t}) = \sum_{t \in T} (\lambda_{e,n1,t} - \lambda_{e,n,t} - trc_{n,n1,t} - opc_{n,t}) * fl_{e,n,n1,t} \tag{2.16}$$

where $opc_{n,t}$ is defined as the operating costs at node n in month t and $trc_{n,n1,t}$ as the cost associated with transporting gas from node n to node $n1$. Therefore, if n is a liquefaction node $l(n)$, $opc_{n,t}$ would reflect the costs of liquefying a unit of natural gas. If n is a liquefaction node then $n1$ has to be a regasification node, thus $trc_{n,n1,t}$ would be

[9]Equation 2.13 holds true if the demand node has no further connections, i.e., is a no-transit country. In case of a country such as Poland, physical flows of the Russian exporter to Poland have to equal the volumes sold to Poland plus all transit volumes.

the short-run marginal LNG transport costs from node n to node $n1$. The optimization problem is subject to some physical transport constraints such as the pipeline capacity:

$$cap_{n,n1,t} - \sum_{e \in E} fl_{e,n,n1,t} \geq 0 \quad \forall n, n1, t \qquad (\phi_{n,n1,t}). \tag{2.17}$$

Thus, the sum over all transport flows (decided on by the traders) through the pipeline between nodes n and $n1$ has to be lower than the respective pipeline capacity $cap_{n,n1,t}$. The dual variable $\phi_{n,n1,t}$ represents the value of an additional unit of pipeline capacity. Along the lines of Inequality 2.17, we also account for capacity constraints on liquefied ($\zeta_{l,t}$ being the corresponding dual variable) and regasified volumes ($\gamma_{r,t}$), as well as LNG transport levels (ι_t).[10]

This optimization problem may also be interpreted as a cost minimization problem assuming a benevolent planner, since in equilibrium there will be gas flows between two nodes n and $n1$ until the absolute difference of the dual variables associated with the physical market clearing constraint (Equation 2.12) of the two nodes ($\lambda_{e,n1,t} - \lambda_{e,n,t}$) equals the costs of transporting gas from node n to node $n1$. Hence, $\lambda_{e,n,t}$ can be interpreted as the exporter's marginal costs of supplying natural gas (including production costs $\lambda_{e,p,t}$) to node n, as shown in Equation 2.9.

2.2.2.2 The Storage Operator's Problem

Each storage facility is operated by one storage operator $s \in S$. The storage facilities are assumed to be located in the importing regions. The storage operator maximizes its revenues by buying gas during months with low prices and reselling gas during months with high prices. In our model, we assume storage operators are price takers[11] and, due to the nature of our modeling approach, also have perfect foresight.[12] Each storage operator faces a dynamic optimization problem of the following form:

$$\max_{si_{s,t}, sd_{s,t}} \Pi_s(si_{s,t}, sd_{s,t}) = \sum_{t \in T} \beta_{d,t}\,(sd_{s,t} - si_{s,t}). \tag{2.18}$$

[10] The interested reader is referred to Appendix A.1 for a detailed description of the omitted capacity constraints.

[11] This assumption must be made in order to reduce model complexity and ensure solvability. Yet, the direction of the identified effects remains unchanged if storage operators are modeled as Cournot players.

[12] When analyzing a supply disruption, this assumption may overestimate the price decreasing effect of storage. For a description of how we handled this issue, see Section 2.3.3

Using injection $si_{s,t}$ as well as depletion $sd_{s,t}$ in month t, we can define the motion of gas stock ($st_{s,t}$), i.e., the change in stored gas volumes, as:

$$\Delta st_{s,t} = st_{s,t+1} - st_{s,t} = si_{s,t} - sd_{s,t} \quad \forall s,t \qquad (\sigma_{s,t}). \tag{2.19}$$

Additionally, the maximization problem of the storage operator is subject to some capacity constraints:

$$cap_{s,t} - st_{s,t} \geq 0 \quad \forall s,t \qquad (\epsilon_{s,t}) \tag{2.20}$$

$$cf_s * cap_{s,t} - si_{s,t} \geq 0 \quad \forall s,t \qquad (\rho_{s,t}) \tag{2.21}$$

$$cf_s * cap_{s,t} - sd_{s,t} \geq 0 \quad \forall s,t \qquad (\theta_{s,t}). \tag{2.22}$$

Hence, we assume that storage capacity can be linearly transferred (by use of the parameter cf_s) to the restriction on maximum injection ($si_{s,t}$) and depletion ($sd_{s,t}$).

2.2.2.3 Price Determination

The equilibrium problem comprises the first-order conditions derived from the different optimization problems as well as the market clearing conditions previously discussed. In addition, we have to include one last market clearing condition:

$$\sum_{e \in E} tr_{e,d,t} + sd_{s,t} - si_{s,t} = \frac{int_{d,t} - \beta_{d,t}}{slope_{d,t}} \quad \perp \quad \beta_{d,t} \text{ free} \qquad \forall d,t. \tag{2.23}$$

The last market clearing condition (Equation 2.23) states that the final demand for natural gas, represented by a linear demand function (where $int_{d,t}$ and $slope_{d,t}$ represent its intercept and slope, respectively), and the gas volumes injected ($si_{s,t}$) into the storage facility at node $s(d)$ are met by the sum over all gas volumes sold on the wholesale market by traders e and gas volumes depleted ($sd_{s,t}$) from storage facility s. Thus, the dual variable associated with Equation 2.23 ($\beta_{d,t}$) represents the wholesale price in demand node d in month t.

Our model of the global gas market is defined by the stated market clearing conditions and capacity constraints, as well as the FOCs of the respective maximization problems.[13] The model is programmed in GAMS as a MCP and solved using the PATH solver (Dirkse and Ferris, 1995, Ferris and Munson, 2000).

[13]See Inequality 2.11 and Appendix A.1 for the remaining FOCs of our model.

2.2.3 Disentangling Prices in a Spatial Equilibrium Model

Figure 2.2 illustrates our methodology to disentangle import prices into price-increasing and price-decreasing components that we subsequently use to evaluate a certain import country's strategic position in the global gas market. In Section 2.2.1, we discuss a simple oligopoly model with a single market, asymmetric players and a competitive fringe. Here, natural gas prices equal the sum of an average oligopoly mark-up and average marginal supply costs of the Cournot players. In contrast, the model presented in Section 2.2.2 allows us to incorporate more complex market settings, such as additional import regions, long-term supply contracts as well as production and transport capacity constraints. As a result of the added complexity, price influencing factors are more diverse.

As seen in the exporter's FOC for optimal trade to demand node d (see Inequality 2.11), the exporter is willing to trade with demand node d as long as the price β_d covers his supply costs $\lambda_{e,d}$ and his individual oligopoly mark-up $cv_e * slope_d * tr_{e,d}$. If an exporter is obliged to deliver LTC volumes to a certain import node, he may even be willing to accept a β_d that is smaller than the sum of supply costs and oligopoly mark-ups. This economic disadvantage for the exporter is denoted by $\chi_{e,d}$ in the model.

According to the oligopoly pricing formula deduced in Section 2.2.1, we are now able to identify to which extend marginal supply costs and oligopoly mark-ups explain the different market prices β_d. The influence of marginal supply costs equals the average of all Cournot player's $\lambda_{e,d}$. Each $\lambda_{e,d}$ can be further subdivided into production costs, transport costs and scarcity rents for transport and production infrastructure. Therefore, by taking the average of all aforementioned supply cost components, we can identify to what extent these components explain prices.

The price influence of the exporters' oligopoly mark-ups is defined as the average of each Cournot player's mark-up. For our analysis, we also need to identify the price-reducing effects of competitive fringe players. We therefore introduce the so-called "maximal oligopoly mark-up", which is the hypothetical mark-up that Cournot oligopolists could realize at a demand node if there were no gas volumes from a competitive fringe available. Thus, as stated in Section 2.2.1, the fringe producers reduce the maximal oligopoly mark-up by $slope_d * tr_d^{CF}$ and the fringe storages by $slope_d * sd_d$. Besides fringe suppliers, LTC's may also have a price decreasing effect that can be identified by taking the average LTC opportunity costs of all Cournot players, $\chi_{e,d}$.

Now, as we are able to disentangle the import price simulated by the equilibrium model into price-increasing and price-decreasing components, we use this approach in Section 2.4 to evaluate the market position of different countries during a supply crisis. There we

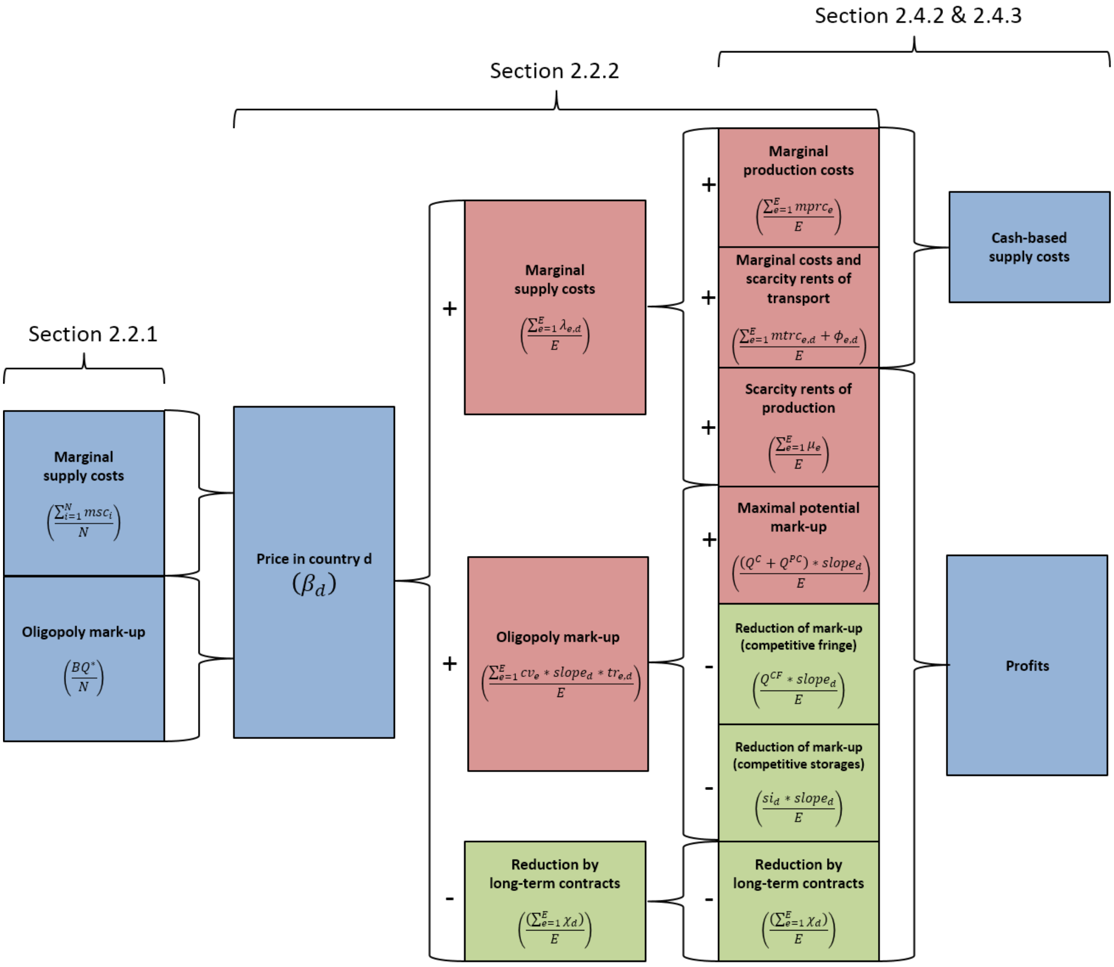

FIGURE 2.2: Disentangling Prices in a Spatial Equilibrium Model

will distinguish between "cash-based supply costs" and exporters' "profits". We define "cash-based supply costs" as monetary costs for using transport infrastructure (marginal costs and scarcity rent) and gas production. The scarcity rent of production and the oligopoly mark-up may both be interpreted as monetary profit for the exporter.

2.3 Data, Assumptions and Scenario Setting

In this section, the data used in our global gas market model as well as the scenario settings of our analysis are described. This section's description focuses on the demand side and the role of long-term contracts in the global gas market. In addition to the information provided in this section, we list details on data used for production capacities, costs, infrastructure capacities and transport costs in Appendix A.2.

2.3.1 Demand

To study the economics of a disruption of the Strait of Hormuz and the effects on regional import prices with a high level of detail, we put a special focus on the demand data. In particular, monthly demand functions must be derived.

The total gas demand of a country and its sensitivity to prices are heavily affected by the sectors in which the gas is consumed. Gas consumption in the heating sector mainly depends on temperature and therefore has a seasonal pattern. On the other hand, gas consumption in industry has no seasonal and temperature-dependent demand pattern, making demand rather constant. Concerning price sensitivity, it is fair to assume that gas demand in the heating sector is rather insensitive to prices, since the gas price does not strongly change the heating behavior and since the heating technology is fixed in the short-term. On the contrary, in power generation, the gas-to-coal spread has a higher impact on gas demand, implying high price sensitivity. Moreover, price sensitivities may also vary by country: It is reasonable to assume that, e.g., Japan (because of its tight generation capacity situation) is less price sensitive in power generation than Germany.

To derive a country's gas demand function, we have to account not only for the aforementioned aspects, but for the different sectoral shares of total demand as well. In addition, owing to different seasonal demand patterns of each sector, the sectoral share of total demand may vary by month. If, for example, heating demand takes a large share of some country's total gas demand in January, then the corresponding demand function would be rather price insensitive. On the contrary, if in July, gas is mainly used in power-generation, the demand function would be rather price sensitive.

Our aim is to consistently derive country-specific monthly linear demand functions accounting for sectoral shares, seasonalities and price sensitivities. In the following, we outline our approach to determine these functions and the accompanying data sources.

First, we use country-specific annual demand data for the years 2010 and 2012. Demand data per country for those years is taken from IEA (2011c), IEA (2011b) and ENTSOG (2011). IEA (2011c) provides consumption data on a country by country basis for the year 2010. For natural gas demand in 2012, we rely on forecasts from IEA (2011b) and ENTSOG (2011).

In a second step, annual demand is split into monthly demand, using historical monthly consumption data provided by, e.g., IEA (2011c), and FGE (2010). Concerning the linear demand functions, sufficient data is only available for 27 nodes representing China, India and most of the OECD countries. For the other countries, we assume monthly demand to be inelastic and exhibit no seasonality.

Next, we distinguish two groups of sectors: We assume "industry and power (IP)" to have a higher price sensitivity than "heating and miscellaneous (HM)". IEA (2011c) provides sectoral shares of gas demand in industry, heat and power generation on an annual basis. For the heating sector, we derive monthly demand data from heating degree days provided by, e.g., Eurostat (European countries) or National Resources Canada (Canada)[14]. We further assume miscellaneous gas demand to exhibit no seasonal fluctuation. We derive the monthly demand for "industry and power generation" as a residual of total demand minus heating demand and minus miscellaneous demand. The monthly demand for both groups, IP and HM, serves as a reference demand with which linear demand curves for each group may be derived.

Monthly reference prices are provided by IEA (2011c) for the majority of countries. We add monthly price information from the spot indices Henry Hub, Title Transfer Facility (TTF) and National Balancing Point (NBP). For all European countries where no data is publicly available, we use the European average gas price provided by IEA (2011c).

Having set up reference price-volume combinations, we still have to determine the monthly price sensitivities in the relevant countries for both demand groups IP and HM to derive specific linear demand functions. We thereby stick to an approach that is commonly used in modeling literature (e.g., Egging et al., 2010, Holz et al., 2008 or Trüby, 2013) by assuming point elasticities in the reference point. While we assume the demand elasticity of the HM group to be approximately -0.1 in all countries with a price sensitive demand function, we differentiate within the IP group. Because of the high degree of oil-price indexation as well as the tight capacity supply in Japan, we assume natural gas demand of the Asian countries to be less price sensitive than the other countries (-0.1 vs. -0.4).[15] These elasticity assumptions are in line with, e.g., Neumann et al. (2009) and Bauer et al. (2011) who assume a price elasticity of -0.3, or Egging et al. (2010) who assume price elasticities between -0.25 and -0.75.

Having derived monthly country-specific demand curves for IP and HM with different price sensitivities, we aggregate both demand functions horizontally. The resulting demand functions account for different seasonal demand patterns, different sectoral shares of total demand and different price sensitivities, therefore varying by month and country.[16]

[14] http://www.nrcan.gc.ca/energy/sources/natural-gas/monthly-market-update/1173

[15] These elasticity values provide the best fit with actual market outcomes in 2010. Please refer to Appendix A.4 for information on how prices in select countries change when the assumed elasticity is varied.

[16] Horizontal aggregation of two linear demand functions leads to a kinked demand function. Our modeling approach is only able to handle differentiable functions. After having checked all equilibrium price/quantity combinations, we can exclude the market outcomes in the steeper part of the kinked demand function. Therefore, we only use the less steep part in our analysis.

Overall, the model covers a gas demand of 3267 bcm for 2010 and 3426 bcm in 2012. This equals 99% of both global gas consumption in 2010 reported by the IEA (2011c) and global gas demand in 2012 as forecasted in IEA's Medium-Term Oil and Gas Markets report (IEA, 2011b). We model 49% of total global demand to be price sensitive and 51% to be inelastic. In Asia/Oceania, 379 of 645 bcm of total demand is elastic (59%), whereas in Europe and North America, more than 90% of total demand is modeled as elastic demand functions. The comparably low share of Asian elastic demand is acceptable for our study because most of the Asian countries with inelastic demand are gas producers and are therefore import independent (e.g., Malaysia, Indonesia or Australia).

2.3.2 Long-term Contracts in the Global Gas Market

Long-term contracts still play a significant role in the natural gas market, in particular in Europe and Asia. Therefore, our model also accounts for LTCs. For Europe, data on LTCs are based on information provided by Gas Matters[17]. LTCs are also important for LNG deliveries: In 2010, about 60 bcm were traded on a spot and short-term basis[18] (GIIGNL, 2010). Of the total LNG trades that occured in 2010 (300 bcm), 80% were carried out as a result of long-term contracts.

As precise information on actual LTCs is not widely available, we model long-term contracts as a minimal delivery per annum from an exporting to an importing country, e.g., 6.4 bcm have to be shipped from Qatar to Italy over the course of the year. In other words, because the annual natural gas imports can be flexibly optimized during a year, we can neglect monthly minimal deliveries. Since our study focuses on security of supply effects during a disruption, we focus on the minimal deliveries instead of take-or-pay volumes, which serve as a means to guarantee "security of demand" for certain exporters.

Long-term contracts are often oil price indexed. This holds true in particular for the Asian LNG importers (Japan Crude Cocktail). However, our model derives prices endogenously, thus allowing the LTC reference prices to be determined via implicit modeling.[19] Our analysis focuses on a short time frame, i.e., one year.

[17] http://www.gasstrategies.com/home

[18] GIIGNL defines short-term contracts as contracts with a duration of less than 4 years. Since our analysis focuses on the effects of an LNG disruption, it is necessary to include LNG long-term contracts in the model. Neglecting that fact would presumably overestimate the flexibility of LNG trade and therefore underestimate the severity of a disruption of the Strait of Hormuz. Since we lack more detailed data and do not have information about potential flexibilities (neither in long- nor in short-term contracts), we stick to an amount of 240 bcm contracted in the long-term. We further assume this to be the contracted volume for 2012 as well.

[19] It is unclear how prices in an oil-price indexed LTC would react to a blockage of the Strait of Hormuz, as this depends on the specific contract structure as well as the change in the oil price. Therefore, the

2.3.3 Scenario Setting

In our study, we simulate two scenarios. In the reference scenario, gas flows between November 2012 and October 2013 are computed assuming no disruption of the Strait of Hormuz. In the other scenario, we simulate a 6-month blockage of the Strait of Hormuz beginning in November. As our model is non-stochastic, we fix storage levels in November based on the results from the reference scenarios. Otherwise, market players would anticipate the blockage and fill the storages in advance (perfect foresight assumption). We, however, implicitly assume that storage operators have information about the length of the disruption. Concerning LNG long-term contracts, we proportionately diminish the annual minimum take/delivery quantity to match the length of the disruption (i.e., a 12 bcm contract is reduced to 6 bcm). This is in line with a reference LNG contract provided by GIIGNL (2011), according to which a blockage is a *force majeure* and relieves the contracting parties from the take/delivery obligation.

2.4 Results of the numerical analysis

2.4.1 Prices

To analyze the fundamental price effects of a disruption of the Hormuz Strait, Figure 2.3 gives the monthly gas prices for Japan, the UK and the USA in both scenarios (no disruption and 6-month disruption).[20]

First, we observe rather identical price curves for the USA. In our simulations, the USA neither import nor export significant amounts of LNG in 2012. Therefore, US gas prices are not affected by the blockage of the Strait of Hormuz.

Second, it can be seen that UK's natural gas price is connected to and affected by incidents on the global LNG market.[21] Whereas in the reference run the gas price varies between US$220/kcm in summer and US$250/kcm in winter, we observe an increase in the gas price when simulating a 6-month long blockage. Once the disruption starts, the UK gas price immediately increases by up to 31% in the winter months (US$328/kcm in January).

approach used in this paper is, in our view, only tractable in a partial equilibrium analysis such as the one presented.

[20]We use the market clearing price of the US southern demand node as a proxy for the monthly price of the USA.

[21]Around 14 bcm of the total LNG imports in 2010 (18.7 bcm) stem from long-term LNG contracts (GIIGNL, 2010).

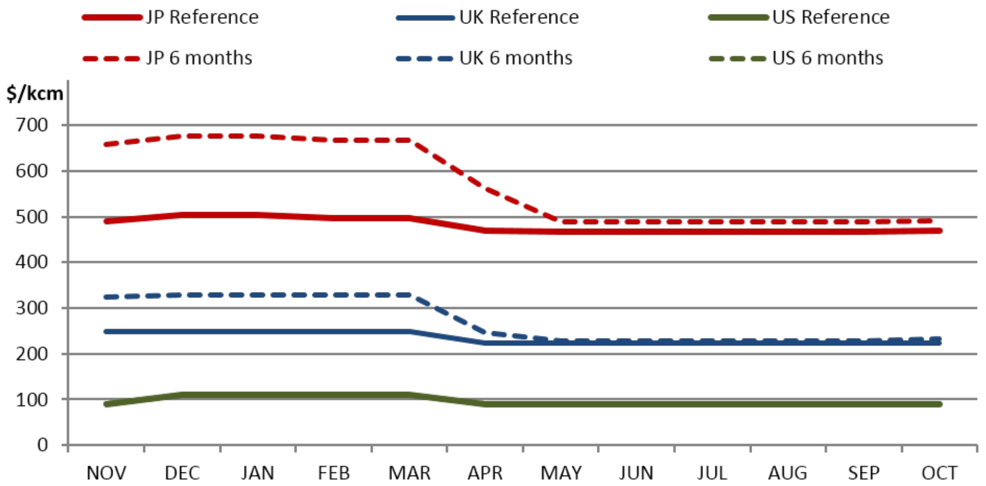

FIGURE 2.3: Price Effects of a Disruption of the Hormuz Strait in Three Selected Countries

Third, we notice that Japan, which relies solely on LNG imports, is most affected by the disruption of Qatar's and United Arab Emirates' LNG exports. The monthly gas price in Japan varies between US$467/kcm and US$505/kcm in the reference case. A 6-month long blockage of Hormuz Strait increases the gas price in Japan by nearly 34% (to more than US$677/kcm in January).

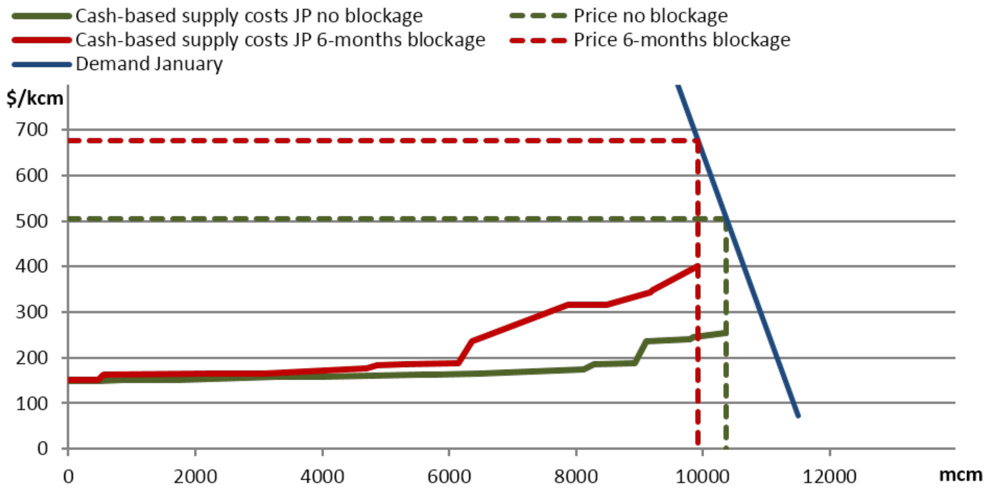

FIGURE 2.4: Changes in Japan's Supply Cost Curve after a Disruption of the Hormuz Strait

Thus, for both countries (Japan and the UK), we observe increasing prices during the disruption. However, it remains unclear whether an exporter's profits increase or whether higher supply costs cause the increase in prices. As an example, Figures 2.4 and 2.5 provide closer insight into the formation of January prices in both scenarios for Japan and the UK, respectively. Both figures contain the respective country's January demand function and the cash-based supply cost curves for both scenarios.[22]

Concerning Japanese supplies, we observe a remarkable increase in supply costs, whereas in the UK, supply costs in both scenarios are nearly identical except for the rightmost part of the curve. Increasing prices, however, seem to be also driven by higher profits for the suppliers in both countries. Yet, neither figure provides an indication as to what factors drive prices most.

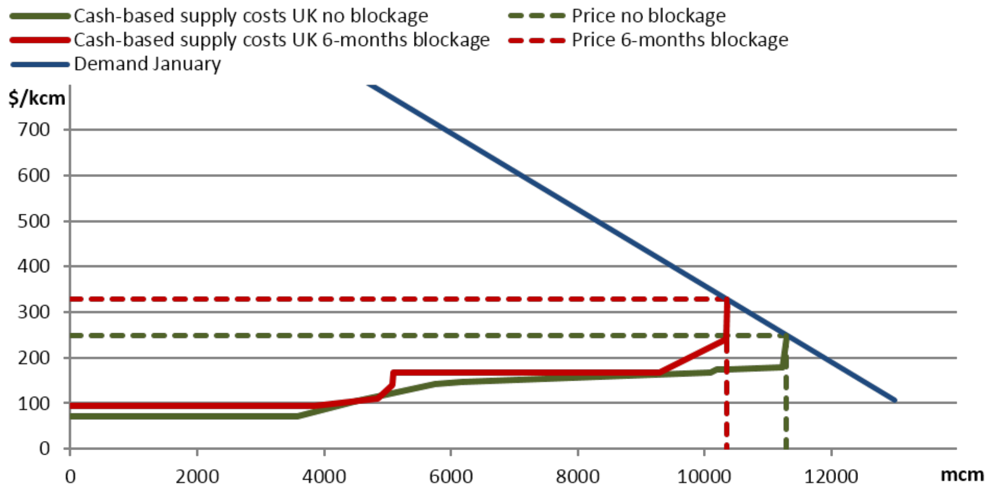

Figure 2.5: Changes in UK's Supply Cost Curve after a Disruption of the Hormuz Strait

Therefore, the observed price effects raise two questions: (1) Why does the import price level differ among different countries, even in the reference scenario? (2) What drivers explain the different price reactions after a supply shock? To answer these questions, we apply the approach introduced in Section 2.2.3. Using the dual variables from our simulation model, we are able to quantify price components that help us evaluate the strategic market positions of different countries. To give an application of our methodology, we next focus on the January prices of Japan and the UK in the reference scenario and during the supply shock.[23]

2.4.2 Price Structure in the Reference Scenario

To explain the price differences between Japan and the UK, we first take a look at Figure 2.6. The diagram illustrates the different components of Japanese and British import prices in January in the reference scenario (no disruption).

[22] According to the terminology used in Section 2.2.3, cash-based supply costs include marginal costs of production and transport plus a scarcity rent for transport infrastructure.

[23] Concerning the USA, the abundant domestic production makes the country independent from imports. This does not only explain the low prices, but also the insensitivity to prices during the global supply shock (disruption of the Strait of Hormuz).

As stated in Section 2.2.3, we distinguish between "cash-based supply costs" and "profits". We define "cash-based supply costs" as those costs that the exporter actually has to bear in order to deliver gas to an importing country (i.e., marginal costs of production and transport as well as congestion rents for transport infrastructure). The scarcity rent for production capacity is monetary profit for the exporter. Therefore, it is part of what we refer to as "profits". Another component of the profits is the average mark-up, which oligopolistic players can realize in a certain import market. The term "maximal potential oligopoly mark-up" labels the mark-up that exporters could realize if the complete demand of a country was satisfied by Cournot players. However, gas purchases from price-taking players or depletion from storages lowers the "maximal potential mark-up". In other words, the presence of a competitive fringe reduces the oligopoly rents. Last, LTCs have a decreasing effect on import prices and, in particular, the exporters' margin. Since LTCs are modeled as minimal deliveries from an exporter to an import country, the LTC is a binding constraint for the exporter. This can be interpreted as an economic disadvantage that the exporter has to bear or, conversely, a price advantage for the importer.

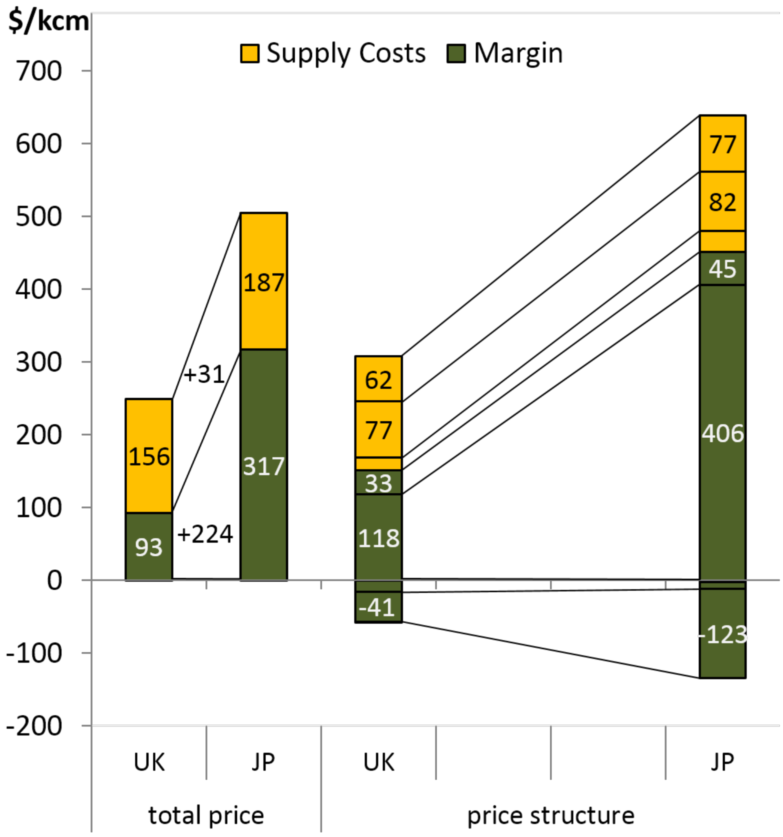

FIGURE 2.6: Structure of British and Japanese Import Gas Prices in the Reference Scenario

As Figure 2.6 reveals, the total January price difference between Japan and the UK is US$255/kcm, yielding US$31/kcm to be explained by higher supply costs. The "profits" account for the major price difference (US$224/kcm). Whereas the scarcity rent for production capacity has a similar impact on prices in both countries, the "maximal potential oligopoly mark-up" explains most of the differences between the "profits". Compared with the UK, we assume the gas demand of Japan to be more inelastic. Thus, the high Japanese dependency on natural gas lets Cournot players realize higher mark-ups in Japan than in the UK.

Yet, both countries are able to limit the oligopolistic mark-ups: The UK has significant domestic production (which we assume to be provided by price-taking producers) and storage reserves that in total lead to a price reduction of US$56/kcm (-US$41/kcm and -US$15/kcm, respectively). Japan, in contrast, only has small capacities of domestic natural gas production and seasonal underground gas storages, which only reduce the gas price in total by US$12/kcm. Japan's key advantage in limiting oligopoly mark-ups is its access to long-term contracted LNG volumes. In our setting, the contracts lead to an import price reduction of US$123/kcm. In other words, without the secured deliveries by long-term contracts, Japan would be much more likely to be exploited by its suppliers.

2.4.3 Structure of Price Reactions during a Supply Disruption

After having provided insight into the price structure of both Japan and the UK in the reference scenario, we focus next on the price increase during a blockage of Hormuz Strait. Figure 2.7 illustrates the January price level in both countries without a disruption (topmost bar) and with a 6-month disruption (lowest bar). Additionally, the middle bars of the figure display the cost components leading to an increase and decrease of the gas price during the disruption.

Marginal transport and production costs: We observe a slight increase in those two cost components because gas must be imported from more distant sources and gas production is intensified during the blockage. However, since both production and transport capacities already have high utilization rates (compared with the global average) in the reference scenario, marginal production and transport costs only explain a fraction of the total price increase in Japan and the UK.

Scarcity rent of transport: A blockage of the Hormuz Strait results in an outage of approximately 30% of global LNG trade volumes. LNG importers therefore need to find alternative sources of supply, which makes the available LNG liquefaction capacity (which we account to transport infrastructure) scarce. Costs resulting from transport scarcity explain US$52/kcm of the total price increase in Japan, but only US$32/kcm in the UK. The difference can be explained by taking a closer look at both countries' market

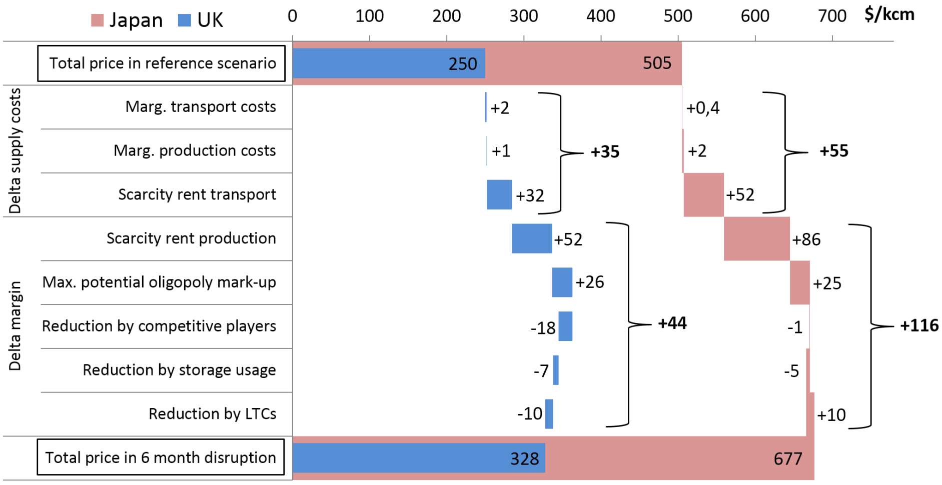

Figure 2.7: Structure of the Import Price Increase during a 6-month Disruption of the Hormuz Strait in Japan and the UK

positions: Japan depends solely on LNG imports, is price insensitive and competes for supply with other countries in the same situation (such as South Korea). The UK, however, is more sensitive to prices and, being connected to the European pipeline grid, is linked to producing countries such as Norway, the Netherlands and even Russia. Thus, the UK is less willing to buy gas from LNG terminals where capacity is scarce and prices are consequently high. Most of the increase in transport scarcity rent in the UK results from bottlenecks in the European pipeline grid, especially during deliveries from Russia. Japan, in contrast, has to rely on the LNG volumes still available to the global gas market during the blockage of the Hormuz Strait. As Japan competes for LNG supplies (and therefore also for LNG transport capacities) with other LNG-dependent importers, the opportunity costs of the transport value chain to deliver LNG to Japan increase during the blockage.

Scarcity rent of production: Production capacity costs explain the major part of the total price increase in Japan (US$86/kcm) and in the UK (US$52/kcm). The price increases induced by the scarcity rents of production are therefore higher than those induced by the transport scarcity rents. This indicates that given a blockage of the Strait of Hormuz, production capacity on a global scale is more scarce than transport capacity. Japanese import prices are, however, more affected by the scarcity of production capacity than are the British ones. The reason for the difference is similar to that of the transport scarcity rents. Whereas the UK has alternative sources of supply connected by pipelines, Japan competes with other LNG importers for the production volumes of LNG exporting countries. The opportunity costs of producing gas to sell to Japan at a later point in time therefore increase when the supply side becomes tighter as a result of a blockage of the Hormuz Strait.

Maximal potential oligopoly mark-up: On the one hand, countries reduce demand during a disruption of Hormuz Strait, which decreases the potential mark-up *ceteris paribus*. On the other, as Qatar (QA) and the United Arab Emirates (AE) are not able to export gas, the number of oligopoly players decreases, which in turn increases the potential mark-up. In our setting, we observe that in both Japan and the UK, the impact on the price increase is approximately US$25/kcm.

Reduction by price-taking players: During the disruption, the UK increases domestic and polypolistic production, which reduces the import price increase by US$18/kcm. Japan, in contrast, covers only a small fraction of total gas supply with domestic production. Therefore, its ability to lessen the import price increase during a blockage of the Strait of Hormuz is limited.

Reduction by storage usage: The UK augments its storage depletion by 160 mcm during the disruption, leading to a decrease in the import price by US$7/kcm. Even though the storage usage in Japan is only increased by 100 mcm, we observe a reduction of US$5/kcm. This indicates that in improving a country's market position, storages increase in importance as countries grow more insensitive to prices.

Reduction by LTCs: The UK holds several LTCs, meaning it has secured deliveries from certain exporters. These LTCs lead to a reduction of the price increase by US$10/kcm during the disruption. Long-term contracts and the corresponding contractual obligations for certain LNG exporters (Algeria, Nigeria and Trinidad) to deliver gas to the UK result in opportunity costs for the exporters. These costs can be interpreted as a realization of their price risk. Concerning Japan, LTCs explain a surprising US$10/kcm of the price increase during a blockage of the Strait of Hormuz. While LTCs lead to a price decrease of US$123/kcm in the reference scenario, LTCs only decrease the import price by US$113/kcm in the scenario with a 6-month disruption. This interesting observation can be explained by the fact that Qatar is one of the more important sources of contracted LNG volumes that, in the event of a blockage of the Strait of Hormuz, have to be substituted by non-contracted LNG volumes. Consequently, the price decreasing effect of Japanese LTCs is reduced in the case of a 6-month disruption.

So far, we have identified three factors that explain why a blockage of the Strait of Hormuz would affect the Japanese import price twice as much as the British one. First, Japan's import dependency on LNG forces Japan to compete for supplies in the disturbed LNG market. Therefore, scarcity rents for both transport and production are affected stronger than in the UK, where the connection to the European pipeline grid provides a viable alternative to LNG gas during the disruption. Second, during the crisis, the UK profits from price-taking domestic production and storage gas reserves that limit the mark-up rents for oligopolistic players. Japan, in contrast, has only small capacities of domestic production and underground storage and is therefore more exposed to Cournot behavior. Third, LTCs help the UK to decrease prices by securing gas deliveries that would normally be sold to the UK at higher price levels. Japan also has significant volumes of LTCs helping to overcome the crisis; however, since part of Japan's LNG long-term contracts are supplied by Qatar (and hence not available in case of a blockage of the Strait of Hormuz), the decreasing price effect in Japan is reduced in comparison with the reference scenario.

2.4.4 The Spatial Impact of Supply Disruptions

As we have seen so far, the supply shock of a Hormuz Strait blockage has a differential impact on importing countries because of their spatial location, i.e. the connection to exporters, e.g. via pipelines. In a spatial oligopoly model the question is whether also the location of the shock affects the importing countries differently. Therefore we derive another scenario of a 6 months lasting blockage of gas flows: in this setting, we assume that gas transits from Russia to Europe are blocked in the Ukraine – a situation that has already occurred in 2009, although for a shorter time period. In the Ukraine scenario, the Hormuz Strait is not blocked.

Figure 2.8 compares the price impacts of the Hormuz disruption and the Ukraine disruption: the US gas price is again not affected by the Ukraine scenario. In Germany and the UK, the price effect of both disruptions is in a similar range. The locational influence of the supply shock becomes obvious when comparing the prices of Italy and Japan for both scenarios. In Italy we observe a strong price increase during the Ukraine disruption (+US$239/kcm), which is more than three times as high as in the Hormuz scenario. In Japan the Hormuz disruption (+US$171/kcm) affects prices by far more than the Ukraine disruption (+US$32/kcm). The reason for this result is similar to the finding from the previous section. Italy has to compensate for missing pipeline based imports from Russia. In order to do so, Italy has to attract LNG volumes by higher prices and the other main supplier Algeria increases its oligopolistic markup in the absence of Russian gas. Japan does not receive any gas which is transited through the Ukraine. Therefore no missing volumes have to be compensated. However, since Europe attracts more LNG in the Ukraine scenario than in the reference scenario, LNG prices rise globally, thus also in Japan.

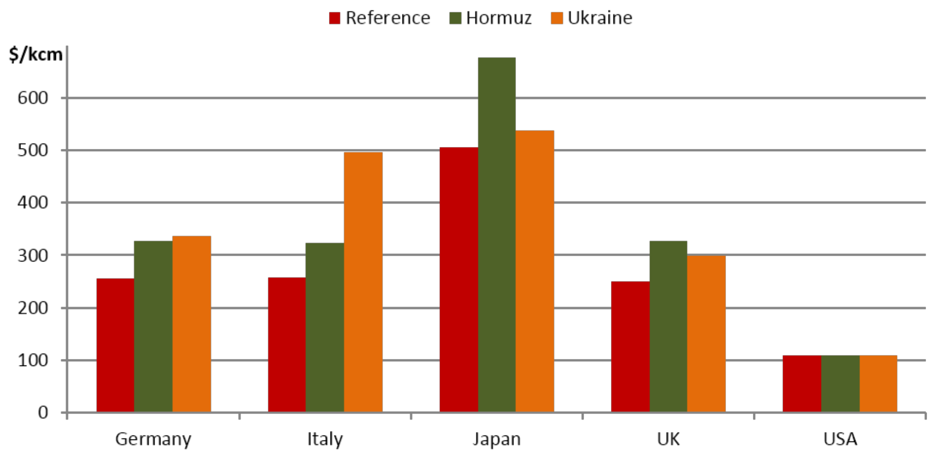

FIGURE 2.8: Select Import Prices during a 6-month Disruption of the Hormuz Strait and Ukraine Gas Transits Respectively

2.5 Conclusions

The political situation in the Persian Gulf is exacerbating. Since the beginning of 2012, Iran has threatened to block the Strait of Hormuz, the world's most important liquefied natural gas choke point. Because regional security of supply depends on the individual supply structure, a potential blockage would affect gas supplies differently depending on the region of the world.

In our paper, we raise the question in which regions would gas import prices be most affected by a blockage and why. For this purpose, we interpret the case of a blockage of the Strait of Hormuz as a supply shock in a spatial oligopoly. We analyze the compensation of missing Qatari gas supplies and compare regional price effects. Moreover, we develop a framework to disentangle regional prices into components and characterize them as price-increasing or price-decreasing components. Identifying the main price drivers allows us to quantify the supply situation in different regions.

We find that the gas price increases most in Japan. We also observe that gas price increases in the UK are significantly lower than those in Japan. US gas prices are hardly affected, as the country is rather independent from global gas trade.

We identify three reasons why a blockage of the Strait of Hormuz affects the import price in Japan much more than that in Britain. First, Japanese gas supplies fully depend on the disturbed liquefied natural gas market. The UK, on the other hand, has access to the European pipeline grid, which is supplied by important producers such as Russia and Norway. Thus, the UK faces an alternative market that – as opposed to the liquefied natural gas market – is only accessible by European (and not global) competitors. In turn, Japan has to compete globally for liquefied natural gas supplies. This translates into higher scarcity rents that Japan has to pay in order to receive liquefied natural gas volumes.

Second, the UK is less exposed to market power than Japan. Unlike in Japan, UK profits from price-taking domestic production and underground long-term storages (which act as a competitive fringe), thus decreasing mark-up rents of oligopolistic players.

Third, long-term contracts limit the price increase in the UK, since they secure gas volumes that otherwise would have been sold to the UK at higher prices. In contrast, the price decreasing effect of long-term contracts diminishes in Japan: The blockage of the Strait of Hormuz suspends long-term contracts between Qatar and Japan. Therefore, Japan loses its price advantage from the Qatari long-term contracts volumes. In other words, during the disruption, the missing volumes have to be replaced at comparably higher prices.

However, a supply disruption does not only affect differently diverse demand regions. Also the location of the disruption matters in a spatial market. To illustrate this effect we simulate a fictitious 6-month blockage of Ukrainian gas transits to Europe. We find that Italian gas prices are by far more affected in the Ukraine scenario than in the Hormuz scenario whereas for Japan the Hormuz disruption has the most severe price consequences.

This study investigates the regionally dispersed price effects following a supply shock in the natural gas market. However, mainly due to computational issues, some simplifying assumptions had to be made in our analysis. First, we assume perfect foresight, which may be a strong simplification, particularly for storage operators. Second, we model storage operators as price takers, despite the fact that a supply shock may allow them to maximize profits by initially refraining from storage depletion and thereby further increasing gas market prices. Third, we use a partial equilibrium model of the global gas market, thus failing to consider, e.g., the interdependencies between the oil and gas market. The interaction of substitutive fuels, such as oil and gas, could affect regional prices differently during a supply shock. In particular, the analysis of global inter-fuel competition using a model that accounts for strategic behavior in the respective markets is an interesting possibility for further research.

Chapter 3

Quantity-setting Oligopolies in Complementary Input Markets – the Case of Iron Ore and Coking Coal

3.1 Introduction

The research presented in this paper is inspired by an important energy source that exhibits the characteristics of a complementary input factor: coking coal. Coking coal is a complementary input to iron ore for steel production. Both goods are indispensable when making crude steel using the so-called "oxygen route", i.e., first producing the pig iron in a basic oxygen furnace and, second, using the pig iron in a blast furnace to create the final product, crude steel. From an energy economics perspective, this industry example is of particular interest because (i) the goods are complements, (ii) each of the inputs is of little use in alternative applications (e.g., power plants typically use coals of different quality), (iii) international trading of both commodities is highly concentrated and (iv) only a few (large) firms are active in both input markets (parallel vertical integration), i.e., produce both coking coal and iron ore, although none of the firms is vertically integrated in the production of steel. Given this market setting, the paper presented investigates the strategy of Cournot-behaving mining companies that own both a coking coal and an iron ore division. Do these firms optimize the divisions' output on a firm-level or according to each division separately (division-by-division)?

In order to answer this question, our analysis comprises two steps: First, we derive a stylized theoretical model to investigate the profitability of firm-level optimization in a setting with two homogeneous Cournot duopolies of complementary goods. In total, three firms are active in both duopolies: Two firms each serve solely one of the markets and one firm serves both markets. The latter firm can either optimize both divisions' output separately or on a firm-level. Comparing total profits of the integrated firm allows us to answer our research question from a theoretical point of view. We consider two cases: one with unlimited capacities and one incorporating a binding capacity constraint on one of the divisions' output.

The actual markets for coking coal and iron ore are, however, more complex as (i) both markets have more than two suppliers, (ii) there are multiple firms which are parallel vertically integrated, (iii) production costs are heterogeneous, (iv) both markets are spatial with multiple demand and supply regions and (v) several producers face a binding capacity constraint. We therefore, in a second step, develop and employ a numerical, spatial, multi-input oligopoly simulation model of the coking coal and iron ore market, calibrated with data from a unique data set for the years 2008 to 2010. We run the model for a range of assumed demand elasticities for the complementary product (pig iron) to assess the profits of the integrated companies in both cases, i.e., the optimization on a firm-level or on a division-level. Furthermore, we compare the simulation results of three specific market settings to the actual market outcomes: In addition to one perfect competition scenario, we assess one scenario assuming division-by-division optimization of all integrated firms and another one assuming firm-level optimization of the integrated companies' business units. We then assess which of these three scenarios best explains the actual market outcomes with regard to trade flows, production volumes and prices of the two commodities. Concerning trade flows, we use three statistical measures to evaluate which setting provides the best fit.

The theoretical model confirms that firm-level optimization is more beneficial compared to division-by-division optimization. However, if one of the divisions' production capacity is limited, we show that there exists a critical capacity constraint (i) below which optimization on a firm-level and on a division-level yield indifferent results, (ii) above which firm-level optimization is always beneficial and (iii) that becomes smaller with a lower demand elasticity.

Applying the simulation model for the coking coal and iron ore market yields three main findings: First, the lower the pig iron demand elasticity is, the more profitable the firm-level optimization is compared to the division-level optimization for an integrated mining company. However, for demand elasticities lower than -0.5 to -0.6, the benefits of firm-level optimization tend to zero. Second, comparing simulation results and actual market outcomes for the years 2008 to 2010 with respect to trade flows, prices and production volumes, the scenario assuming perfect competition, other than the two scenarios that assume players to behave in a Cournot-manner, does not match actual market outcomes. Third, the scenario assuming division-level optimization provides a more consistent fit with actual market outcomes than the firm-level optimization scenario, although one scenario does not unambiguously dominate the other. Thus, no indication is found that mining companies integrated into coking coal and iron ore production have applied firm-level optimization during the years 2008 to 2010.

At least two explanations for this finding are possible: First, because of capacity constraints, firm-level optimization only generates additional profits compared to division-level optimization if demand for the final product (pig iron) is rather inelastic. Second, additional management costs (increased organizational and transactional costs) that go along with firm-level optimization may outweigh additional profits. Hence, division-level optimization may leave sources of profits untapped but can be the profit-optimizing strategy of a mining company integrated in both coking coal and iron ore production.

Our research is motivated by two strands of literature. The starting point is the seminal publication by Cournot (1838) concerning the theory of complementary oligopolies. More recent papers on the topic of strategic behavior and complementary goods were inspired by Singh and Vives (1984), who develop a duopoly framework that allows for the analysis of quantity- and price-setting oligopolies assuming goods to be substitutes, independent or complements. Building on Singh and Vives' finding, a whole body of literature emerged, devoting its attention to analyzing the problem of complementary monopolies under different setups. However, the setting in which we are interested is different from the ones assumed in most of the papers belonging to this strand of literature: In our setting, the supply of each complement is characterized by an oligopoly, i.e., there are few substitutes for each complement, whereas most of the papers belonging to the body of literature referred to above assume each complementary good to be produced by a monopolist. Salinger (1989) is the only one to use a similar setting as the one presented in this paper. Second, concerning empirical literature, two analyzes on strategic behavior on the coking coal market have inspired our research: Graham et al. (1999) and Trüby (2013). Graham et al. (1999) simulate the coking coal trade for the year 1996 for several supply- and demand-side market power cases. Trüby (2013) analyzes different market structures such as Cournot or Stackelberg behavior of mining companies to find evidence of non-competitive behavior. Further empirical papers dealing with the analysis of coking coal and iron ore trading have been published (e.g., Labson, 1997, Toweh and Newcomb, 1991 or Fiuza and Tito, 2010). However, to the best of our knowledge, there has yet to be a publication that handles the strategic interaction between both markets or that applies the theory of complementary inputs to a real-world setting.

Consequently, this paper contributes to the literature in three ways: First, we add a new dimension to the existing literature on the strategic behavior of coking coal producers by taking into account the iron ore market and the complementarity of both goods in pig iron production. Second, we extend the literature on resource market simulations by developing a spatial multi-input equilibrium model that accounts for coking coal and iron ore as complementary inputs and enables the simulation of market power on a firm-level. Third, we assess the strategic behavior of firms that produce both coking coal and iron ore, thereby specifically accounting for capacity constraints.

The remainder of this paper is structured as follows: Section 3.2 introduces our theoretical framework and establishes our theoretical findings. Section 3.3 presents the motivation for our industry example, explains the structure of the simulation model used to model the coking coal and iron ore market and describes the numerical data used in this study. Section 3.4 analyzes the results obtained from the model simulations. More specifically, Subsection 3.4.1 analyzes, from the perspective of individual firms, the impact of firm- versus division-level optimization on the firms' profits. Subsection 3.4.2 assesses which of the three scenarios best explains the actual outcomes of the coking coal and iron ore market. Subsection 3.4.3 briefly discusses the strategic implications of these findings. Finally, Section 3.5 concludes.

3.2 Quantity-setting Complementary Oligopolies

In the setting we are interested in, supply of each complement, coking coal and iron ore, is characterized by a quantity-setting (Cournot) oligopoly. Each of the two complementary goods is considered as homogeneous. Furthermore, the setting is characterized by the existence of a number of parallel vertically integrated firms, i.e., mining companies which produce both coking coal and iron ore. Consequently, we model two simultaneous Cournot equilibria both of which influence the composite good's demand and thus the price of the two complementary goods. The approach chosen in this paper resembles the one in Salinger (1989), who uses a similar setting of complementary oligopolies to investigate how different definitions of the terms "upstream" and "downstream" change the impact of a vertical merger on competition. Following Salinger (1989), we assume players active in one input market to take the price of the other complement as given, thus we assume $\frac{\partial p_1}{\partial x_2} = \frac{\partial p_2}{\partial x_1} = 0$.

This assumption implies that we abstract from the "tragedy of the anticommons" problem. The problem was first described by Sonnenschein (1968), who pointed out the duality between a Bertrand duopoly with substitutes and a Cournot complementary monopoly. Sonnenschein (1968) showed for a setup in which each complementary good is produced by one monopolist and each monopolist maximizes its profit by choosing the optimal quantity of its good, an incentive arises to undercut total output of the other complement. In his setting an oversupply of one of the complements would cause its price to drop to zero (or to marginal costs if they are assumed to be greater than zero), leaving all the profits to the other complement's supplier. In the end, this would lead to a race-to-the-bottom in quantities. The unique Nash-equilibrium where such a deviation is not profitable is one where no firm produces at all. This somewhat paradox (and unrealistic) result relies heavily on the effect that even the slightest excess supply of one of the goods lets its price drop to zero. An effect which already Sonnenschein himself referred to as "somewhat obscure".[24] [25]

In the following, we will use a stylized theoretical model to investigate the profitability of firm-level optimization in a setting with two homogeneous Cournot duopolies of complementary goods. In Subsection 3.2.1, unlimited production capacity is assumed. In Subsection 3.2.2, we first investigate if the introduction of a binding capacity constraint on one of the complementary goods of the parallel vertically integrated firm may change the favourability of firm-level optimization. Second, we propose and proof three conjectures characterizing the profitability of firm-level optimization and the effect of capacity constraints.

3.2.1 A Model of Two Complementary Duopolies With Unlimited Capacities

We start out by considering a simple market of three firms producing two complementary goods. Firm 1 holds two divisions, one (c_1) produces complement C (coking coal) and the other (i_1) produces complement I (iron ore). The other two firms each are specialized

[24] This remark can be found in footnote 4 of Sonnenschein (1968).

[25] Another interesting aspect of complementary goods and Cournot competition was first brought forward by Singh and Vives (1984). They develop a duopoly framework that allows to analyse quantity- and price-setting oligopolies (Bertrand, 1883) assuming goods to be substitutes, independent or complements. The two authors proof that in the case of a complementary monopoly companies prefer to offer price instead of quantity contracts, as this maximizes their profits. Amongst other things, Häckner (2000) shows that this finding also holds true under more general assumptions including a setting with more firms (each producing one complementary good). In this paper both input markets are characterized by oligopolies with firms having production constraints. Therefore, if firms were assumed to engage in Bertrand competition and production capacity would be unconstrained prices of each complement would equal marginal costs and, thus profits would amount to zero. In the case of capacity constraints it has been shown that first-order conditions for profit maximization may have a kink, such that equilibria may not be well defined. Therefore, companies would prefer quantity contracts over price contracts in our setting.

and each own one division. Firm 2 solely produces coking coal (c_2) and the third firm solely produces iron ore (i_2). Thus, there are $N = M = 2$ producers of each complement coking coal and iron ore. For simplification of the analysis, production costs are assumed to be zero, although this does not qualitatively alter the results. Complements I and C may be combined in fixed proportions (here: one unit each) to produce the composite good pi (pig iron), i.e., it holds true that $x_{pi} = x_i = x_c$ with $x_c = \sum_n^N x_c^n$ and $x_i = \sum_m^M x_i^m$.

In addition, we assume full compatibility among the complements and perfect competition in the market for the composite good, such that NxM composite goods exist, all of which are available at price $p_{pi} = p_i + p_c$. Thus each complement's price ($p_i \left[\sum_m^M x_i^m, p_c\right]$ and $p_c \left[\sum_n^N x_c^n, p_i\right]$) depends on the supply of the complement ($\sum_m^M x_i^m$ or $\sum_n^N x_c^n$) as well as the price of the other complement. However, the price of the other complement is perceived as a cost component due to the assumption $\frac{\partial p_1}{\partial x_2} = \frac{\partial p_2}{\partial x_1} = 0$. We also rule out that there is product differentiation in the composite good market, thus all $N \times M$ composite goods are perfect substitutes as well. Initially, we do not assume the composite good's inverse demand function to be of a specific functional form.

Assuming, that firm 1 chooses to optimize the output of divisions c_1 and i_1 *not* on a firm-level but division-by-division, the profit functions of the four divisions are given by

$$\Pi_{i_m} = p_i x_i^m \tag{3.1}$$

$$\Pi_{c_n} = p_c x_c^n. \tag{3.2}$$

Taking, for example, the first partial derivate of the profit function of division i_1 yields the following first-order condition:

$$\frac{\partial \Pi_{i_1}}{\partial x_i^1} = p_i + \left(\frac{\partial p_i}{\partial x_i^1} \frac{\partial x_i^1}{\partial x_i^1} + \frac{\partial p_i}{\partial p_c} \frac{\partial p_c}{\partial x_i^1} + \frac{\partial p_i}{\partial x_i^{-m}} \frac{\partial x_i^{-m}}{\partial x_i^1} \right) x_i^1 = 0 \tag{3.3}$$

with x_i^{-m} being the iron ore production of the competitors. Due to the assumption that the firms engage in Cournot competition, it holds true that $\frac{\partial x_i^{-m}}{\partial x_i^1} = 0$. As discussed previously, in our model we assume that $\frac{\partial p_1}{\partial x_2} = \frac{\partial p_2}{\partial x_1} = 0$, hence Equation 3.3 simplifies to

$$\frac{\partial \Pi_{i_1}}{\partial x_i^1} = p_i + \frac{\partial p_i}{\partial x_i^1} \frac{\partial x_i^1}{\partial x_i^1} x_i^1 = 0. \tag{3.4}$$

In order to derive the market results we assume the demand function to be linear in form, i.e., $p_{pi} = a - bx_{pi}$. The first partial derivative of the profit function of division i_1 yields the following first-order condition, which due to the assumed symmetry looks analogue for the other firms:

$$\frac{\partial \Pi_{i_1}}{\partial x_i^1} = p_i - bx_i^1 = 0. \tag{3.5}$$

Solving the resulting system of equations allows us to derive equilibrium output and prices under division-by-division optimization:

$$x_{pi}^* = x_i^* = x_c^* = \frac{a}{2b}, \quad p_c^* = p_i^* = \frac{a}{4} \quad \text{and} \quad p_{pi}^* = \frac{a}{2}. \tag{3.6}$$

Next we now consider a setup in which firm 1 optimizes the output of its divisions c_1 and i_1 simultaneously, i.e., on a firm-level. In literature, firm-level optimization is often referred to as parallel vertically integration (PVI). To distinguish the results of firm-level optimization to division-level optimization, we use the notation "PVI" in the following. In its general form, i.e., without a specific functional form of the (inverse) demand function, the profit function is given by

$$\Pi_{PVI} = p_i x_i^{PVI} + p_c x_c^{PVI}. \tag{3.7}$$

Taking the first partial derivate of Equation 3.7 with respect to x_i^{PVI} and x_c^{PVI} yields:

$$\frac{\partial \Pi_{PVI}}{\partial x_i^{PVI}} = p_i + \left(\frac{\partial p_i}{\partial x_i^{PVI}} \frac{\partial x_i^{PVI}}{\partial x_i^{PVI}} + \frac{\partial p_i}{\partial p_c} \frac{\partial p_c}{\partial x_i^{PVI}} + \frac{\partial p_i}{\partial x_i^{-m}} \frac{\partial x_i^{-m}}{\partial x_i^{PVI}} \right) x_i^{PVI} + \frac{\partial x_c^{PVI}}{\partial x_i^{PVI}} p_c = 0 \tag{3.8}$$

$$\frac{\partial \Pi_{PVI}}{\partial x_c^{PVI}} = p_c + \left(\frac{\partial p_c}{\partial x_c^{PVI}} \frac{\partial x_c^{PVI}}{\partial x_c^{PVI}} + \frac{\partial p_c}{\partial p_i} \frac{\partial p_i}{\partial x_c^{PVI}} + \frac{\partial p_c}{\partial x_c^{-n}} \frac{\partial x_c^{-n}}{\partial x_c^{PVI}} \right) x_c^{PVI} + \frac{\partial x_i^{PVI}}{\partial x_c^{PVI}} p_i = 0. \tag{3.9}$$

We already know that $\frac{p_i}{x_c} = \frac{p_c}{x_i} = 0$ and $\frac{\partial x_i^{-m}}{x_i^m} = \frac{\partial x_c^{-n}}{x_c^n} = 0$. Keeping in mind that in this example a factor intensity (*fin*) of 1 is assumed, in case of a parallel vertically integrated firm $\frac{\partial x_c^{PVI}}{\partial x_i^{PVI}} = \frac{\partial x_i^{PVI}}{\partial x_c^{PVI}} = fin = 1$. Thus, a firm-level optimizing firm knowing that an increase in one of the complements output needs an equally large increase of the other complement in order to increase the output of the composite good, would always find it beneficial to increase output of both goods at the same time. Assuming a linear inverse demand function of the composite good and using Equations 3.8 and 3.9, respectively, the resulting first-order conditions are:

$$\frac{\partial \Pi_{PVI}}{\partial x_i^{PVI}} = a - 2bx_i^{PVI} - bx_i^2 + p_c = p_i + p_c - bx_i^{PVI} = 0 \tag{3.10}$$

$$\frac{\partial \Pi_{PVI}}{\partial x_c^{PVI}} = a - 2bx_c^{PVI} - bx_c^2 + p_i = p_i + p_c - bx_c^{PVI} = 0. \tag{3.11}$$

Taking a closer look at the Equations 3.10 and 3.11, we see that due to the complementarity of the goods, in order to maximize its overall profits, the mining company which optimizes output on a firm-level has to take into account not only the production of its direct competitors, but also the price of the complementary good. Solving again the resulting system equations allows us to derive equilibrium output and prices under firm-level optimization:

$$x_{pi}^* = x_i^* = x_c^* = \frac{2a}{5b}, \quad p_c^* = p_i^* = \frac{a}{5} \quad \text{and} \quad p_{pi}^* = \frac{2a}{5}. \tag{3.12}$$

By comparing the equilibrium solutions, i.e., with (Equations 3.12) and without (Equations 3.6) firm-level optimization, we find that firm-level optimization results in higher supply of the composite good and, therefore, of the two complementary inputs, which in turn leads to lower prices. Hence, firm-level optimization increases consumer welfare.

TABLE 3.1: Market Outcomes Based on Strategy Choice of the Integrated Firm

	Division-level	**Firm-level**
Price of composite good	$\frac{a}{2}$	$\frac{2a}{5}$
Price of complements	$\frac{a}{4}$	$\frac{a}{5}$
Quantity ($x_{pi} = x_i = x_c$)	$\frac{a}{2b}$	$\frac{3a}{5b}$
Each firm's output	$x_i^m = x_c^n = \frac{a}{4b}$	$x_i^{PVI} = x_c^{PVI} = \frac{2a}{5b}$ $x_i^2 = x_c^2 = \frac{a}{5b}$
Each firm's profit	$i^m = c^n = \frac{a^2}{16b}$	$PVI = \frac{4a^2}{25b} \quad i_2 = c_2 = \frac{a^2}{25b}$

While consumers benefit from firm-level optimization, the specialized, i.e., not parallel vertically integrated firms lose market share and make less profit. This is due to the fact that firm-level optimization effectively internalizes a negative externality. The externality is negative due to the the fact that $\frac{\partial p_1}{\partial x_2} = \frac{\partial p_2}{\partial x_1} = 0$ (see also Salinger, 1989). If a company, which is specialized in producing one of the complements, chooses to reduce its output, the production of the composite good is reduced as well, thereby raising the composite good's price. This increases the price of the company's complement, while the other complement's price is not changed (because of $\frac{\partial p_1}{\partial x_2} = \frac{\partial p_2}{\partial x_1} = 0$). However, due to the reduction of the composite good's output, the output of the other complement, too, is reduced. Consequently, reducing the output of one of the complements causes a negative externality on the firms producing the other complement. Hence, the PVI company, internalizing this negative externality, is willing to supply a larger amount of both inputs, which then leads to a reduction of the output of the remaining independent companies (see Table 3.1). Another interesting aspect is that, in contrast to Cournot oligopoly with substitutes and no capacity constraints, there is no merger paradox. That is, profits of the firm-level optimizing company (which may be interpreted as a merger situation) are always larger than the combined profits of the two divisions under division-level optimization (equivalent to a non-merger situation), again due to the internalization of the negative externality.

Summing up, we recalled that a parallel vertically integrated company maximizes its profits by optimizing output of both goods on a firm-level. Assuming unlimited production capacity, we showed that firm-level optimization of divisions producing different complements is always profitable, i.e., it increases overall profit of the holding.

3.2.2 Profitability of Firm-level Optimization under Constrained Capacity

As shown in Subsection 3.2.1, the profitability of firm-level optimization of a parallel vertically integrated company arises from increasing the output of both complements compared to the case of division-level optimization. Therefore, the question arises whether a constraint restricting the potential output of one of the two complements may alter the result that firm-level optimization is beneficial.

In order to do so, we need to recall from Subsection 3.2.1 that, first, an unconstrained integrated firm behaves in a manner similar to a Stackelberg leader, i.e., by internalizing the negative externality of the two complements, he increases his output compared to the case of division-level optimization (see Table 3.1). Second, the integrated firm maximizes its profit by supplying the same amount of both complements (in case of a factor intensity of both goods of 1), i.e., it provides both complements as a bundle. However, in case of a binding capacity constraint on one of the complements, the firm could also choose to supply different quantities of its two goods. Consequently, one can rewrite the profit function of the parallel vertical integrated firm from the previous subsection (Equation 3.7) as:

$$\Pi_{PVI} = (p_i + p_c)x_b + p_i x_i^{PVI} + p_c x_c^{PVI} \tag{3.13}$$

with x_b referring to the amount of bundled sales supplied to the market, thus it represents at the same time sales of iron ore as well as coking coal, while x_i^{PVI} and x_c^{PVI} need not be sold at a similar ratio. Thus the firm's total coking coal and iron ore output amounts to $x_b + x_i^{PVI}$ and $x_b + x_c^{PVI}$, respectively. In the following, using Equation 3.13 and a linear demand function, we would like to investigate the profitability of firm-level optimization in the event of a binding capacity constraint in more detail. Therefore, we propose three conjectures that we will proof subsequently:

Conjecture 1 *Given a specific linear demand function, there exists a critical capacity limit, $\overline{x}_b$, that makes the integrated firm indifferent between firm-level and division-level* *optimization, i.e., profits are identical for both strategies. For capacity limits lower than* $\overline{x}_b$ *profits of both strategies remain identical as well.*

Conjecture 2 *Given a specific linear demand function, for every capacity limit* $\hat{x}_b$ *that fulfills* $\hat{x}_b > \overline{x}_b$*, firm-level optimization is profitable despite a binding capacity constraint.*

Conjecture 3 *The less elastic the linear inverse demand function of the composite good, the lower becomes the critical capacity constraint,* $\overline{x}_b$*.*

Concentrating first on Conjecture 1, we need to show that for a given linear inverse-demand function of the composite good, there is a capacity limit to one of the complements $\overline{x}_b$ that causes the difference between the division-level profits, $\pi_c^1 + \pi_i^1$, and the firm-level profits, π^{PVI}, to be zero.[26] For this purpose, we start by deriving the equilibrium profit of firm-level optimization using the first-order conditions of the three firms (one integrated and two specialized firms):

$$\frac{\partial \Pi_{PVI}}{\partial x_i^{PVI}} = -bx_i^{PVI} - bx_b + p_i = 0 \tag{3.14}$$

$$\frac{\partial \Pi_{PVI}}{\partial x_c^{PVI}} = -bx_c^{PVI} - bx_b + p_c = 0 \tag{3.15}$$

$$\frac{\partial \Pi_{PVI}}{\partial x_b} = -bx_b - bx_c^{PVI} - bx_i^{PVI} + p_c + p_i = 0 \tag{3.16}$$

Assuming a binding capacity constraint on the iron ore output of the integrated firm ($\overline{x}_b$), the first and third first-order conditions (Equations 3.14 and 3.16) will not be needed as the firm's optimal iron ore output is $\overline{x}_b$ (hence, $x_i^{PVI} = 0$), otherwise the capacity constraint would not be binding.

Knowing that the first-order conditions of the non-integrated firms remain unchanged (see Equation 3.10) and using $p_{pi} = p_i + p_c$ as well as Equation 3.15 yields

$$p_i = \frac{2a - 3b\overline{x}_b}{5}, \quad p_c = \frac{a + b\overline{x}_b}{5}, \quad x_c^{PVI} = -\frac{4}{5}\overline{x}_b + \frac{a}{5b}. \tag{3.17}$$

Therefore, the integrated firm's profit function in case of a binding capacity constraint is

$$\pi^{PVI} = \frac{a^2 + 12ab\overline{x}_b - 14b^2\overline{x}_b^2}{25b}. \tag{3.18}$$

We know from Subsection 3.2.1 that the profit of the integrated firm applying division-level optimization amounts to $2 * \frac{a^2}{16b} = \frac{a^2}{8b}$ with each division supplying $\frac{a}{4b}$ (see Table

[26] We use x_b since if the capacity constraint on one of the complements is binding, the firm will choose to produce at least the same quantity of the other complement, hence it will supply $\overline{x}_b$ bundles.

3.1). In order to proof Conjecture 1, we thus need to show that when the capacity constraint is $\overline{x}_b = \frac{a}{4b}$ profits under firm-level optimization equal the profits of division-level optimization:

$$\pi^{PVI} = \frac{a^2 + 12ab\frac{a}{4b} - 14b^2\left(\frac{a}{4b}\right)^2}{25b} = \frac{4a^2 - \frac{7a^2}{8}}{25b} = \frac{\frac{25a^2}{8}}{25b} = \frac{a^2}{8b}, \tag{3.19}$$

which is the case. Now, if we consider division-level optimization with one division being constrained in its output, e.g., the iron ore division($\overline{x}_i^2$), the function of profits (depending on the capacity constraint) is identical to that of firm-level optimization (see Appendix B.1). In other words, if the capacity limit equals or is lower than the optimal quantity of the division-level strategy, profits of the parallel vertically integrated firm remain unchanged by optimizing on a firm-level, which is what we wanted to proof.

Regarding Conjecture 2, we need to show that for capacity constraints that are higher than $\overline{x}_b = \frac{a}{4b}$ profits of firm-level optimization are higher than that of division-level optimization. We already know that the optimal output of the unconstrained integrated firm under firm-level optimization is $\frac{2a}{5b}$. Taking a look at equilibrium output of x_c^{PVI} stated in Equation 3.17, we see that x_c^{PVI} is zero for $\hat{x}_b > \frac{a}{4b}$, because output in this model is restricted to be non-negative. Therefore, total output when optimizing on a firm-level is equal to $\hat{x}_b$ for $\hat{x}_b > \overline{x}_b = \frac{a}{4b}$. In this case, equilibrium prices and the integrated firm's profits are given by

$$p_i = p_c = \frac{a - b\hat{x}_b}{3}, \quad \pi^{PVI} = \frac{2a\hat{x}_b - 2b\hat{x}_b^2}{3} \quad \text{for } \hat{x}_b > \overline{x}_b. \tag{3.20}$$

Hence, for $\hat{x}_b > \overline{x}_b$ it holds true that the profits of firm-level optimization change by

$$\frac{\partial \pi^{PVI}}{\partial \hat{x}_b} = \frac{2a - 4b\hat{x}_b}{9} \quad \text{for } \hat{x}_b > \overline{x}_b, \tag{3.21}$$

with $\frac{\partial \pi^{PVI}}{\partial \hat{x}_b} > 0$ for $\frac{a}{4b} < \hat{x}_b < \frac{2a}{5b}$, which proofs Conjecture 2. Figure 3.1 illustrates the integrated firm's profits of division-level and firm-level optimization depending on the iron ore capacity.

Focussing now on Conjecture 3, we would like to show that the steeper the inverse demand function is the lower the optimal quantities supplied in case of division-level optimization $\frac{a}{4b}$ (see Table 3.1) and thus the lower the critical capacity constraint becomes. Therefore, we need to establish the relationship between the ratio of a, the maximum willingness-to-pay, and b, the slope of the inverse demand function, and the assumed (absolute) point elasticity ϵ. Since it can be easily shown that a and b in the linear

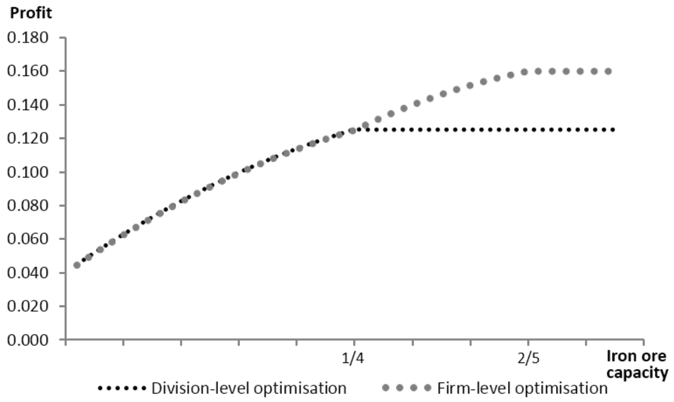

FIGURE 3.1: Profits of the Integrated Firm Optimizing on a Firm-level versus a Division-level Depending on the Iron Ore Production Capacity

demand case can be written as:

$$a = p_{ref} + b * x_{ref} \tag{3.22}$$

$$b = \frac{p_{ref}}{x_{ref}} * \frac{1}{\epsilon} \text{ with } \epsilon > 0, \tag{3.23}$$

with p_{ref} and x_{ref} being a reference price and demand, respectively, it holds true that

$$\frac{a}{b} = (1 + \epsilon) * x_{ref}. \tag{3.24}$$

Consequently, the lower the elasticity in the reference point, ϵ, i.e., the steeper the linear inverse demand function, the lower the optimal quantities when firms optimize their quantities separately. Thus, the less elastic the linear inverse demand function of the composite good, the lower the critical capacity constraint, $\overline{x}_b$ becomes (Conjecture 1). The intuition behind this finding is that the steeper the demand function, i.e., the lower the point elasticity, the lower the equilibrium output. The lower the equilibrium output is the less restrictive is the capacity constraint. Furthermore, the less restrictive the capacity constraint of the integrated firm, the higher is the effect of firm-level optimization (avoiding marginalization of both divisions).

3.3 A Spatial Equilibrium Model of the Global Coking Coal and Iron Ore Market

3.3.1 Steelmaking and the Markets for Coking Coal and Iron Ore

In general, there are two main routes to produce crude steel, which is an alloy of iron and carbon. One option, also referred to as the "oxygen route", is an integrated steel-making process involving blast furnace (BF) production of pig iron followed by a basic oxygen furnace (BOF). Alternatively, an electric arc furnace (EAF) process may be applied (the so called "electric route"), which mainly uses recycled steel (steel scrap) for steelmaking, and may also use direct reduced iron (DRI) to substitute steel scrap. Roughly 30% of global steel supply is produced using EAFs, with the remainder relying on integrated steel-making.

The main difference between the two production methods is that the basic oxygen steelmaking process is self-sufficient in energy, i.e., the energy is generated during the process by the reaction of oxygen and carbon, with coke being the main source of carbon. This is not the case with EAF steelmaking, as an EAF mainly relies on the use of electricity for melting the steel scrap and DRI. Therefore, no coke is used in electric arc furnaces. Against the background that coke is essentially coking coal without impurities, it is obvious that almost the entire global coking coal supply is used in coke ovens and, therefore, in the basic oxygen steelmaking process. Furthermore, due to its chemical properties and the existence of cheaper alternative coal types (mainly thermal coal and lignite), coking coal is not used in electricity generation. Albeit to a lesser extent, this also holds true for iron ore, with the reason being that the major part of total steel scrap supply is used in EAFs, thereby reducing the need for direct reduced iron. In 2012, pig iron production amounted to 1112 Mt, while direct reduced iron production was 71 Mt, i.e., DRI accounted for 6% of global iron production (WSA, 2013). Consequently, coking coal and iron ore are complementary goods needed to produce pig iron, with both inputs being (almost exclusively) used in this single application.

Furthermore, both markets, the one for iron ore as well the one for coking coal share two interesting characteristics: First, international trade of both commodities is highly concentrated, as the biggest four exporting companies in the coking coal and iron ore market were responsible for 45% and 67% of total trade volume in 2010, respectively. Second, three global mining companies, namely BHP Billiton, Rio Tinto and Anglo American, are among the top four exporting companies in both markets. Hence, not only are they parallel vertically integrated companies, i.e. they produce both complementary inputs, but, in addition, they may have considerable market power. Given the setting of complementary inputs and market concentration, integrated companies active in both markets may have incentives to maximize their profits by on a firm-level jointly choosing their coking coal and iron ore production volumes on a firm-level and not separately, i.e., division-by-division.

3.3.2 Model Logic and Formulation

The partial equilibrium model presented in this section is programmed as a mixed complementary problem (MCP). The model aims at maximizing annual profits of the global mining companies producing coking coal and iron ore subject to production constraints and given the various costs along the supply-chain, such as seaborne and inland transport costs. Section 3.2, albeit in a simplified setting (i.e., non-spatial market, with only one consuming region and homogeneous players) already discusses a firm's profit function under independent optimization of the business units and under firm-level optimization. Here, the discussion of the model focuses only on the first-order and the market clearing conditions, thus we do not explicitly write down the respective profit functions. Similar to the model presented in the previous section, we assume that the composite good's price ($\lambda_{d,y}$) in demand region d linearly depends on the composite good's (pig iron) demand (which is equal to pig iron production $pi_{d,y}$). Thus, $\lambda_{d,y} = int_{d,y} - slo_{d,y} * pi_{d,y}$.[27] [28]

The model distinguishes the physical transports of input factor f by mining company n in year y produced in mine m to a demand market d ($tr_{n,f,m,d,y}$) and the sales of a company to a market ($sa_{n,f,d,y}$). If the firm optimizes output on a firm-level, it can also sell both composites as a bundle ($sa^b_{n,d,y}$).

Transports $tr_{n,f,m,d,y}$ are constrained by the annual production capacity $cap_{n,f,m,y}$ of mine m. Hence, the amount of transported volumes is subject to the following constraint

$$cap_{n,f,m,y} - \sum_{d \in D} tr_{n,f,m,d,y} \geq 0 \quad \forall n, f, m, y \qquad (\mu_{n,f,m,y}), \tag{3.25}$$

thereby $\mu_{n,f,m,y}$ represents the value of an additional unit of production capacity at mine m in year y, which may also be interpreted as a scarcity rent of production capacity.

For each input, the sum of transported volumes to a demand market has to equal the sales of each company. If firm-level optimization is enabled the parameter sim_n is equal to 1.

$$\sum_{m \in M(n)} tr_{n,f,m,d,y} = sa_{n,f,d,y} + sa^b_{n,d,y} * sim_n \quad \forall n, f, d, y \qquad (v_{n,f,d,y}), \tag{3.26}$$

thereby $v_{n,f,d,y}$ can be interpreted as the physical value of the transported goods, i.e., the sum of production costs, scarcity rent and transport costs.

[27] Although all sets, parameters and variables used throughout this subsection are explained in the text, the reader is referred to Table B.1 in Appendix B.2 for an overview of the nomenclature.

[28] To keep the formulae as simple as possible, all parameters used in the model description have been adjusted for the factor intensity.

A mining company is only willing to produce and transport a good to a market if the sum of production costs, scarcity rent and transport costs is covered by the resulting physical value in the market.

$$\begin{aligned}\frac{\partial Ł_{\Pi_n}}{\partial tr_{n,f,m,d,y}} = &- v_{n,f,d,y} + pco_{f,m,y} + tco_{f,m,y} \\ &+ \mu_{n,f,m,y} \geq 0 \quad \perp \quad tr_{n,f,m,d,y} \geq 0 \qquad \forall n, f, m, d, y.\end{aligned} \tag{3.27}$$

Each mining company n maximizes its profit by selling volumes to demand region d as long as the price of the input factor ($\rho_{f,d,y}$) exceeds the value of the good $v_{n,f,d,y}$. In case the company is assigned market power (which is indicated by setting the binary parameter $cva_{n,y}$ equal to one), $\rho_{f,d,y}$ must not only exceed physical delivery costs but also the company's mark-up, which depends on the slope of the composite good's demand function ($slo_{d,y}$) and sales volume of the company ($sa_{n,f,d,y}$ and $sa^b_{n,d,y} * sim_n$ in case of firm-level optimization).

$$\begin{aligned}\frac{\partial Ł_{\Pi_n}}{\partial sa_{n,f,d,y}} = &- \rho_{f,d,y} - cva_{n,y} * slo_{d,y} * (sa_{n,f,d,y} + sa^b_{n,d,y} * sim_n) \\ &+ v_{n,f,d,y} \geq 0 \quad \perp \quad sa_{n,f,d,y} \geq 0 \qquad \forall n, f, d, y.\end{aligned} \tag{3.28}$$

If an integrated mining company decides to optimize its divisions on a firm-level it has to decide additionally about the amount of bundles of complementary input factors that it sells to each market. The price of both input factors, i.e., the bundle has to equal the oligopolistic mark-up (see Equation 3.16) plus the physical value of both inputs.

$$\begin{aligned}\frac{\partial Ł_{\Pi_n}}{\partial sa^b_{n,d,y}} = &- \sum_f (\rho_{f,d,y}) - cva_{n,y} * slo_{d,y} * \left(\sum_f (sa_{n,f,d,y}) + sa^b_{n,d,y} * sim_n \right) \\ &+ \sum_f v_{n,f,d,y} \geq 0 \quad \perp \quad sa^b_{n,d,y} \geq 0 \qquad \forall n, d, y.\end{aligned} \tag{3.29}$$

Finally, in order to model an oligopoly in complementary goods the model encompases three market clearing conditions:

$$\lambda_{d,y} = int_{d,y} - slo_{d,y} * pi_{d,y} \quad \perp \quad \lambda_{d,y} \quad \text{free} \qquad \forall d, y \tag{3.30}$$

$$pi_{d,y} = \sum_{n \in N} (sa_{n,f,d,y} + sa^b_{n,d,y} * sim_c) \quad \perp \quad \rho_{f,d,y} \quad \text{free} \qquad \forall f, d, y \tag{3.31}$$

$$- \lambda_{d,y} + \sum_{f \in F} \rho_{f,d,y} \geq 0 \quad \perp \quad pi_{d,y} \geq 0 \quad \forall d, y. \tag{3.32}$$

These market clearing conditions represent three aspects: First, Equation 3.30 determines the price of pig iron ($\lambda_{d,y}$) using the inverse linear demand function. Second, Equation 3.31 states that each input's total sales (including bundles of input factors) to demand region d needs to equal total pig iron demand ($pi_{d,y}$). This equation is used to model coking coal and iron ore as complementary goods, with the composite good being produced using a fixed-proportion production technology. Finally, Inequality 3.32 needs to be incorporated to establish the relationship between input factor prices ($\rho_{f,d,y}$) and pig iron price ($\lambda_{d,y}$). For simplification, we assume that the pig iron price is fully explained by the prices of coking coal and iron ore, i.e., does not include any further marginal costs for the production process. This does not effect the results qualitatively though as the final product's price is of no further importance for our analysis.

3.3.3 Data and Scenario Setting

This subsection describes the data of the coking coal and iron ore market that we use in the numerical simulation. The dataset comprises demand, production and transport data of the years 2008 to 2010.

3.3.3.1 Demand Data

Iron ore consumption data in international statistics (e.g., World Steel Association (WSA)) is usually specified in metric tons thereby abstracting from the iron content in the ore (Fe-content). This however complicates our analysis: As we are interested in iron ore consumption as an input in pig iron production, it necessitates information on the amount of pure iron contained in the consumed ore. For example, a country has an annual consumption of 1 million tonnes (Mt) of iron ore. It is supplied by one producer delivering 0.7 Mt of 40% Fe and another delivering 0.3 Mt of 60% Fe. Thus, the country consumes 0.46 Mt of pure iron. A second country also consumes 1 Mt of iron ore, but the material has an iron content of 65% Fe. Hence the country consumes 0.65 Mt of pure iron. Even though both countries consume 1 t of iron ore, the pure iron consumption as an input for pig iron production is nearly 50% higher in the second country.

To cope with this problem, we use annual pig iron production data provided by WSA as a proxy for the actual iron ore consumption, thereby assuming that 1 Mt of pure iron is consumed to produce 1 Mt of pig iron.

Concerning coking coal we do not face this problem as we account for coking coal consumption specified in energy units (IEA, 2012). However, it is necessary to define the factor intensity of coking coal in pig iron production. Comparing coking coal consumption and pig iron production we assume a factor intensity of 70% which means that 0.7 Mt of coking coal are needed to produce 1 Mt of pig iron.

We assume that in the simulation model both coking coal and iron ore are exclusively used for pig iron production. In reality, 6% of global annual iron ore production serves as input for so-called direct reduced iron (DRI). Concerning coking coal, IEA statistics suggest that some minor quantities (4% globally) of coking coal are used for power generation as well. We correct our data for this in the following to limit complexity of our analysis. For the same reason, we abstract from stocking of iron ore or coking coal, which can be observed in both markets.

As stated in section 3.3, linear price-demand functions for pig iron are required in order to simulate different market settings. To derive those country specific demand functions we stick to an approach that has been widely used in literature on market models programmed as a mixed complementary problem (MCP): Using a reference price, a reference volume and an elasticity yields slope and intercept of the demand function. We use the annual pig iron production as reference volume. The reference price, however, is more difficult to obtain since we are not interested in the real pig iron price (containing price elements such as labour costs) but only the part of the price that can be explained by those input factors being in the scope of our analysis, i.e., the prices of coking coal and iron ore. The reference price is therefore calculated as follows

$$p_{pi} = p_i + p_c. \tag{3.33}$$

The annual average prices of coking coal and iron ore are derived based on information from BGR (2008-2011) and BREE (2011).

3.3.3.2 Production Data

We include detailed iron ore production data containing mine-by-mine production costs and region specific iron contents (World Mine Cost Data Exchange, 2013). Concerning coking coal we integrate the dataset of Trüby (2013) comprising mine-by-mine production costs as well. The production costs have to be interpreted as free on board costs, i.e., inland transport costs are already taken into account. Additionally, we analyse historic coking coal and iron ore production data of the most important export companies such as Vale, Rio Tinto, BHP Billiton (BHPB), Anglo American/Kumba, XStrata or FMG using their annually published production reports. Using those data sources in addition to annual country specific production and export volumes (iron ore: WSA (2010, 2011, 2012), coking coal: IEA (2012)), we obtain a detailed and nearly complete dataset of both factor market's supply side.

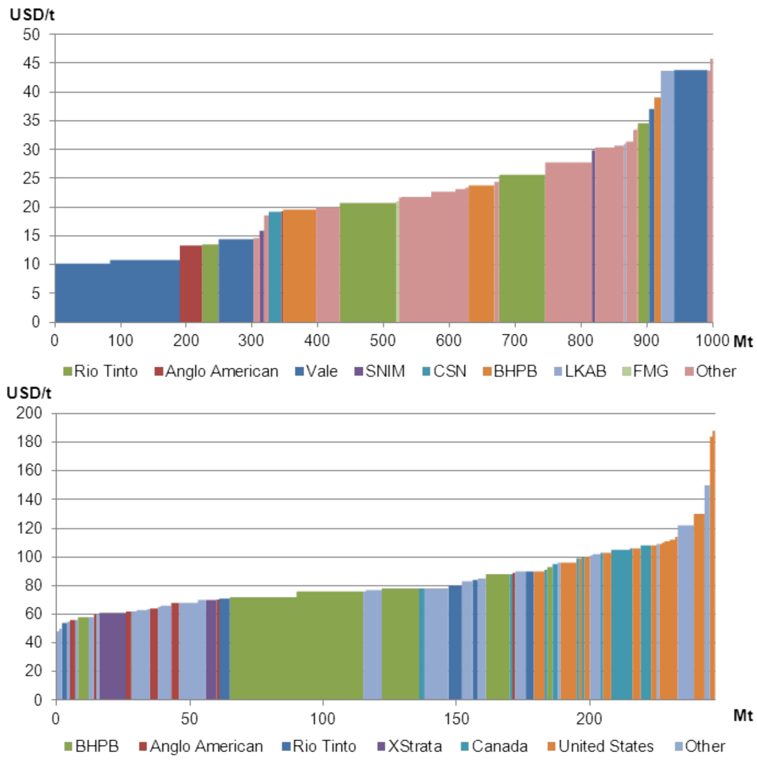

FIGURE 3.2: Coking Coal and Iron Ore FOB Cost Curves of Major Exporters in 2008

However, for two major producing countries it is difficult to access detailed mine sharp production data in both markets: China and India. For China, World Steel Dynamics (2011) provides us with cost and capacity information on iron ore production differentiating between several cost levels. Concerning Chinese coking coal production and both inputs in India, we use the annual iron ore production from WSA respectively the annual coking coal production from IEA (2012), however, not differentiating between different mines. This simplification does not severely affect our analysis as both in China and in India there is no dominant iron ore or coking coal producer that has a significant influence on global trade. Therefore, we assume an atomistic supply side in those two countries, i.e., coking coal and iron ore producers from both countries are modeled as competitive players.

Firms modeled as Cournot players are Vale, RioTinto, BHPB, FMG, Anglo American (Kumba), CSN, LKAB and SNIM in the iron ore market and Rio Tinto, BHPB, Anglo American and XStrata in the coking coal market. In line with Trüby (2013), we model US coking coal exporters as one Cournot player (US_CC), since the main export ports and the inland transport rails are controlled by one player and market power is assumed to be exerted via the infrastructure. Other smaller and mostly domestic producers are assumed to market their production volumes as competitive players.

Figure 3.2 shows the global FOB supply cost curves of major coking coal and iron ore exporters in 2008. Note that this figure does not reflect the seaborne traded iron ore volumes exactly since exporters also partly supply their domestic markets as well. We observe that regarding production costs the big three iron ore exporters Vale, Rio Tinto and BHP Billiton are for most part in the lower half of the global FOB cost curve.

3.3.3.3 Transport Data

The dataset used in this analysis comprises distances between major export and import ports using a port distance calculator. Additionally, the dataset contains freight rates of 2008 to 2010 of bulk carrier transports on numerous shipping routes. Using freight rates and transport distances we calculate a proxy for the seaborne transport costs. For most of the inland transport routes, costs are already accounted for since the cost data are free on board (FOB), i.e., the costs comprise production, inland transport and port handling costs. The only exception is inland transports from Russia to Europe respectively China where rail freight rates are used.

To limit model complexity, we do not explicitly account for capacity limitations of neither port nor rail infrastructure nor ship capacities. We implicitly assume that scarce bulk carrier capacities are already represented by the freight rates. Capacity limitations of export port or rail infrastructure both are subsumed under the production capacity of a production region. For example, if a production region has a capacity of 100 and the according port only has a capacity of 80, the production capacity we use in our model is 80.

3.4 Results of the Numerical Analysis

3.4.1 The Profitability of Parallel Vertical Integration in the Coking Coal and Iron Ore Market

We apply our computational model to investigate whether or not firms benefit from behaving parallel vertically integrated, i.e., optimizing output of the complementary goods on a firm-level. Therefore, in a first step, we simulate the coking coal and iron ore market for the years 2008 to 2010 to derive the profitability of the integrated companies Anglo American, Rio Tinto and BHP Billiton. Since the strategy choice of the competitors may influence the profitability of the own strategy, we model a simple static simultaneous game with two stages. In the first stage, each integrated company chooses between two strategies: "optimizing on a firm-level (FL)" and "optimizing on a division-level (DL)". In the second stage, all companies in the coking coal and iron ore market (also companies active in only one of the markets) set the production quantities, thereby knowing each of the integrated companies' strategy choices, FL or DL. Thus, in total we simulate 8 model runs and use each company's total profit margin as payoff function.[29]

The question arises if the proposed two-stage game is a realistic representation of the market. Is an integrated company able to credibly commit optimizing both divisions separately and can this be observed by the other players? The commitment to division-level optimization could be realized by incentive contracts for the division managers, e.g., by remuneration depending on profitability of the division. Although these contracts are unlikely to be seen by the other players, division-level optimization could be observable by founding a subsidiary company for, e.g., the iron ore business. Ideally, the holding would sell minor shares of the subsidiary in order to further incentivize that each division is optimizing itself separately. Although in reality, coking coal and iron ore businesses of integrated companies are rather subdivisions[30] than subsidiaries, the strategy DL could per se be committed to in a credible and observable way.

Figure 3.3 illustrates the profitability of choosing FL over DL for each of the three integrated companies given the other companies' strategy choices and the assumed demand elasticity. The profitability is derived as the difference in profit margins between option FL and option DL. These results seem to confirm Conjecture 3 from 3.2.2: The more inelastic the demand is, the higher is the additional benefit of choosing FL over DL. With an increasing demand elasticity the additional benefit of FL converges to zero.[31]

As stated in 3.2.2, capacity constraints of at least one of the complementary goods seem to be one explanation for the decreasing profitability of strategy FL. For BHP Billiton, for example, the iron ore capacity is binding in all three years as soon as the demand elasticity (in absolute terms) is higher than 0.5. Rio Tinto's coking coal capacity is binding in all of the scenarios and the iron ore capacity becomes binding for elasticities of 0.3 and 0.4 and higher. This might be an explanation why the additional benefit of strategy FL is generally higher for BHP Billiton than for Rio Tinto.

[29]Since we have no data about fixed costs of iron and coking coal mining, we focus on the profit margin, i.e., price minus marginal costs times quantity sold. This is sufficient for our analysis since we only compare differences of profit margins whereas fixed costs only change the level of the total profits.

[30]Interestingly, for both Rio Tinto and BHP Billiton, the head offices of the iron ore divisions are situated in Perth, the coal divisions in Brisbane and the holdings in Melbourne.

[31]For BHP Billiton, we observe slightly negative values for the years 2008 and 2009. This phenomenon can be explained by numerical issues during the solution process of the model.

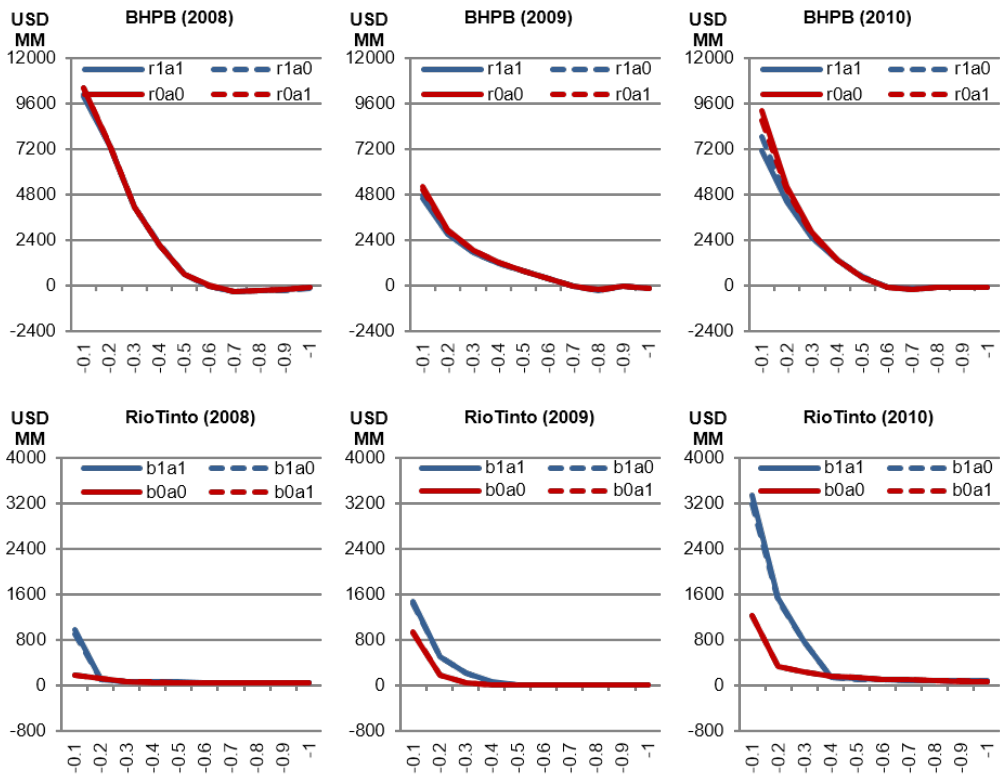

FIGURE 3.3: Additional Profits from Firm-level (1 = FL) vs. Division-level (0 = DL) Optimization Depending on the Other Integrated Companies' Strategy (b = BHP Billiton, r = Rio Tinto, a = Anglo American)

3.4.2 A Comparison of Three Market Settings

So far, the model results revealed that FL is a beneficial strategy for integrated companies if the demand is rather inelastic or, in other words, if the production capacity of both complementary goods is not scarce. However, the outcomes of FL and DL are equal when higher demand elasticities are assumed. In the following, searching for evidence whether or not integrated players optimize their coking coal and iron ore divisions on a firm-level, we investigate which of the strategy choices and which demand elasticities best represent historical market outcomes. Therefore we compare model results and historical market outcomes, i.e., prices, trade flows and production volumes.

In total, we focus on three market settings in this section: First, we investigate whether non-competitive behavior is observed in both the iron ore and the coking coal market. Hence, we run a scenario in which all players in the market behave in a perfectly competitive manner ("Perfect competition"), i.e., act as price takers. Second, we run another two model simulations each assuming Cournot behavior in both markets. One in which Anglo American, BHP Billiton and Rio Tinto each optimize output on a firm-level ("Firm-level") and another one in which each of those firms' coking coal and iron ore business units optimize their profits separately "Division-level"). By comparing model

TABLE 3.2: P-values of the F-tests ($\beta_0 = 0$ and $\beta_1 = 1$) for a Range of Elasticities

Coking coal	Perfect competition 2008	2009	2010	Division-level 2008	2009	2010	Firm-level 2008	2009	2010
e = -0.1	0.01**	0.00***	0.00***	0.08*	0.04**	0.03**	0.64	0.14	0.49
e = -0.2	0.01***	0.00***	0.00***	0.22	0.06*	0.04**	0.39	0.08*	0.44
e = -0.3	0.01***	0.00***	0.00***	0.46	0.12	0.14	0.37	0.11	0.33
e = -0.4	0.01***	0.00***	0.00***	0.64	0.26	0.50	0.36	0.14	0.36
e = -0.5	0.01***	0.00***	0.00***	0.71	0.54	0.93	0.32	0.14	0.31
e = -0.6	0.01***	0.00***	0.00***	0.63	0.92	0.59	0.27	0.13	0.20
e = -0.7	0.01***	0.00***	0.00***	0.41	0.92	0.20	0.19	0.11	0.10*
e = -0.8	0.01***	0.00***	0.00***	0.26	0.56	0.08*	0.11	0.09*	0.08*
e = -0.9	0.00***	0.00***	0.00***	0.13	0.38	0.07*	0.08*	0.05*	0.07*
e = -1.0	0.00***	0.00***	0.00***	0.10*	0.12	0.07*	0.06*	0.04**	0.06*
Iron ore	Perfect competition 2008	2009	2010	Division-level 2008	2009	2010	Firm-level 2008	2009	2010
e = -0.1	0.00***	0.00***	0.00***	0.85	0.15	0.32	0.87	0.41	0.55
e = -0.2	0.00***	0.00***	0.00***	0.88	0.62	0.72	0.91	0.89	0.95
e = -0.3	0.00***	0.00***	0.00***	0.66	0.87	0.95	0.74	0.79	0.73
e = -0.4	0.00***	0.00***	0.00***	0.37	0.62	0.79	0.59	0.25	0.41
e = -0.5	0.00***	0.00***	0.00***	0.18	0.13	0.44	0.42	0.03**	0.19
e = -0.6	0.00***	0.00***	0.00***	0.09*	0.01**	0.19	0.27	0.00***	0.09*
e = -0.7	0.00***	0.00***	0.00***	0.04**	0.00***	0.09*	0.17	0.00***	0.05*
e = -0.8	0.00***	0.00***	0.00***	0.02**	0.00***	0.05**	0.08*	0.00***	0.03**
e = -0.9	0.00***	0.00***	0.00***	0.01***	0.00***	0.05**	0.06*	0.00***	0.03**
e = -1.0	0.00***	0.00***	0.00***	0.01***	0.00***	0.01**	0.06*	0.00***	0.01**

Significance levels: 0.01 '***' 0.05 '**' 0.1 '*'

outcomes to actual price, production and trade data for the time period from 2008 to 2010, we aim at identifying the setting which has the better fit with the realized values. To compare trade flows we use three statistical tests discussed in Appendix B.3.[32]

Starting with the analysis of the "Perfect competition" setting, we find that the test statistics of the F-test allow us to reject the null hypothesis ($\beta_0 = 0$ and $\beta_1 = 1$) on a 99.9% level for both goods in all years and elasticities (Table 3.2). Interestingly, whereas this result is confirmed by higher Theil's inequality coefficients and lower Spearman rank correlation coefficients in the case of iron ore in all years, this is not the case with coking coal trade flows in 2008 (Figure 3.4).

However, considering prices and production in the perfect competition setting (PC) in addition to the trade flows, we conclude that the two market settings, in which players behave in a non-competitive manner, outperform the perfect competition setting. The model when run with all players acting as price takers cannot reproduce iron ore prices for most part of the elasticities that were investigated (Figure 3.5). In addition, total

[32] Trade flows for both commodities at all demand elasticities as well as actual trade flows in the respective years are available from the authors upon request.

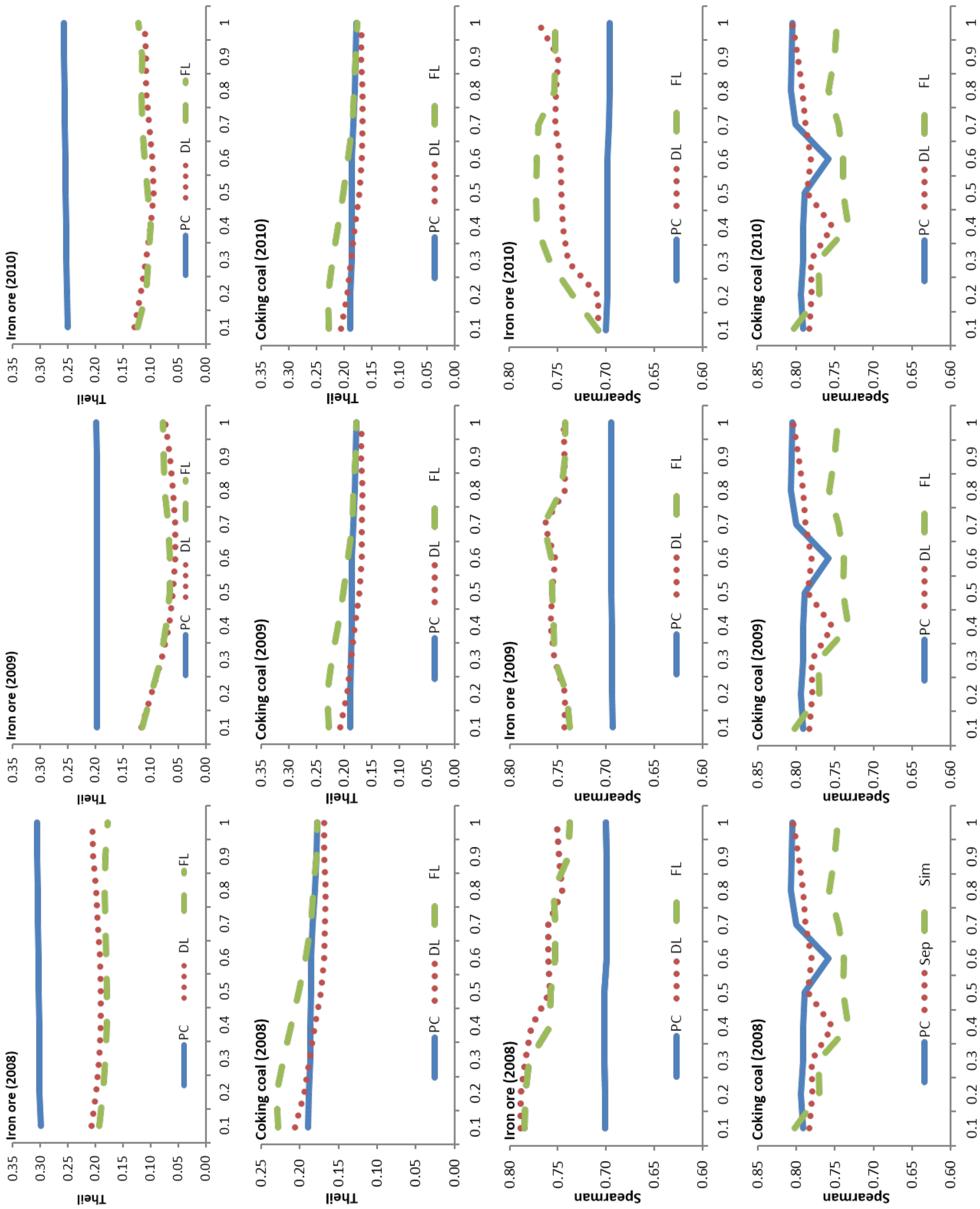

Figure 3.4: Theil's Inequality Coefficient and Spearman Rank Correlation Coefficient Contingent on the Demand Elasticity

production of both commodities is too high in this market setting and, more importantly, the model cannot capture production behavior of the largest company in each market (Figure 3.6), i.e., Vale in the case of iron ore and BHP Billiton in the case of coking coal: For almost each assumed demand elasticity, these producers produce up to full capacity.

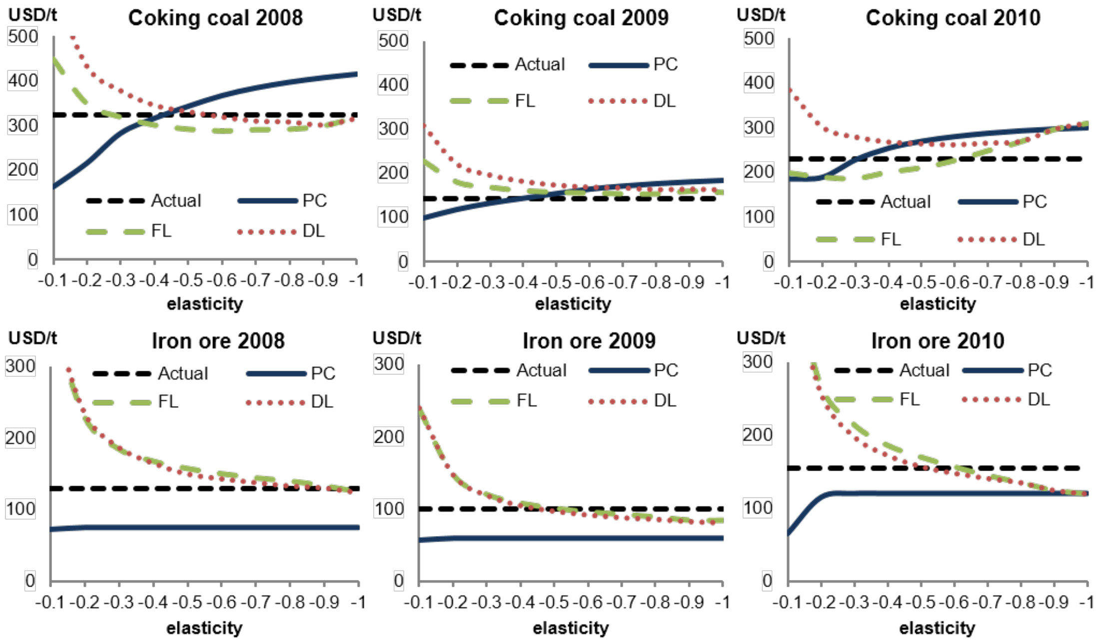

FIGURE 3.5: Coking Coal and Iron Ore Prices Contingent on the Demand Elasticity

Concerning the comparison of the FL and the DL setting, the picture is more ambiguous. Starting out by looking at the results of the hypothesis tests for iron ore trade flows, one may be drawn to the conclusion that both of the two Cournot settings are able to reproduce actual trade flows, as for a large part of the range of elasticities we investigated the hypothesis tests cannot reject the null hypothesis. Contrasting the findings of the linear hypothesis test with Theil's inequality coefficient and Spearman's *rho*, we see from Figure 3.4 that both non-competitive settings perform similarly well in the case of iron ore. For coking coal, the DL setting performs better than the FL setting as Theil's inequality coefficient is lower and Spearman's *rho* is higher than in the DL setting .

Concerning prices we observe that the FL setting generates lower coking coal prices and higher iron ore prices than the DL setting, although the simulated iron ore prices are very similar with the difference never exceeding 8%. Iron ore prices match the actual market outcome for the years 2009 and 2010 for an assumed demand elasticity of -0.5 to -0.6. In this range of elasticities for the year 2008, the simulation results overestimate the actual iron ore prices by US$20/t (DL) and US$27/t (FL). Concerning coking coal the DL setting fits the actual coking coal price of 2008 for an assumed demand elasticity of -0.5 to -0.6 whereas the FL setting underestimates the price by US$35/t. In contrast, for 2009, the FL setting is closer to the actual coking coal price than DL in the whole range of simulated elasticities. For a demand elasticity of -0.5 to -0.6 the differences to the actual values are US\$15/t and US\$30/t, respectively. For the year 2010 and a demand elasticity of -0.6, the FL setting seems more appropriate to represent the coking coal price.

Finally, we take another look at the company's production output depicted in Figure 3.6. Whereas the iron ore production is similar in both scenarios (see the example of Vale in Figure 3.6), the coking coal production volumes differ significantly in the case of BHP Billiton and the US coking coal player. The FL case overestimates the actual production volumes of BHP in the whole range of elasticities in all years. In the DL case the BHP production volume is matched at elasticities of -0.5 to -0.7 between 2008 and 2010. The US coking coal production in the FL case is always lower than in the DL case. For lower elasticities the DL case is closer to the actual production whereas the production volumes converge for higher elasticities in the years 2008 and 2010.

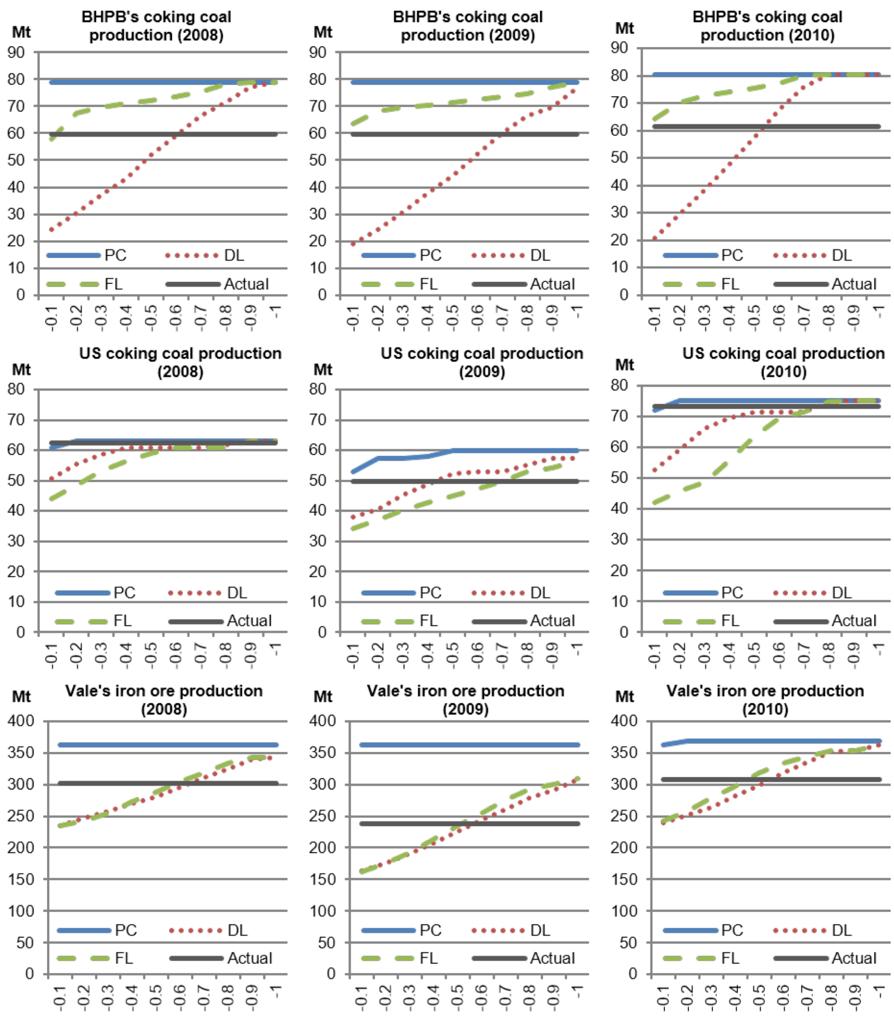

Figure 3.6: Production of Vale, BHP Billiton and US Coking Coal Producers Depending on the Demand Elasticity and the Market Setting

Summing up, we found no evidence supporting the idea that players in the two commodity markets behave in a perfectly competitive manner. Consequently, the two non-competitive market settings resulted in market outcomes that match actual outcomes better than in the perfect competition case. Regarding the comparison of the case of DL and FL optimization of the business units' profits, we did not find overwhelming evidence to dismiss one of the two settings. But, the results of the statistical tests and the comparison of production and price data draw a more consistent picture in the DL than in the FL setting, with the model performing best for elasticities of -0.5 and -0.6.

3.4.3 Strategic Implications

The comparison of actual market outcomes and model results provide an indication that the DL setting best represents the market outcome. However, since the analysis did not allow to unambiguously opt for one setting this subsection aims at delivering an economic argument why the three merged companies might indeed have chosen strategy DL over FL in reality.

If a firm decides to optimize both the coking coal and the iron ore division on a firm-level (i.e., choosing strategy FL), a sophisticated organizational structure is required such that the economic agents within the firm are incentivized to act in a way which in fact leads to a global optimum. Both divisions have specialized knowledge regarding their specific markets, they possess a high technical know how, they know their production costs and capacities and have an idea about their own market position compared to their competitors. However, to make both divisions act according to strategy FL, it is required that both divisions coordinate themselves to sell the optimal combination of coking coal and iron ore to a demand market. And even more challenging, the division managements have to be incentivized to act as such. Höffler and Sliwka (2012) discuss that symmetric incentives based on the units' performance provide incentives for haggling within the organization whereas symmetric incentives based on the overall profit would lead to free-rider behavior because of reduced individual responsibility for the overall performance. The authors state that these inefficiencies become stronger with increasing interdependencies between units. They find that asymmetric incentive structures which make one unit dominant in the organization could reduce these inefficiencies: The dominant unit should have unit based incentives whereas the other unit should have incentives based on the overall profit.

Although asymmetric incentive structures reduce organizational inefficiencies, simultaneous optimization of the divisions nevertheless incurs additional transactional and organizational costs. Coming back to the finding from Section 3.4.1 an integrated company will only choose FL over DL, if the additional profit from FL is sufficiently high to overcompensate the additional transactional and organizational costs incurred by strategy FL. As seen before, this is only the case if the production capacity of both goods is sufficiently high to benefit from FL by increasing the output. The lower the demand elasticity becomes, the less restrictive the capacity constraint. In the real world application, we have seen that BHP Billiton is the leading company in the coking coal market but faces a binding capacity constraint in the iron ore market the higher the assumed demand elasticity is. Therefore, the extra benefit of FL versus DL tends to zero for higher elasticities whereas it can become significant for lower demand elasticities. The simulation model, however, reproduced market results more consistently when simulating elasticities of -0.5 to -0.6 where the benefit of firm-level optimization was converging to zero.

3.5 Conclusions

In this paper, we have examined the strategic behavior of quantity-setting mining companies that are relevant players in the both the coking coal and the iron ore market. This setting is of particular interest in the analysis of energy and resource markets since (i) both goods are complementary inputs for steel production, (ii) both goods have little alternative use, (iii) both goods exhibit high supply-side concentration and (iv) some of the biggest producers are active on both markets. Given these characteristics, this paper investigated whether the integrated mining companies optimize their output on a firm-level or on a division-level.

We first assessed the profitability of firm-level optimization in a theoretical model of two homogeneous Cournot duopolies of complementary goods that interact with each other. We considered two cases: one with unlimited capacities and one with a binding capacity constraint on one of the divisions' output. Firm-level optimization is always profitable if capacities are unlimited. However, we proved three conjectures for the case in which one of the divisions faces a binding capacity constraint. There exists a critical capacity constraint (i) below which the parallel vertically integrated firm is indifferent between firm-level and division-level optimization, (ii) above which firm-level optimization is always beneficial and (iii) that becomes smaller with a lower demand elasticity.

Next, we investigated whether these findings also hold for a real-world application. The markets for coking coal and iron ore are more complex than the theoretical model as (i) there are more than two suppliers in each market, (ii) there are more than one firm that are parallel vertically integrated, (iii) production costs are heterogeneous,

(iv) both markets are spatial markets and (v) most of the producers face a binding capacity constraint. Therefore, we developed a numerical spatial multi-input equilibrium model of both markets based on a unique data set. Assessing the profitability of the integrated companies, the results from the theoretical model were confirmed in the simulation. The coking coal market leader BHP Billiton generates additional profits from firm-level optimization under low elasticities because, in this case, the iron ore capacity is not binding. With increasing demand elasticity, the benefits of simultaneous optimization tend to zero. Lastly, we compared the model results of one simulation assuming division-level optimization and one assuming firm-level optimization to the actual price, trade flow and production data for the years 2008 to 2010. Although no scenario is dominant, the scenario assuming division-level optimization fitted the actual market outcomes slightly better. Hence, the simulation did not reveal any evidence of firm-level optimization over the respective years.

Apart from the arguments made within this analysis, there may be other economic reasons for division-level optimization that were not the main focus of this paper and could be interesting for further research. For example, the firm-level optimization of two business units could create inefficiently high organizational costs. Furthermore, it may therefore be challenging to create incentives for both divisions to not optimize the division but rather to optimize on a firm-level. Since this analysis focused on a comparison of historic and model-based market outcomes, it may be insightful to further assess the strategic investment of companies in a prospective analysis. The decision whether to grow in one or the other complementary factor market, thereby altering the own strategic position or the one of the competitor, may be another interesting sequel to this paper.

Chapter 4

CO_2 Abatement Policies in the Power Sector under an Oligopolistic Gas Market

4.1 Introduction

The European Union and its member states have established a variety of policies to foster carbon dioxide (CO_2) abatement in the electricity sector. One EU-wide instrument is the European Union Emissions Trading System (EU-ETS), which defines an emissions quota and forces CO_2-intensive industries such as electricity generation, cement, paper or iron and steel production to buy allowances to emit CO_2. Besides the EU-ETS, there are various national CO_2 reduction policies in place such as numerous subsidy regimes for renewable (RES) power generation or a coal tax levied in the Netherlands. Emissions quota systems such as the EU-ETS are considered to be a cost efficient instrument to achieve a defined CO_2 abatement target (see, e.g., Böhringer and Rosendahl, 2011). Given a fixed CO_2 emissions quota, additional policies such as RES subsidies or taxes have no effect on CO_2 reduction but cause deviations from the cost-efficient CO_2 reduction. Hence, given constant fuel costs for different policies, it can be shown analytically that taxes or subsidies increase the costs of the power system.

However, there are good reasons to claim that fuel costs, at least for natural gas, are not constant but rather influenced by climate policy interventions: First, climate policies affect the gas demand of the power sector. The EU-ETS or a coal tax, for example, fosters fuel switching from coal to gas. RES subsidies, on the contrary, have a negative impact on power generation from natural gas. Second, natural gas supply in Europe is highly concentrated. In 2012, the European OECD member countries purchased roughly

70% of their total gas demand from Russia, Norway, Algeria or the Netherlands. In each of these countries, one state-owned gas company manages almost the entirety of gas sales. Given the high market concentration, changing gas demand functions through policy intervention can influence gas prices significantly. In this context, Newbery (2008) has shown analytically that the EU-ETS reduces the price elasticity for gas consumption in the electricity sector, strengthens the market power of gas suppliers and increases gas prices. Increasing gas prices imply higher power system costs.

The overall power system cost effect of combining other carbon reduction policies such as a coal tax or a fixed bonus for RES with the EU-ETS seems unclear: On the one hand, combining the EU-ETS with additional policies causes efficiency losses (e.g., tax distortions). On the other hand, policies and their effects on gas demand may cause a gas price reaction in the oligopolistic gas market. However, the direction of the change in gas price and therefore the overall effects on power system costs are ambiguous.

Thus, this paper aims at answering the question as to how carbon reduction policies in combination with the EU-ETS affect the power system costs and therefore the costs of CO_2 abatement, thereby accounting for gas market effects. This research focuses on two carbon reduction policies which I introduce in addition to the EU-ETS: A location- and technology-independent fixed bonus RES subsidy and a coal tax. The analysis is conducted following four hypotheses:

1. A coal tax increases gas prices, a fixed RES bonus decreases gas prices. (H1)
2. A coal tax increases power system costs compared to an EU-ETS-only regime. (H2)
3. A fixed RES bonus reduces power system costs compared to an EU-ETS-only regime. (H3)
4. Higher market power in the gas market amplifies the outlined effects. (H4)

In order to assess these hypotheses, a stylized theoretical model is used to analyze the interaction of gas and electricity markets given the respective policies and the EU-ETS. From this theoretical analysis, I identify three effects of a policy intervention on power system costs. First, applying the example of a RES subsidy, I find that the direct impact of a subsidy on the power generation depends on the fuel type. Gas generation decreases, whereas coal and RES generation increases. This *direct effect* of a subsidy on power system costs is always positive, i.e., in the first step system costs increase due to the subsidy. However, secondly, if the subsidy affects gas price and demand, the changing gas price leads to a different equilibrium on the power market. This effect is denoted as *indirect quantity effect*. Third, the subsidy changing the gas price affects the costs of each unit of gas purchased by the power sector. This effect is denoted as the *indirect price effect*. Both indirect effects of a subsidy can be positive or negative. If they are negative, the effects may overcompensate the direct cost effect. Thus, a climate policy such as a RES subsidy can, in theory, reduce power system costs.

To quantify these effects and to verify the hypotheses for a real-world example of the European power and gas markets, I develop a calibrated simulation tool which models the long-term interaction of both markets by combining a power market and a gas market simulation model. The approach that is commonly used to simulate electricity markets in partial analyses is large-scale linear dispatch and investment simulation models. In this analysis, the model DIMENSION is applied (see Richter, 2011). Partial analyses concerning market power on the natural gas market are often conducted using mixed complementarity problem (MCP) models, enabling the simulation of Cournot oligopolies. In this study, I apply the long-term global gas market model COLUMBUS (see Hecking and Panke, 2012 or Growitsch, Hecking, and Panke, 2014). Both models are integrated as follows: The power market model is used to derive a gas demand function, which is then applied in the gas market model. The resulting gas price is then fed back into the power market model.

The integrated simulation model is applied to three scenarios for the years 2015, 2020, 2030 and 2040. The scenarios include an EU-ETS only scenario as a reference, an EU-ETS plus coal tax scenario and third, an EU-ETS plus fixed RES bonus scenario.

Concerning H1, I find from the simulation that a coal tax has ambiguous effects on gas prices whereas for each fixed RES bonus scenario, the gas prices decrease. H2 holds, i.e. a coal tax increases power system costs. Furthermore, the results reveal that a fixed bonus RES subsidy can decrease overall costs of the power system (H3): In the simulated cases the indirect price effect overcompensates the increasing costs incurred by the sum of the direct and indirect quantity effect. The simulation also confirms H4, i.e., that higher gas market power amplifies the effects outlined above.

The policy implications of these findings should not suggest that CO_2 abatement becomes more efficient through a fixed RES bonus. The results should only reveal that the costs of the *European power system* decrease. Decreasing costs of the power system result from decreasing purchase costs for natural gas. Therefore, lower power system costs imply lower revenues for natural gas suppliers. Hence, one motive for introducing a fixed bonus RES subsidy could be to redistribute welfare from non-European gas suppliers to European power utilities or end users.

This research is based on literature on the economic effects of overlapping climate policies[33]. This strand of literature traces back to Tinbergen (1952), who argues that the number of policies should equal the number of policy objectives. In other words, if the sole objective was to reduce CO_2 emissions, only one policy should be used. Sijm (2005), for example, concludes that in the presence of a CO_2 emissions quota system, the CO_2-reduction effect of any other policy becomes zero. In this light, Böhringer et al. (2008) show that additional CO_2 emission taxes for sectors covered by the EU-ETS have no effect on CO_2 reduction but increase overall costs. Concerning RES-E subsidies, Böhringer and Rosendahl (2011) argue that, combined with the EU-ETS, these policies increase CO_2 abatement costs without affecting CO_2 reduction.

However, literature also provides economic justifications in favor of interacting policies (see, for example, Sorrell and Sijm, 2003)[34]: Additional policies may correct market failures with respect to technology innovation and market penetration, raise fiscal incomes, redistribute welfare, reduce other environmental externalities or reduce the import dependence on oil and gas imports. Lastly, some argue that additional policies could improve the static efficiency of the EU-ETS, i.e., correct market failures other than the negative externality of CO_2 emissions such as supply-side concentration. Bennear and Stavins (2007), for example, state that market power plus environmental externalities can create the need for multiple policies. Whereas Bennear and Stavins (2007) focus on market power and externalities in the same market, Newbery (2008) takes into account market power in the upstream market. According to Newbery (2008), the EU-ETS, internalizing CO_2 emissions in the power sector, fosters market power in the upstream fuel market (natural gas) thereby increasing CO_2 abatement costs.

In this light, this research contributes to the existing literature on overlapping climate policies in the electricity sector by assessing two policies in combination with the EU-ETS, thereby explicitly accounting for oligopolistic behavior in the gas market. It extends the current debate on overlapping regulations by showing that policy interventions do not only affect the regulated market but also have feedback effects on upstream markets and potential market power, as seen in the gas market. Furthermore, this research shows that the policies in focus are capable of redistributing welfare between market participants across different markets.

Additionally, this research contributes to the literature on modeling electricity and gas market interaction in three dimensions: First, the model developed in this paper combines the high level of detail of LP power market simulations with the oligopolistic behavior of the MCP gas market models. Second, the electricity sector's inverse gas

[33] For a detailed overview see Fischer et al. (2010) or del Río González (2007).

[34] However, it is important to stress that analyzing the effectiveness and efficiency of currently applied policies with respect to these justifications is beyond the scope of this paper.

demand functions are derived endogenously during the simulation. Third, the model enables the simulation of gas market power on power utilities.

The paper is structured as follows: In Section 4.2, I show the interactions between policies, the gas market and the power market and the resulting cost effects in a stylized theoretical analysis. Section 4.3 presents the methodology used in this paper, i.e., the combining a LP power market model with a MCP gas market model in a numerical analysis. The model parameterization and the scenario design are discussed in Section 4.4. Section 4.5 assesses the hypotheses of this paper by applying the integrated power and gas market model for a case study of 11 European countries. Section 4.6 concludes.

4.2 A Stylized Model of Carbon Reduction Policies Affecting Power System Costs

In this section, the interactions between carbon reduction policies, power generation by fuel type and power system costs are analyzed using a stylized model. In a first step, a fixed gas price (i.e., no interaction with the gas market) is assumed. In a second step, the reaction of the gas market to changing gas demand from the power sector is included. Thirdly, a graphical analysis of the interaction is presented. The modeled electricity market is equipped with three technologies: coal C, gas G and renewables R. Let x_C, x_G and x_R denote the amount of electricity supplied by each technology, respectively. K denotes the total power system costs. The power generation of each technology depends on the fixed bonus subsidy for renewables[35] s and the specific full costs of power generation g, c and r, i.e., long-run marginal costs.[36] Variables c and r are assumed to be constant, whereas the gas generation costs g are affected by changing gas prices. Subsidies for renewables affect gas demand and, therefore, gas prices. Thus, the gas-specific generation costs g depend on the subsidy s. This yields the following power system costs:

$$\begin{aligned} K(x_R(s,g(s)), x_C(s,g(s)), x_G(s,g(s)), g(s)) = \\ (r-s)x_R(s,g(s)) + sx_R(s,g(s)) + cx_C(s,g(s)) + g(s)x_G(s,g(s)). \end{aligned} \tag{4.1}$$

Electricity demand D is inelastic and equals the sum of the generated power of all three technologies,

$$D = x_R + x_C + x_G. \tag{4.2}$$

[35] In the following, the fixed bonus subsidy for renewables becomes the central focus of this analysis. The effects of a coal tax are similar.

[36] The full costs of power generation comprise capital costs, fixed operation and maintenance costs and fuel costs. The specific full costs represent the full-costs per unit, i.e., long-run marginal costs.

There is a cap E on CO_2 emissions. Total emissions depend on the specific CO_2 emissions per technology, e_C, e_G and e_R. The renewable emissions e_R are assumed to be zero, and $e_C > e_G$. Total emissions are given by:

$$E = e_C x_C + e_G x_G. \tag{4.3}$$

For a situation in which $c < g < r$ and $s = 0$. Let x_C^0, x_G^0 and x_R^0 denote the equilibrium power generation and DR the residual demand. Assume $x_C^0 > 0$ and $x_G^0 > 0$. Then,

$$DR = D - x_R^0 = x_C^0 + x_G^0. \tag{4.4}$$

4.2.1 Cost Effects Given Fixed Gas Prices

In the following, I derive the cost effects of a fixed bonus RES subsidy on power system costs, given that gas prices are not affected by the subsidy.

Proposition 1: Assuming a constant gas price and, hence, constant generation costs g, a subsidy s increases power system costs K.

Although this is implied already by the first welfare theorem, the following proof turns out to be instructive for the further discussions in this section.

Proof of Proposition 1:
Differentiating the power system costs K with respect to the subsidy s yields:

$$\begin{aligned}\frac{dK}{ds} &= \frac{\partial K}{\partial x_R}\frac{dx_R}{ds} + \frac{\partial K}{\partial x_C}\frac{dx_C}{ds} + \frac{\partial K}{\partial x_G}\frac{dx_G}{ds} \\ &= \frac{\partial K}{\partial x_R}\frac{\partial x_R}{\partial s} + \frac{\partial K}{\partial x_C}\frac{\partial x_C}{\partial s} + \frac{\partial K}{\partial x_G}\frac{\partial x_G}{\partial s} \\ &= r\frac{\partial x_R}{\partial s} + c\frac{\partial x_C}{\partial s} + g\frac{\partial x_G}{\partial s}.\end{aligned} \tag{4.5}$$

Next, two Lemmata are needed to proceed the proof of Proposition 1.

Lemma 1: Subsidy s increases coal-fired generation x_C, whereas it decreases gas-fired generation x_G, i.e., $\frac{\partial x_C}{\partial s} > 0$ and $\frac{\partial x_G}{\partial s} < 0$.

Proof of Lemma 1:
Equations 4.3 and 4.4 yield the equilibrium quantities x_C^0 and x_G^0, respectively, i.e., the equilibrium given the residual demand and emission constraint:

$$x_C^0 = \frac{E - e_G DR}{e_C - e_G} \tag{4.6}$$

$$x_G^0 = \frac{e_C DR - E}{e_C - e_G}. \tag{4.7}$$

Let subsidy s have a positive impact on renewable generation or, put differently, decrease residual demand DR, that is:

$$\frac{\partial DR}{\partial s} = -\frac{\partial x_R}{\partial s} < 0. \tag{4.8}$$

Thus, assuming a constant CO_2 cap E and using Equations 4.6, 4.7 and 4.8 yields:

$$\frac{\partial x_C}{\partial s} = \frac{\partial DR}{\partial s}\frac{-e_G}{e_C - e_G} > 0 \tag{4.9}$$

$$\frac{\partial x_G}{\partial s} = \frac{\partial DR}{\partial s}\frac{e_C}{e_C - e_G} < 0. \tag{4.10}$$

This **proves Lemma 1.**

Lemma 1 implies that increasing generation of renewables through a subsidy in combination with a CO_2 quota system increases coal-fired generation whereas gas-fired generation, i.e., the more expensive but less CO_2-intensive technology, decreases.

Hence, from Equations 4.5, 4.9 and 4.10, the total cost effect of a renewable subsidy can be derived to equal:

$$\frac{dK}{ds} = r\frac{\partial x_R}{\partial s} + c\frac{e_G}{e_C - e_G}\frac{\partial x_R}{\partial s} - g\frac{e_C}{e_C - e_G}\frac{\partial x_R}{\partial s} = \frac{\partial x_R}{\partial s}(r + \frac{ce_G - ge_C}{e_C - e_G}). \tag{4.11}$$

Since the generation of renewables x_R increases with the subsidy, a subsidy increases total power system costs if and only if the term in brackets becomes positive. Rearranging Equation 4.11 yields:

$$g < r(1 - \frac{e_G}{e_C}) + c\frac{e_G}{e_C}. \tag{4.12}$$

Lemma 2: $g < r(1 - \frac{e_G}{e_C}) + c\frac{e_G}{e_C}$ is equivalent to $x_G^0 > 0$.

Proof of Lemma 2:

Assume that Condition 4.12 does not hold, i.e.,

$$g = \hat{g} + h > r(1 - \frac{e_G}{e_C}) + c\frac{e_G}{e_C} = \hat{g} \quad , h > 0. \tag{4.13}$$

Thus, the power system costs K^0 in the equilibrium become:

$$K^0 = (\hat{g} + h)x_G^0 + rx_R^0 + cx_C^0 = r(1 - \frac{e_G}{e_C})x_G^0 + c\frac{e_G}{e_C}x_G^0 + rx_R^0 + cx_C^0 + hx_G^0. \quad (4.14)$$

Assume another situation with $x_G^1 = 0$ and system costs K^1. Zero gas-fired generation results allows for more available emission allowances compared to the situation in which $x_G^0 > 0$, thus:

$$x_C^1 = x_C^0 + \frac{e_G}{e_C}x_G^0. \quad (4.15)$$

Since power demand is assumed to be constant and $\frac{e_G}{e_C} < 1$, generation of renewables has to increase in order to compensate for the decreasing gas-fired generation:

$$x_R^1 = x_R^0 + (1 - \frac{e_G}{e_C})x_G^0. \quad (4.16)$$

Thus, the power system costs K^1 become:

$$K^1 = rx_R^0 + r(1 - \frac{e_G}{e_C})x_G^0 + cx_C^0 + c\frac{e_G}{e_C}x_G^0 < K^0, \text{ since } h > 0. \quad (4.17)$$

Hence, $x_G^0 > 0$ and $g > r(1 - \frac{e_G}{e_C}) + c\frac{e_G}{e_C}$ would not be a cost-efficient equilibrium. This **proves Lemma 2.**

From Lemmas 1 and 2 it follows that, given $x_C^0 > 0$, $x_G^0 > 0$, a binding CO_2 cap, $c < g < r$ and fixed gas price, i.e., fixed generation costs g , a positive subsidy for renewables s increases power system costs K. This **proves Proposition 1**.

The economic interpretation of Proposition 1 is that a subsidy for renewables has the same effect as the exchanging of one unit of gas-fired generation for a more expensive unit of a bundle of renewable generation and coal-fired generation, which is an equally CO_2-intensive option as gas-fired electricity generation.

4.2.2 Cost Effects Accounting for a Gas Market Reaction

The section before has shown that a RES subsidy increases power system costs, given that the gas price is constant. In the following section, the power system costs are derived given the assumption that the gas price is affected by the RES subsidy.

Proposition 2: Assuming that the subsidy s affects the gas demand function and therefore the equilibrium gas price and the gas generation costs g, the overall effect of a subsidy s on power system costs K is ambiguous.

Proof of Proposition 2:

Differentiating K with respect to s yields:

$$\begin{aligned} \frac{dK}{ds} &= \frac{\partial K}{\partial x_R}\left(\frac{\partial x_R}{\partial s} + \frac{\partial x_R}{\partial g}\frac{\partial g}{\partial s}\right) \\ &+ \frac{\partial K}{\partial x_C}\left(\frac{\partial x_C}{\partial s} + \frac{\partial x_C}{\partial g}\frac{\partial g}{\partial s}\right) \\ &+ \frac{\partial K}{\partial x_G}\left(\frac{\partial x_G}{\partial s} + \frac{\partial x_G}{\partial g}\frac{\partial g}{\partial s}\right) \\ &+ \frac{\partial K}{\partial g}\frac{\partial g}{\partial s}. \end{aligned} \tag{4.18}$$

Thus, the subsidy affects electricity generation of each fuel type directly. Since the subsidy also affects the gas price and therefore gas generation costs, a subsidy also affects the electricity generation indirectly via g. Rearranging Equation 4.18 yields:

$$\begin{aligned} \frac{dK}{ds} &= r\underbrace{\frac{\partial x_R}{\partial s}}_{(+)} + c\underbrace{\frac{\partial x_C}{\partial s}}_{(+)} + g\underbrace{\frac{\partial x_G}{\partial s}}_{(-)} && \text{(direct effect)} \\ &+ \left(r\underbrace{\frac{\partial x_R}{\partial g}}_{(+)} + c\underbrace{\frac{\partial x_C}{\partial g}}_{(+)} + g\underbrace{\frac{\partial x_G}{\partial g}}_{(-)}\right)\underbrace{\frac{\partial g}{\partial s}}_{(?)} && \text{(indirect quantity effect)} \\ &+ x_G\underbrace{\frac{\partial g}{\partial s}}_{(?)}. && \text{(indirect price effect)} \end{aligned} \tag{4.19}$$

The direct effects of a subsidy have been discussed in the previous section: Subsidy s decreases x_G but increases both x_C and x_R. The direct cost effect is positive (see Proposition 1). When taking into account the gas market reaction, a subsidy s can increase or decrease the gas price and therefore gas generation costs g.[37] Hence, the sign of $\frac{\partial g}{\partial s}$ is ambiguous. A subsidy has two indirect effects on total power system costs. First, the indirect price effect is quite intuitive: If the subsidy s increases/decreases the gas price, i.e., gas generation costs g, the costs of gas purchased by the power sector increase/decrease. Second, the indirect quantity effect is more complex, as explained by Lemma 3:

Lemma 3: The indirect quantity effect becomes negative if and only if $\frac{\partial g}{\partial s} < 0$, i.e., if and only if a subsidy decreases the gas price.

[37] Gas generation costs g comprise constant fix costs and fuel costs. Latter are proportional to the gas price depending on the gas plant's degree of efficiency. Therefore gas price changes are in a positive linear relation to changes of gas generation costs g.

Proof of Lemma 3:
It is sufficient to show that $\tau = r\frac{\partial x_R}{\partial g} + c\frac{\partial x_C}{\partial g} + g\frac{\partial x_G}{\partial g} > 0$.

Increasing gas generation costs g increase generation of renewables x_R.[38] Given a constant total power demand D, the effect on the residual demand DR is negative, i.e.,

$$\frac{\partial DR}{\partial g} = -\frac{\partial x_R}{\partial g} < 0. \tag{4.20}$$

Given a constant CO_2 cap E and applying the same proof as Lemmas 1 and 2 shows that $\tau > 0$. This **proves Lemma 3.**

Lemma 3 implies that decreasing gas generation costs g induce an exchange of one unit of a bundle of x_C and x_R for one unit of x_G, which is cheaper and equally CO_2 intensive. Vice versa, an increasing gas generation costs g imply an exchange of one unit of x_G for one unit of a bundle of x_C and x_R, which is more expensive and equally CO_2 intensive.

Summing up, a RES subsidy s that increases the gas price and therefore gas generation costs g has a positive cost effect since, besides the positive direct cost effect, both indirect effects are positive. However, if a RES subsidy s decreases the gas price and gas generation costs g, both indirect cost effects become negative such that they may overcompensate the direct cost effect. Hence, the overall effect of a subsidy s on power system costs K can become negative. This **proves Proposition 2**.

4.2.3 Graphical Analysis

In the following, the effects of the stylized model are discussed in a graphical analysis. Therefore, Figure 4.1 illustrates the effects discussed before: The figure contains 10 diagrams numbered by roman numerals. Diagrams I to III show the relation between subsidy s and quantities x_R, x_C and x_G, respectively. The blue lines illustrate the equilibrium (0), i.e., the reference case with $s = 0$. The variables x_C^0, x_G^0 and x_R^0 are the cost-efficient quantities. A subsidy would decrease x_G and increase x_R and x_C. Note that summing up $x_R(s)$, $x_C(s)$ and $x_G(s)$ horizontally would result in a vertical line, i.e., a subsidy would not affect power demand.

[38] This theoretical model focuses on the long-run marginal costs. Therefore, increasing gas price implies higher long-run marginal costs of gas-fired power plants. Thus, renewables become more competitive compared to gas-fired generation, and x_R increases.

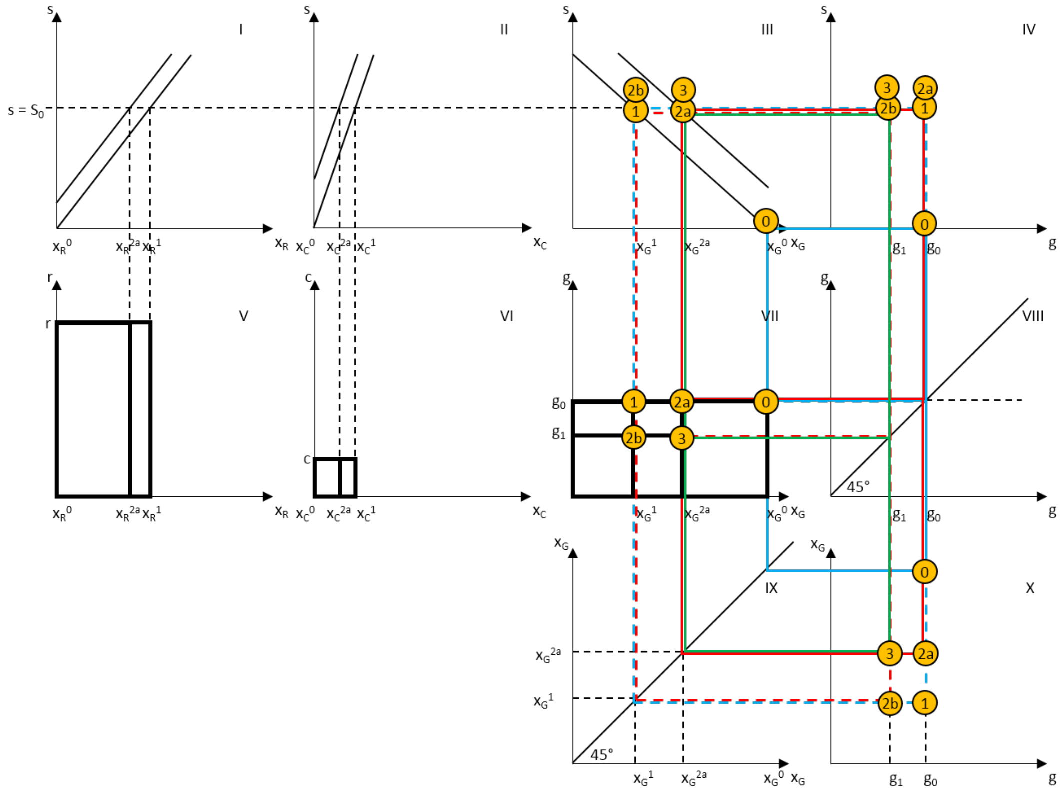

FIGURE 4.1: Effects of a Fixed Bonus RES Subsidy on the Power Market, the Gas Market and Power System Costs

Assume a subsidy $s = S_0$ leads to a new equilibrium (1) with x_C^1, x_G^1 and x_R^1, illustrated by the blue dashed lines. Assume further that in this case, there is no interaction between the gas and the power market, i.e., $\frac{\partial x_G}{\partial g} = 0$ and $\frac{\partial g}{\partial s} = 0$. The latter is illustrated as a vertical line in Diagram IV. Diagrams V to VII illustrate the cost effects of changing subsidies. Since r and c are constant, the cost increases from coal and renewables are depicted by the respective rectangles in Diagrams V and VI. Since $x_G^1 < x_G^0$ and g_0 is assumed to be constant, the costs incurred by gas consumption decrease. However, the overall cost effect (direct cost effect) is positive for the reasons discussed in Section 4.2.1.

Assume next a case (2a) in which the power market interacts with the gas market but gas prices are still constant, i.e., $\frac{\partial x_G}{\partial g} < 0$ and $\frac{\partial g}{\partial s} = 0$ (illustrated by the red solid lines). The gas market equilibrium is given by a price leading to generation costs of g_0 and a quantity x_G^{2a}. This situation can occur if, for example, the gas demand function of the power sector is inelastic or if the gas supply equals gas demand at that particular price. The relationship $x_G^{2a} > x_G^1$ and a constant g_0 results in an outwards shift of $x_G(s)$ in Diagram III. Accordingly, $x_R(s)$ and $x_C(s)$ shift inwards (since the sum of all three terms is constant). The new equilibrium quantities, x_G^{2a}, x_C^{2a} and x_R^{2a}, are located between the equilibrium quantities of case (1) and case (0). Therefore, the power system costs in case (2a) are lower than those in case (1) and higher than those in reference case (0).

This situation illustrates what was referred to as the indirect quantity effect in Equation 4.19.

Assume next a case (2b) in which the gas price and gas generation costs g are affected by the subsidy, i.e., $\frac{\partial g}{\partial s} < 0$ but $\frac{\partial x_G}{\partial g} = 0$ (red dashed lines). Therefore, $x_G^{2b} = x_G^1$. The equilibrium gas price in case (2b) implies different gas generation costs denoted as g_1. Diagram VII illustrates the indirect price effect of Equation 4.19. Total costs are reduced compared to case (1) since each unit of gas costs less.

Case (3), illustrated by the green lines, assumes $\frac{\partial g}{\partial s} < 0$ and $\frac{\partial x_G}{\partial g} < 0$. This is the case that will most likely occur during the simulations in the numerical analysis. A subsidy S_0 leads to a direct quantity effect, which strictly increases costs. Since the gas demand function changes due to the subsidy, the gas market equilibrium changes. If $\frac{\partial g}{\partial s} < 0$, i.e., the subsidy s decreases the gas price and generation costs decrease from g_0 to g_1, the gas consumption of the power sector increases further (assume to $x_G^3 = x_G^{2a}$). The indirect quantity effect therefore reduces the cost increase incurred by the direct effect. However, both effects in sum are still positive. But, if the subsidy causes a sufficient decrease in the gas price, the indirect price effect can lead to a reduction of power system costs as a result of the subsidy.

Figure 4.2 illustrates the cost effects once more, assuming that a RES subsidy decreases gas prices. R^0, C^0 (additional costs) and G^0 (cost savings) are depicted by blue lining and represent the direct effect. The terms R^1, C^1 (cost savings) and G^1 (additional costs) represent the indirect quantity effect (red lines) and G^2 (cost savings) represents the indirect price effect (green lines). As previously discussed, $R^0+C^0+G^0+R^1+C^1+G^1 > 0$, i.e., the direct and indirect quantity effects increase power system costs. However, a sufficiently large G^2 can lead to a subsidy for renewables decreasing overall power system costs.

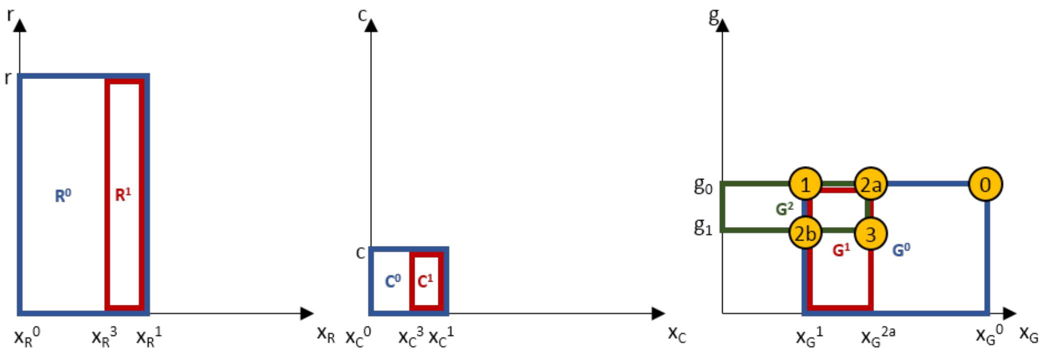

FIGURE 4.2: Cost Effects of a Fixed Bonus RES Subsidy

The magnitude of the effects discussed depend, among others, on the gas market reaction, i.e., how the subsidy affects gas demand and therefore the gas market equilibrium. If there is a high degree of supply-side market power in combination with a gas demand function that has become less elastic from the subsidy, the gas price may even increase as a result of the subsidy, i.e. $\frac{\partial g}{\partial s} > 0$. In that case, overall power system costs strictly increase.

This stylized model shows that the cost effects of subsidies (or similarly, of taxes) depend on the fuel switching characteristics of the respective electricity market. Therefore, I develop an integrated simulation model for both the power and the gas market in the next section.

4.3 Modeling the Interaction of Power and Gas Markets

This research aims at assessing the power system costs of climate policies combined with the EU-ETS, thereby accounting for the interactions between the electricity market and the oligopolistic gas market. Lienert and Lochner (2012) assess the importance of modeling the interdependencies between the power and gas market. In doing so, they develop a linear simulation model combining two LP models: a dispatch and investment power market model and a gas infrastructure model.[39] Abada (2012) develops a gas market MCP model that is able to simulate market power and to incorporate demand functions accounting for fuel substitution. Although this approach implicitly models fuel substitution in the power sector, the author does not explicitly model the electricity sector. In a recent paper by Huppmann and Egging (2014), the authors develop a MCP model that integrates different fuel markets (e.g., gas, coal, oil) as well as fuel transformation such as the electricity sector. Fuel suppliers exert market power against exogenous linear demand functions of energy end users such as the industry, residential or transport sectors. However, fuel producers do not exert market power on the electricity sector. A common modeling approach seen in the literature on climate policy is the use of computed general equilibrium models (CGE). This class of models seeks to derive a Walrasian equilibrium of different sectors of an economy, which are represented by demand and supply functions. Obviously, CGE could be one possible method of modeling the interactions between the gas and power market.

However, this research develops a different methodology by combining a linear European electricity market model with a MCP global gas market model accounting for strategic gas producers. Both aspects enable a highly detailed and therefore more realistic representation of the respective markets as discussed below and in Sections 4.3.1 and 4.3.2.

[39] See Lienert and Lochner (2012) for a detailed overview of this branch of literature.

The model developed in the following accounts for the interdependency of gas and electricity markets in an integrated framework and is suited to i) conduct long-term simulations of dispatch and investment decisions in the electricity market, ii) derive annual gas demand functions of the power sector and iii) simulate market power in the gas market.

Electricity markets are often modeled as linear cost minimization models (see Figure 4.3), an approach which implicitly assumes a perfectly competitive electricity market. LP electricity market models, such as the DIMENSION model (Richter, 2011) applied in this analysis (see Section 4.3.1), derive the cost-minimal amount of power plant dispatch and investment, from which additional information such as fuel demand or CO_2 emissions can be computed. Because of the high level of detail and to limit model complexity, many power market models are partial equilibrium model, i.e., the interactions with other markets are not modeled. Gas prices, for example, are exogenous inputs into the model. Gas demand from the power sector is a model outcome but does not have feedback effects on the gas market or gas prices.

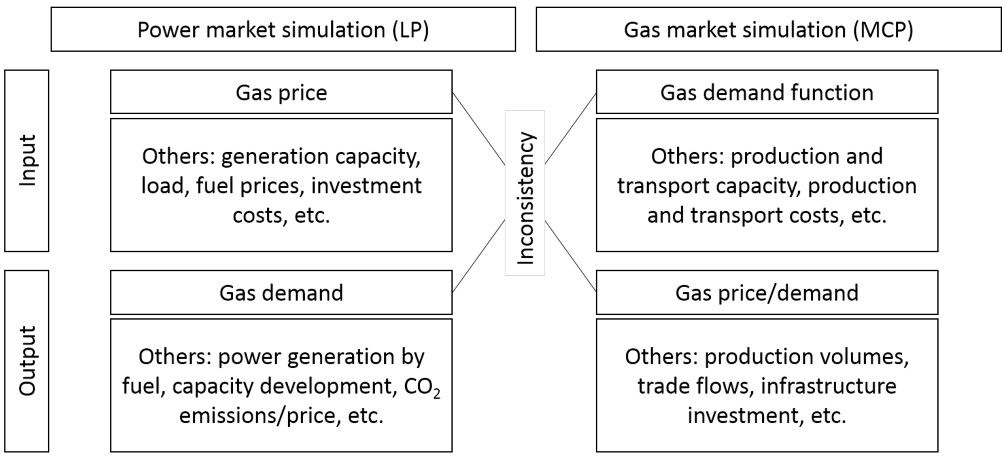

Figure 4.3: Inconsistencies of Partial Analytical Electricity and Gas Market Models

A common approach to model resource markets (and global gas markets in particular) are partial equilibrium models formulated as mixed complementarity problems (MCP).[40] MCP models, like the COLUMBUS gas market model applied in this analysis (see Section 4.3.2), allow for the simulation of strategic behavior of oligopolistic gas exporters. This requires the representation of the demand side such as, e.g., gas demand by the electricity sector using the inverse demand functions in an analytical form. The specification of the demand function is exogenous to the model. Often, demand functions are derived from historical or, for the future, from assumed price/demand combinations plus an assumption about the demand elasticity. The model outcome is a gas market equilibrium of production volumes, trade flows, demand and prices. However, since

[40] See, for example, Trüby and Paulus (2012) for steam coal, Trüby (2013) for coking coal, Hecking and Panke (2014) for the interaction of iron ore and coking coal or Gabriel et al. (2005) for natural gas.

the demand functions are exogenous to the model, the model does not account for any interaction with other markets such as the electricity market.

Consequently, with respect to the research question, both models used standalone would yield inconsistent results (see Figure 4.3). Therefore, I present a new approach to integrate both models. Since natural gas is an input factor for power production, or vice versa the power sector is an end consumer of natural gas, the core idea is to link both market simulations by the demand functions. The demand functions represent the end users' (i.e., the power generators') demand for natural gas. A four-step procedure links both market models consistently (see Figure 4.4):

1.) Create n random samples of gas prices and run the DIMENSION electricity market model for each sample. Each simulation yields annual gas demands.

2.) Use the derived price/demand samples to approximate annual inverse demand functions $p(x)$ in an analytical form. The resulting demand functions are therefore outputs of the power market model.

3.) Use the demand functions as inputs of the COLUMBUS gas market model to derive the oligopolistic gas market equilibrium.

4.) Use the gas market equilibrium prices as inputs of the DIMENSION model and derive the power market outcome.

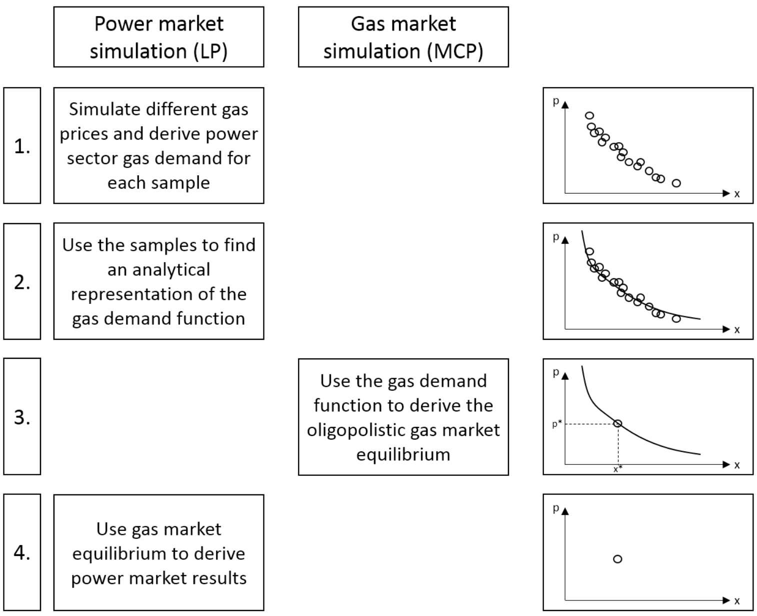

FIGURE 4.4: Integration of LP Power Market and MCP Gas Market Model

In the following, the simulation models DIMENSION and COLUMBUS as well as the model integration approach are explained in greater detail.

4.3.1 The Linear Electricity Market Model DIMENSION

The linear electricity market model DIMENSION[41], developed by the Institute of Energy Economics at the University of Cologne, is designed for long-term analyses of the European power system up to 2050. As such, DIMENSION and its predecessor DIME have been backtested and applied in numerous long-term power market studies both in research (see, e.g., Hagspiel et al., 2014) and policy advising (see, e.g., Fürsch et al., 2012).

The model minimizes power system costs by deriving the cost-optimal power plant dispatch and investment. The power system can be subdivided into different geographical units such as countries, which are connected by net transfer capacities. Assumptions on annual power demand are broken down to hourly load patterns of typical days differentiated by, e.g., weekend/weekday or summer/winter. The hourly load is assumed to be inelastic and has to be met by the supply side, i.e., by conventional power plants and renewables. The hourly feed-in of renewables with zero variable costs such as wind or solar PV is exogenous to the model and also derived from typical days. The dispatch of conventional power plants is endogenous to the model and depends on the variable costs, flexibility and capacity of the power plants. The initial capacity of the generating units is exogenous to the model, but the model endogenously optimizes investment in new power plants and renewables, depending on investment costs, future power plant utilization rates and a discount factor.

The DIMENSION model is a useful tool to simulate the effects of different power market policies in long-term analyses. The EU-ETS, for example, can be modeled by setting annual CO_2 boundaries. If such a boundary is binding, CO_2 allowances are scarce, which fosters power generation by more expensive but less CO_2-intensive power plants. A coal tax can be modeled by increasing the exogenously given coal price, and a fixed RES bonus can be modeled by reduced or negative variable costs of renewables. For each parameterization, the model yields the cost-optimal power plant dispatch and investment decisions, from which other information such as the annual gas demand can be derived.

4.3.2 The MCP Gas Market Model COLUMBUS

The MCP gas market model COLUMBUS[42] simulates the global gas market up to 2040. It has been backtested with historic market outcomes in Growitsch, Hecking, and Panke (2014). The model represents the spatial structure of worldwide supply, infrastructure

[41] For a detailed model description, see Richter (2011) or Jägemann et al. (2013).

[42] For a detailed model description, see Hecking and Panke (2012) or Growitsch, Hecking, and Panke (2014).

and demand by a node-edge topology. COLUMBUS derives a market equilibrium by optimizing the dispatch and investment decisions of several gas market actors such as exporters, traders or operators of LNG infrastructure or pipelines. Initial production and infrastructure capacities as well as cost parameters are inputs into the model. Actors can, however, also invest in production and infrastructure at certain investment costs. Concerning the demand side, the model distinguishes all important demand countries by sector (power, industry, residential), each represented by annual inverse demand functions. In the basic COLUMBUS version, demand functions are exogenously defined by historical or, for the future, by assumed price/demand combinations and assumed price elasticities.

COLUMBUS enables the simulation of Cournot behavior of gas exporters, i.e., the simulation of a spatial oligopoly. Modeling a Cournot oligopoly in a MCP requires an analytical representation of the price reaction towards changing output. The functions are common knowledge to all modeled Cournot players. In order to integrate the DIMENSION power market model with COLUMBUS, the annual inverse demand functions of the power sector are derived by DIMENSION and used in COLUMBUS. The details of this approach are presented in the next section.

4.3.3 Integrating Power and Gas Market Simulations

Since this study aims at assessing policies with respect to their long-term effects on power system costs up to 2040, the integrated simulation of electricity and gas market is conducted for the sample years 2015, 2020, 2030 and 2040.[43] Both DIMENSION and COLUMBUS are inter-temporal models that simulate the investment in power plants and gas assets, respectively. In particular, there is an important inter-temporal dependency between gas prices and power sector gas demand, illustrated in Figure 4.5: The gas prices p_i have a direct impact on the dispatch X_i, i.e., the gas consumption of gas-fired power plants. Additionally, the investment I_i in new gas-fired capacity depends not only on the future gas prices $p_{i',(i\leq i')}$ but also on the future utilization of gas-fired plants $X_{i,(i\leq i')}$. In turn, the utilization X_i depends on the past investments $I_{i',(i\geq i')}$.

[43] In order to avoid end effects, the simulation is continued until the year 2070. However, only the model results up to 2040 are important for this analysis.

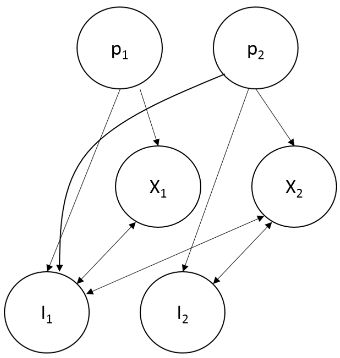

FIGURE 4.5: Inter-temporal Dependency of Gas Prices and Gas Demand in the Power Sector

To limit complexity but to nonetheless cope with the inter-temporal dependency, the model implicitly assumes full gas price certainty in the power market. In other words, gas exporters play a one-shot Cournot game setting all quantities for future exports up to 2040. Power generators regard the resulting equilibrium gas prices as certain. This can be interpreted as a long-term gas contract or a forward purchase of gas. Besides certainty on gas prices, all players in the gas and the power market have perfect foresight on the future of both markets. In order to simulate the Cournot oligopoly in the gas market, the COLUMBUS model requires an inverse demand function that accounts for the hidden inter-temporal relation of gas prices and demand for discrete time steps:

$$f : \mathbb{R}^4 \rightarrow \mathbb{R}^4$$
$$\begin{pmatrix} p_{2015} \\ p_{2020} \\ p_{2030} \\ p_{2040} \end{pmatrix} = f \begin{pmatrix} X_{2015} \\ X_{2020} \\ X_{2030} \\ X_{2040} \end{pmatrix}. \tag{4.21}$$

4.3.3.1 Power Market Simulations of Gas Price Samples

Due to the complex interactions between gas prices, investments in gas-fired power plants and gas demand, it is virtually impossible to trace the relation between prices and demand over time in an analytical functional form. Therefore, we simulate n gas price samples $(p_1, p_2, p_3, p_4)_{\{i,i\in 1\ldots n\}}$ derived from a uniform distribution of prices between 15 and 50 $\text{EUR}_{2010}/\text{MWh}_{\text{th}}$. For each sample of gas prices, we run the DIMENSION model and derive a vector of annual amounts of gas consumption by the power sector $(X_1, X_2, X_3, X_4)_{\{i,i\in 1\ldots n\}}$. The resulting point cloud represents the hidden relation of gas prices and demands for the years 2015, 2020, 2030 and 2040, indexed by 1, 2, 3 and 4, respectively. In particular, it contains information on how the gas price in one year reacts to the changing output of a Cournot gas exporter in the same or a different year. The simulation of a gas market Cournot oligopoly requires the approximation of the point cloud by an analytical representation.

4.3.3.2 Deriving an Inverse Gas Demand Function

The COLUMBUS model requires a continuous and differentiable inverse demand function, as in Equation 4.21. The function consists of different additive components f_{ij}, representing the partial price effect of changing demand X_j on price p_i:

$$\begin{pmatrix} p_1 \\ p_2 \\ p_3 \\ p_4 \end{pmatrix} = f \begin{pmatrix} f_{11}(X_1) + f_{12}(X_2) + f_{13}(X_3) + f_{14}(X_4) \\ f_{21}(X_1) + f_{22}(X_2) + f_{23}(X_3) + f_{24}(X_4) \\ f_{31}(X_1) + f_{32}(X_2) + f_{33}(X_3) + f_{34}(X_4) \\ f_{41}(X_1) + f_{42}(X_2) + f_{43}(X_3) + f_{44}(X_4) \end{pmatrix}. \tag{4.22}$$

It is crucial to the consistency of model results that the inverse demand function has a high fit with the point cloud. Therefore, the point cloud is approximated by a function using a least-squares approach. A variety of test runs indicate that most of the variation in price p_j can be explained by the X_j of the same year j. This is economically intuitive since the power plant dispatch is strongly related to the fuel prices of the same time period. A low demand X_j therefore implies a high p_j. Unfortunately, a linear function does not properly represent the point cloud in most of the simulations. Among a variety of functional forms, the inverse tangens hyperbolicus, also used by Abada (2012) performs best in modeling the component f_{jj}. Furthermore, part of the price variation is also related to gas demands of other years: The demand $X_{j',(j \neq j')}$, representing the inter-temporal relation, also affects p_j because of power plant investment. I choose a linear function for each component $f_{jj',(j \neq j')}$.

This yields the following inverse demand function:[44]

$$\begin{pmatrix} p_1 \\ p_2 \\ p_3 \\ p_4 \end{pmatrix} = \begin{pmatrix} f_{11}(X_1) & + & \beta_{12}X_2 & + & \beta_{13}X_3 & + & \beta_{14}X_4 \\ \beta_{21}X_1 & + & f_{22}(X_2) & + & \beta_{23}X_3 & + & \beta_{24}X_4 \\ \beta_{31}X_1 & + & \beta_{32}X_2 & + & f_{33}(X_3) & + & \beta_{34}X_4 \\ \beta_{41}X_1 & + & \beta_{42}X_2 & + & \beta_{43}X_3 & + & f_{44}(X_4) \end{pmatrix} \tag{4.23}$$

[44] Due to non-linearities, it is beyond the scope of this paper to focus on the mathematical details of the function. During the simulation, the derived function leads to consistent results for the gas and power market and has a good solvability using the PATH-solver in GAMS. Therefore the method of modeling the inter-temporal relations of gas prices and gas demand is used in this paper. Also, the inter-temporal approach is presented here since this topic has been hardly addressed in the literature thus far.

with

$$f_{ii}(X_i) = \alpha_i + \frac{1}{\gamma_i}\text{ath}(\frac{\delta_i - X_i}{\delta_i}) \tag{4.24}$$

and $\alpha_i, \beta_{ij}, \gamma_i, \delta_i$ as parameters. The parameter values are optimized in a non-linear problem with the objective of deriving the demand function that best fits the point cloud of samples. Therefore, the sum of squared deviations between modeled and sampled prices is minimized.

4.3.3.3 Implementing the Inverse Gas Demand Function in COLUMBUS

The inverse demand function is used to model a Cournot oligopoly in COLUMBUS. We assume that there are $k_{k \in K}$ oligopolistic gas exporters supplying a total of X_i in period i. The term x_i^k is the output of each player k and $C_i^k(x_i^k)$ is the respective cost function. Each player maximizes the following profit function for $i_{i \in 1...4}$ time periods:

$$\max_{x_i^k} \Pi_k = \sum_{i=1}^{4} p_i x_i^k - C_i^k(x_i^k), \text{ with } p_i = p_i(X_1, \ldots, X_4) \text{ and } X_i = \sum_{k \in K} x_i^k. \tag{4.25}$$

Taking the first derivative with respect to x_i^k yields the following first-order condition (FOC), with $\lambda_i^k(x_i^k)$ being marginal supply costs, i.e., the player-specific costs of transport, production and infrastructure scarcity rents:

$$\frac{\partial \Pi_k}{\partial x_i^k} = p_i + \sum_{j \in 1...4} \frac{\partial p_j}{\partial x_i^k} x_i^k - \lambda_i^k(x_i^k). \tag{4.26}$$

Thus, the FOC takes into account the changing output x_i^k affecting the prices p_j of all time periods. For the specific inverse demand function used in this simulation (Equation 4.23), the following Karush-Kuhn-Tucker condition is implemented in the model:

$$-p_i - \frac{x_i^k}{\left(\frac{\delta_i - X_i}{\delta_i}\right)^2}\left(-\frac{1}{\gamma_i \delta_i}\right) - \sum_{i \neq j} \beta_{ji} x_i^k + \lambda_i^k(x_i^k) \geq 0 \quad \perp \quad x_i^k \geq 0. \tag{4.27}$$

Besides including the output decision of each player in COLUMBUS, it is necessary to include the inverse demand function. Two equations are required. The first one balances the firm-individual output x_i^k and the total output X_i. The total output can also be interpreted as total demand since in COLUMBUS total annual demand and supply have to be equal. Therefore, the dual variable is the price p_i,

$$\sum_i x_i^k = X_i \quad \perp \quad p_i \text{ free} . \tag{4.28}$$

The second equation balances the price variable p_i and the price function depending on $X_j, (j \in 1 \ldots 4)$. The dual variable is X_i,

$$p_i = \alpha_i + \frac{1}{\gamma_i}\text{ath}(\frac{\delta_i - X_i}{\delta_i}) + \sum_{j,j\neq i} \beta_{ij} X_j \quad \perp \quad X_i \text{ free} . \tag{4.29}$$

4.3.3.4 Deriving the Consistent Market Outcome

Running the COLUMBUS model using the inverse demand function derived from DIMENSION yields equilibrium gas prices $(p_1, p_2, p_3, p_4)^*$ and equilibrium gas demand $(X_1, X_2, X_3, X_4)^*$. The equilibrium gas prices are henceforth used as input fuel prices for the DIMENSION model. Running DIMENSION yields the total power sector gas demand $(\hat{X}_1, \hat{X}_2, \hat{X}_3, \hat{X}_4)$. The higher the fit between the gas demand from the COLUMBUS and the DIMENSION models, the more consistent the model results with respect to the interaction of gas and power markets will be. If the fit is insufficient, the procedure described can be rerun with a higher level of detail, i.e., by simulating more samples (step 1) in a smaller price range around the equilibrium gas prices. If the fit is sufficient, the DIMENSION market outcome can be assumed to be consistent to the COLUMBUS outcome and model results such as the power system costs can be interpreted.[45]

4.4 Assumptions and Scenarios

4.4.1 Assumptions on the Numerical Analysis

The numerical analysis is conducted with a special focus on 11 European countries[46] for the time range between 2013 and 2040. Whereas the COLUMBUS model, which accounts for the entire global gas market, is only run once per scenario, the electricity market model DIMENSION has to be run once for each gas price sample, i.e., 1000

[45] Appendix C.1 provides an assessment of the convergence of the COLUMBUS and the DIMENSION models and shows how the outlined mechanism, i.e., simulating more samples in a smaller price range, improves the convergence of both models.

[46] These countries include Austria, Belgium, Czech Republic, Denmark, France, Germany, Great Britain, Italy, Poland, the Netherlands and Switzerland. The choice of these 11 countries was made because of their importance concerning European CO_2 emissions, their location in the center of Europe and their high gas market integration.

times per scenario.[47] In order to reduce the complexity of DIMENSION and decrease computation time, the number of simulated countries is hence limited to 11. In total, these countries make up for 75 % of current CO_2 emissions of the European power sector and half of the current EU-ETS allowances. Since this study focuses on the power sector, other EU-ETS sectors such as cement production are not included in the modeling. Thus, this approach implicitly assumes the same marginal costs for the proportional CO_2 reduction of other EU-ETS sectors. Although this is clearly a strong assumption, it does not qualitatively change the main messages of this analysis.

In this analysis, the DIMENSION model assumes an emissions quota of roughly 200 million CO_2 allowances for the power sector of the 11 countries in 2050, which equals a 80% CO_2 reduction compared to 2012. The number of allowances is reduced proportionately over time between 2012 and 2050. The analysis assumes implicitly that emissions certificates can be traded among those 11 countries. The quota must be achieved for each year, i.e., the possibility of "banking and borrowing" is excluded. In the basic configuration of this research, any other climate policy such as national RES subsidies or RES targets are, in contrast to the current regulation, not included in the simulation. Concerning the power plant and renewables data, this analysis uses the large-scale database of the Institute of Energy Economics at the University of Cologne, which contains information on ca. 4700 power plants – almost the entire European generation capacity including renewables. The database includes a variety of power plant parameters such as age, lifetime, efficiency, ramp-up times and current investment and operational costs. Concerning future investment costs, the assumption is made that the investment costs for mature technologies are constant, whereas costs decrease for new technologies such as certain renewables. Future investment costs are mainly based on IEA (2013b).

Concerning fuel prices, this analysis is consistent with to the assumptions made in Fürsch et al. (2012), with the exception of gas prices which are modeled endogenously. In contrast, coal prices are exogenous to the model for three reasons: First, there is currently no dominant player active on the global thermal coal market. Thus, a polypolistic coal market can be assumed (see, e.g., Trüby and Paulus, 2012 or Haftendorn and Holz, 2010). Second, whereas for many natural gas exporters the only sales opportunity is Europe via pipeline, coal trade via ship or train is much more flexible concerning the demand side. Third, due to the huge mining capacities in China (in particular), the global coal supply curve is rather flat. If European coal imports were to decline, traditional coal exporters such as Colombia or Russia could easily shift their exports to China or India, where they would crowd out domestic production. Although European coal prices

[47]The number of samples is set to 1000 in this analysis, with results achieving consistent results of gas and power market models.

would decrease after a demand drop, the price effect would be negligible compared to natural gas.

The gas market model COLUMBUS accounts for all major production and demand regions worldwide. The above-mentioned 11 countries are regarded as one demand region. Therefore, an implicit assumption is made that there is a full gas market integration among these countries, which is reasonable considering the well-built transport infrastructure, in particular, of the Northwest European gas market. The annual exogenous demand of these 11 countries, which is composed of the sectoral demand for power, heat and industry, is corrected for the power demand. The power demand is modeled by the demand functions derived through DIMENSION. The heat and industry gas demand functions are assumed to be exogenous. These assumptions as well as the future demand for other countries worldwide follow the IEA (2013b) and IEA (2013a). Parameters on existing infrastructure and production capacities are identical to those of Growitsch, Hecking, and Panke (2014), in which the authors provide a calibration of the model based on historic data. Future production and infrastructure capacities are derived endogenously in the model. However, to account for political or geographical limitations or the resource endowment of supply countries, potential investment in production and infrastructure assets are limited, in line with the future projections of IEA (2013b). Two assumptions are of particular importance for the degree of competition in Europe: First, potential LNG exports from the USA and Canada amount to 60 bcm for 2020 and 200 bcm for 2040.[48] Second, gas trade from Iran and Iraq via Turkey to Europe is excluded.[49] More detailed information concerning model parameters of the DIMENSION and COLUMBUS models are provided in Appendix C.3.

4.4.2 Scenario Setting

To investigate the hypotheses H1 to H3, this study assesses three scenarios of different climate policy regimes in the European power sector. In the scenario "Reference", the only active carbon abatement policy is the EU-ETS. In particular and in contrast to the current real-world regulation, there are no additional RES subsidies such as national feed-in-tariffs in place. The scenario "Coal Tax (CT)" assumes the presence of a coal tax in addition to the EU-ETS. The coal tax is raised for each thermal megawatt-hour of hard

[48]The parameter "potential LNG exports" is an upper boundary on the capacity of LNG export terminals. Hence, this parameter does not necessarily match the exports derived by the model since the model could regard investment or LNG exports to be uneconomical. Furthermore, LNG exports from North America would not necessarily affect the European gas market, since they could also be attracted by Asian importers.

[49]Even though Iran and Iraq are endowed with substantial natural gas resources, future gas sales to Europe are highly uncertain due to the current political situation and the need for transport infrastructure.

coal burned to generate power. The tax is identical for each of the countries considered. A tax of 10 EUR_{2010}/MWh_{th} and a tax of 20 EUR_{2010}/MWh_{th} are simulated. The scenario "Fixed RES Bonus (FB)" assumes a fixed bonus subsidy that is paid to the operator of a renewable power plant for each megawatt-hour of electricity generated. The fixed bonus is independent of technology and location. Fixed bonus subsidies of 5, 10, 20 and 30 EUR_{2010}/MWh_{el} are simulated.

In order to examine hypothesis H4, each of the three scenarios is derived in an additional variant that assumes a different market structure of the gas market: In a fictitious case, I assume a cartel of Norway and Russia. Even though this assumption is not necessarily realistic from a gas market point of view, the sole purpose of this setting is to assess the effects of a higher degree of market power.

4.5 Results of the Numerical Analysis

The simulation results are discussed in four parts: First, I focus on the effects of climate policies on the power market gas demand functions and the resulting equilibrium gas prices. Secondly, the policy effects on power generation by fuel type are discussed. Thirdly, I compare the overall power system costs of the different scenarios with a special focus on the cost effects as discussed in Section 4.2.3. Fourth, I analyze the effects of changing gas market power on the power system costs.

4.5.1 Gas Demand Functions and Equilibrium Gas Prices

Figure 4.6 shows the effects of renewable subsidies on gas demand functions for the years 2015, 2020, 2030 and 2040. "REF" labels reference scenario and "FB10" and "FB20" label a fixed bonus payment of 10 EUR_{2010}/MWh_{el} and 20 EUR_{2010}/MWh_{el}, respectively. The point clouds illustrate gas price/demand combinations simulated by the power market model DIMENSION. The black lines show the approximated demand functions.[50] The yellow square shows the equilibrium gas price/demand combination for the respective year and scenario resulting from the gas market simulation by the COLUMBUS model.

[50] Since the demand function for each scenario is four-dimensional, the dimensionality has to be reduced in order to show it graphically. For the year 2015, for example, the function drawn shows the relation between the gas price and the quantity of the year 2015. In this figure, the other quantities for the years 2020, 2030 and 2040 are set to the resulting gas market equilibrium quantities.

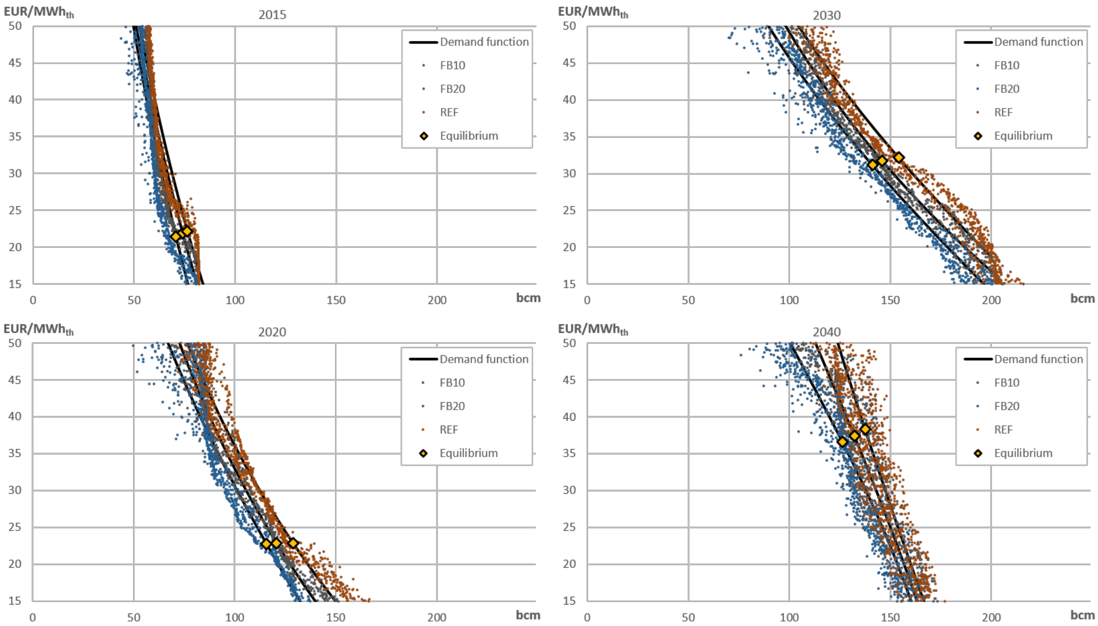

Figure 4.6: Gas Price/Demand Samples, Demand Curves and Gas Market Equilibria for the Fixed RES Bonus Scenarios

The figure shows a similar effect for all four years. Increasing the renewable subsidy shifts the gas demand function inwards. In other words, increasing competition by cheaper renewables decreases the willingness-to-pay for natural gas of the power sector. The shift in the demand curve changes the resulting gas market equilibrium. An increasing fixed bonus for renewables increases the equilibrium gas demand and decreases gas prices. This effect is unambiguous for all subsidy scenarios and all years although the price decrease is very weak for the year 2020.

Figure 4.7 is identical to figure 4.6 but illustrates the effects of a coal tax on the gas demand functions and the resulting gas market equilibria. "CT10" and "CT20" label coal tax scenarios of 10 EUR_{2010}/MWh_{th} and 20 EUR_{2010}/MWh_{th}, respectively. In particular for the years 2015 and 2020, fuel competition between coal and natural gas becomes more intensive because of the coal tax. For this reason, in CT10 and CT20, the power sector becomes very sensitive with regard to natural gas prices. Even though gas demand in equilibrium increases substantially, the gas price decreases. This can be explained by lower oligopoly markups of gas producers because of the less steep and more price elastic demand function induced by the coal tax. For the years 2030 and 2040 the elasticity is not affected as much. Thus, the gas market equilibria show that gas consumption and gas prices increase with the coal tax.

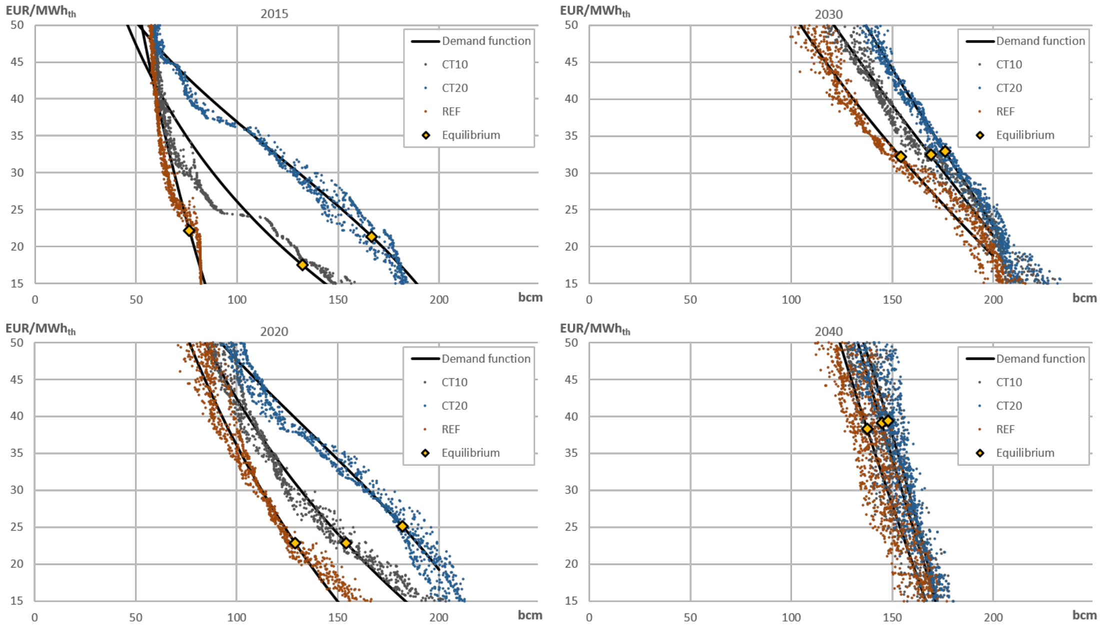

FIGURE 4.7: Gas Price/Demand Samples, Demand Curves and Gas Market Equilibria for the Coal Tax Scenarios

With regard to hypothesis H1, the results confirm the intuition that renewable subsidies cause a decrease in gas prices. Concerning the coal tax the picture is more diffuse. Although in 2030 and 2040 a coal tax causes an increase in gas prices, the example of the year 2015 has provided a valuable exception: If a policy significantly changes the gas demand elasticity, the resulting price effect can contradict to H1 because of the oligopolistic gas market structure.

4.5.2 Effects of Climate Policies on Power Generation

Figure 4.8 depicts the effects on power generation by fuel type when a fixed bonus of 20 EUR_{2010}/MWh_{el} for renewables is introduced. As shown in Section 4.2, such a subsidy has both a direct effect (labeled "Dir.") and an indirect effect (labeled "Ind.") on power generation. The direct effect is derived by comparing the power generation of the Reference scenario $x_{REF}(g_{REF})$ with the power generation of the fixed RES Bonus scenario (FB), but applying the equilibrium gas prices of the Reference scenario $(x_{FB20}(g_{REF}))$. Thus,

$$x_{dir} = x_{FB20}(g_{REF}) - x_{REF}(g_{REF}). \tag{4.30}$$

The indirect effect, which is induced by a changing gas market price, is derived by comparing $x_{FB20}(g_{REF})$ to $x_{FB20}(g_{FB20})$. Thus,

$$x_{ind} = x_{FB20}(g_{FB20}) - x_{FB20}(g_{REF}). \tag{4.31}$$

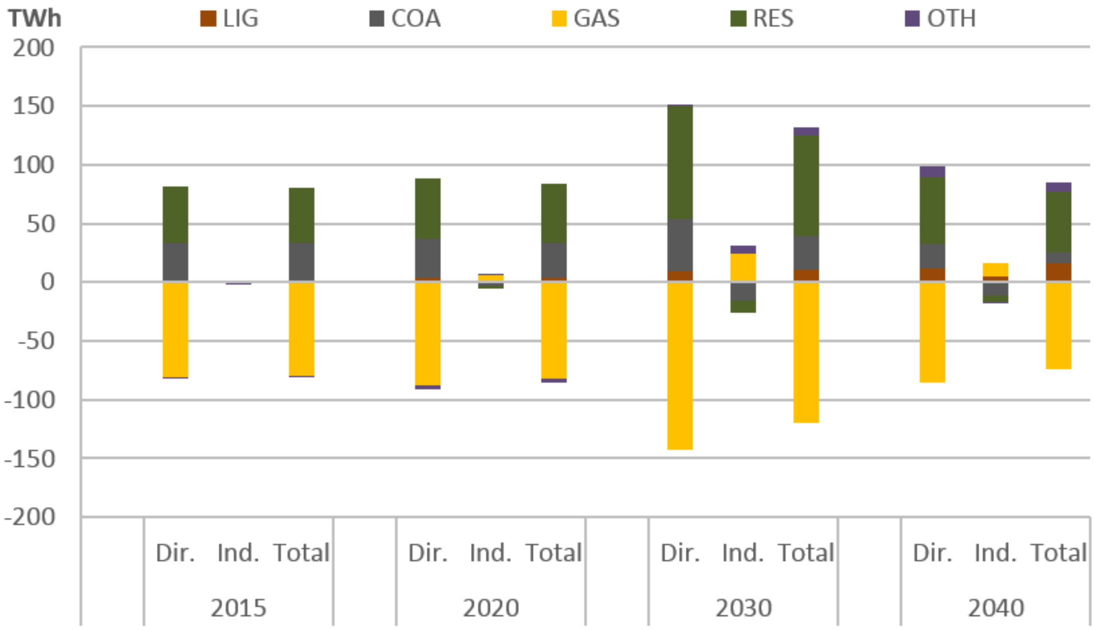

FIGURE 4.8: Effects of a Fixed RES Bonus on Power Generation by Fuel Type

As expected from the stylized model described in Section 4.2, the direct effect of a subsidy under the EU-ETS is an increasing generation of renewables and cheap, but CO_2-intensive, coal and lignite. Gas-fired generation decreases. As discussed in Section 4.5.1, gas prices in equilibrium decrease when a subsidy is introduced. Therefore, the indirect effect of a subsidy via the gas price is an increasing gas-fired generation, whereas generation from renewables, coal and lignite decreases. However, the overall effect is a decreasing gas-fired generation.

Figure 4.9 illustrates the effects of a 10 EUR_{2010}/MWh_{th} coal tax on power generation. The direct effect of a coal tax is a fuel switch from coal to gas. It can be observed that renewable generation also decreases, for example in 2020. Since coal-fired generation is replaced by gas, the CO_2 emissions price decreases, which causes gas to replace renewable generation. The indirect quantity effect is in line with the observations of Section 4.5.1. In 2015, the decreasing gas price leads to another increase in gas-fired generation. From 2020 onwards, the indirect effect is very weak because of the low price effect (2020, 2030) and the low demand elasticity (2040).

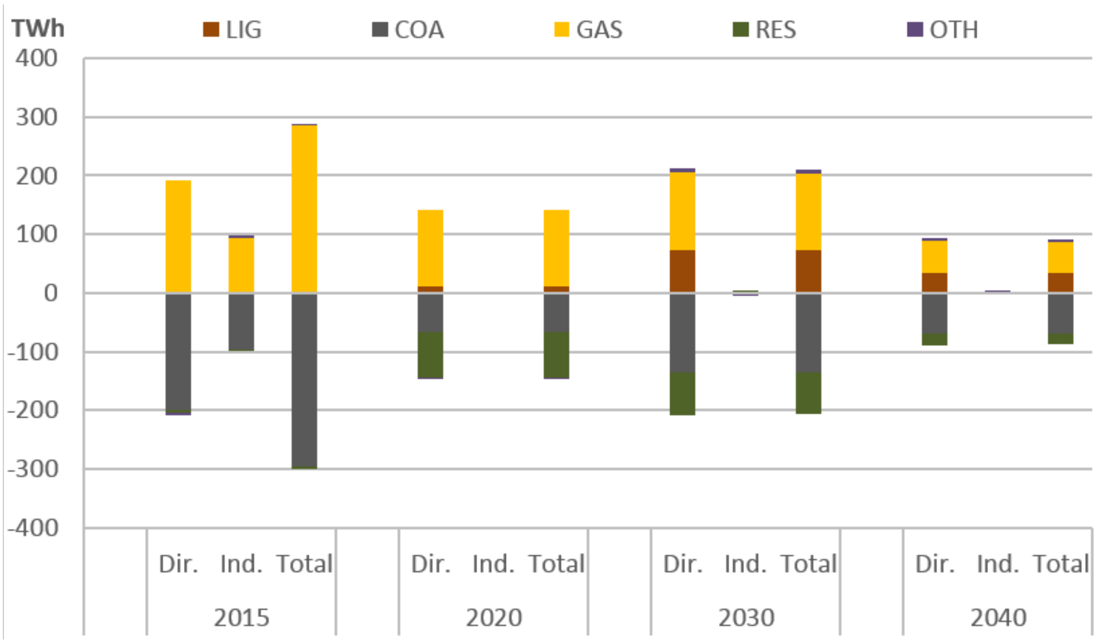

FIGURE 4.9: Effects of a Coal Tax on Power Generation by Fuel Type

4.5.3 Power System Cost Effects of Climate Policies

The power system costs are defined as the relevant costs for dispatch and investment decisions, i.e., fuel costs, fixed operation and maintenance costs and investment costs for new power plants. Subsidy expenses are added to the costs, and tax revenues are subtracted. In this analysis, the costs are summed up for the time range between 2013 and 2040 at a discount rate of 10%.[51]

Figure 4.10 illustrates the cost effects of the fixed bonus RES subsidy and coal tax scenarios. As shown in Section 4.2, the cost difference between the two scenarios can be subdivided into a direct quantity effect (C_{dir}), an indirect quantity effect (C^q_{ind}) and an indirect price effect (C^p_{ind}). In the example of the scenario FB20, the direct quantity effect is derived by comparing the costs of scenario FB20 with the Reference scenario, with both scenarios assuming the gas price of the Reference scenario, g_{REF}:

$$C_{dir} = C_{FB20}(g_{REF}) - C_{REF}(g_{REF}). \tag{4.32}$$

The sum of the indirect quantity effect and the indirect price effect is derived by comparing the costs of the FB20 scenario using the price of the Reference scenario,

[51]Clearly, the discount rate is crucial for results of the numerical simulation in Section 4.5. Although the assumed discount rate affects the magnitude of the simulation results, the effects derived in Section 4.2 remain qualitatively the same. To provide the reader some insight on the sensitivity of the discount rate on the simulation results, Appendix C.2 presents an analysis assuming a discount rate of 3%.

$C_{FB20}(g_{REF})$, to the costs of the FB20 scenario using the gas price of the FB20 scenario, $C_{FB20}(g_{FB20})$. Thus,

$$C^{x}_{ind} + C^{p}_{ind} = C_{FB20}(g_{FB20}) - C_{FB20}(g_{REF}). \tag{4.33}$$

The indirect price effect is derived as the gas price difference between scenario FB20 and the Reference scenario multiplied by the gas consumption of the power sector in the FB20 scenario, x_G^{FB20}:

$$C^{p}_{ind} = (g_{FB20} - g_{REF})x_G^{FB20}. \tag{4.34}$$

As discussed in the previous section a coal tax in the power sector causes a deviation from the cost efficient power generation under the no-tax case. Hence, the direct cost effect of a coal tax is positive, as Figure 4.10 illustrates. In the CT10 scenario, where a coal tax causes gas prices to both increase and decrease (depending on the year), the indirect quantity effect is positive. In other words, changing gas prices forces power generation to deviate from the cost-optimal generation even more than seen in the direct effect. However, the costs of gas purchases decrease, i.e., the indirect price effect reduces costs. Yet, in total, power system costs in the CT10 scenario are higher than in the reference case. In the CT20 scenario, except for the year 2015, gas prices increase. Therefore, a higher gas price increases the costs of gas purchased by the power sector, i.e., the indirect price effect is positive. Hence, these numerical results confirm hypothesis H2: A coal tax increases overall power system costs.

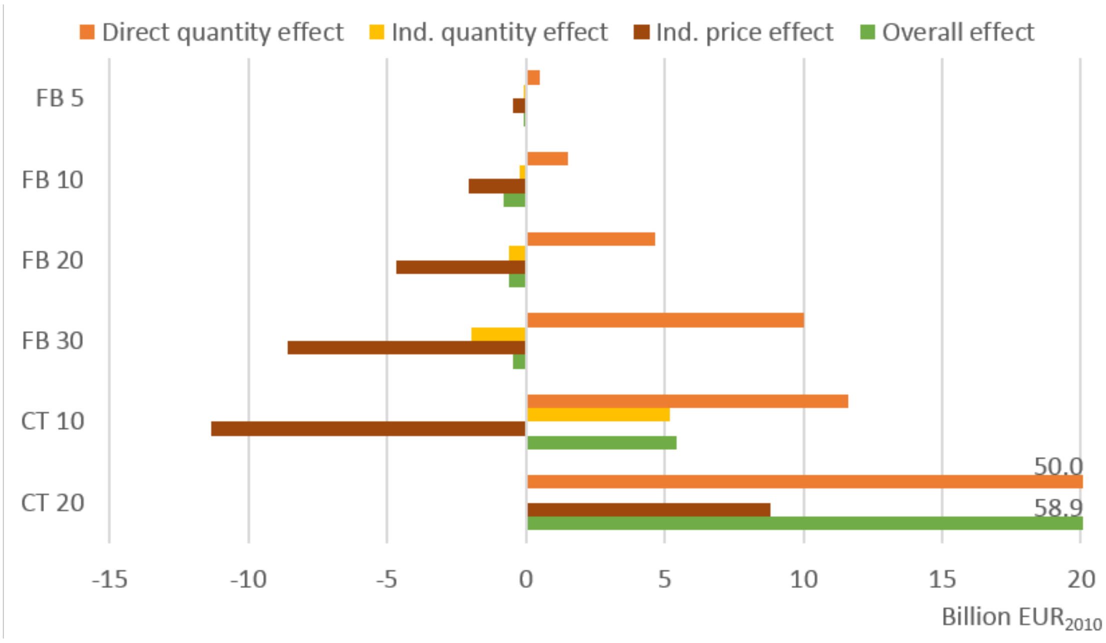

FIGURE 4.10: Power System Cost Effects of Different Levels of Coal Taxes and RES Subsidies

With regard to fixed bonus RES subsidies, Figure 4.10 reveals that the direct cost effect of such a subsidy is positive and increases with the subsidy. However, since the subsidy causes the gas price to decrease, the indirect quantity effect reduces the additional costs incurred by the direct quantity effect. Nonetheless, the sum of both the direct and indirect quantity effect is positive. However, the indirect price effect of a subsidy, i.e., decreasing costs of gas purchased by the power sector, overcompensates the quantity effects. Therefore, this numerical simulation of the European power and gas market confirms hypothesis H3: A fixed bonus RES subsidy may decrease overall power system costs because of the gas price reaction.

4.5.4 Cost Effects of Supply-side Concentration on the Gas Market

A higher supply side concentration on the gas market is simulated by a fictitious cartel of Norway and Russia. For the scenarios FB20 and the CT10, Figure 4.11 compares the gas price reaction (i.e., the price differences to the respective REF scenario) under the standard gas market structure (STANDARD) with the cartel (CARTEL).[52] The gas price reduction in the FB20 scenario is higher in the case of the cartel than in the standard case for each year. In the Coal Tax scenario CT10, the gas price reduction in the cartel case is lower in 2015 than in the standard case, whereas the gas price increase in the years 2020 and 2030 is higher.

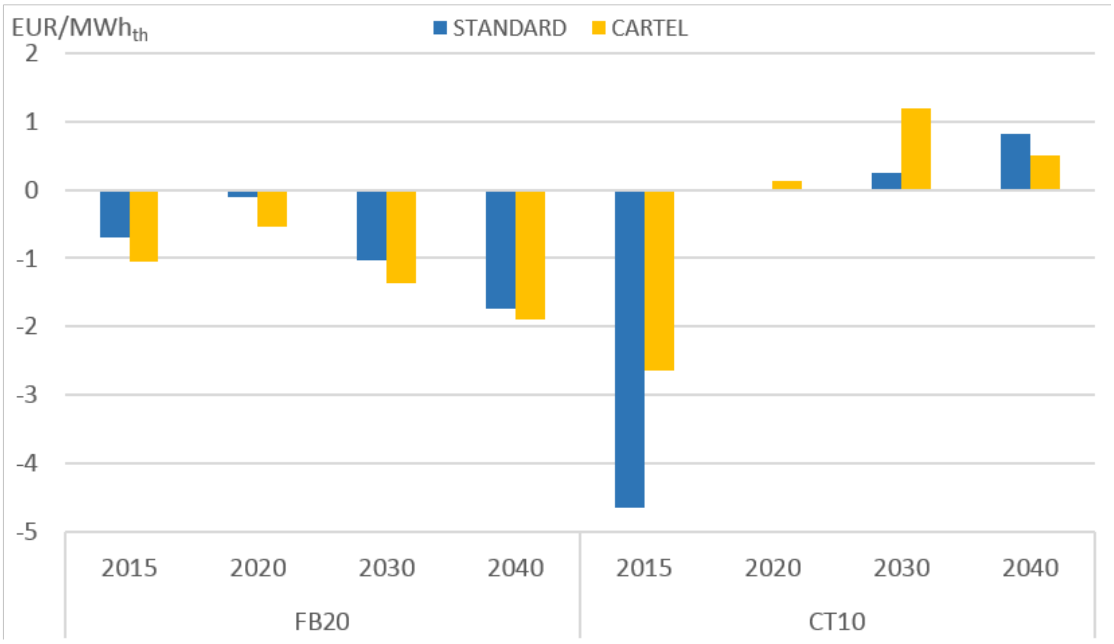

FIGURE 4.11: Effects of Higher Market Power of Gas Suppliers on Gas Prices

[52]For the other scenarios, the results are qualitatively the same.

These price reactions explain the cost effects when different gas supply-side structures are assumed (see Figure 4.12). In the RES subsidy scenarios, the higher price decrease causes a higher indirect price effect such that the overall power system cost reduction is higher in the CARTEL case than in the STANDARD case. In the coal tax scenarios, the opposite holds. To sum up, with regard to hypothesis H4, a higher market power in the gas market amplifies the discussed effects.

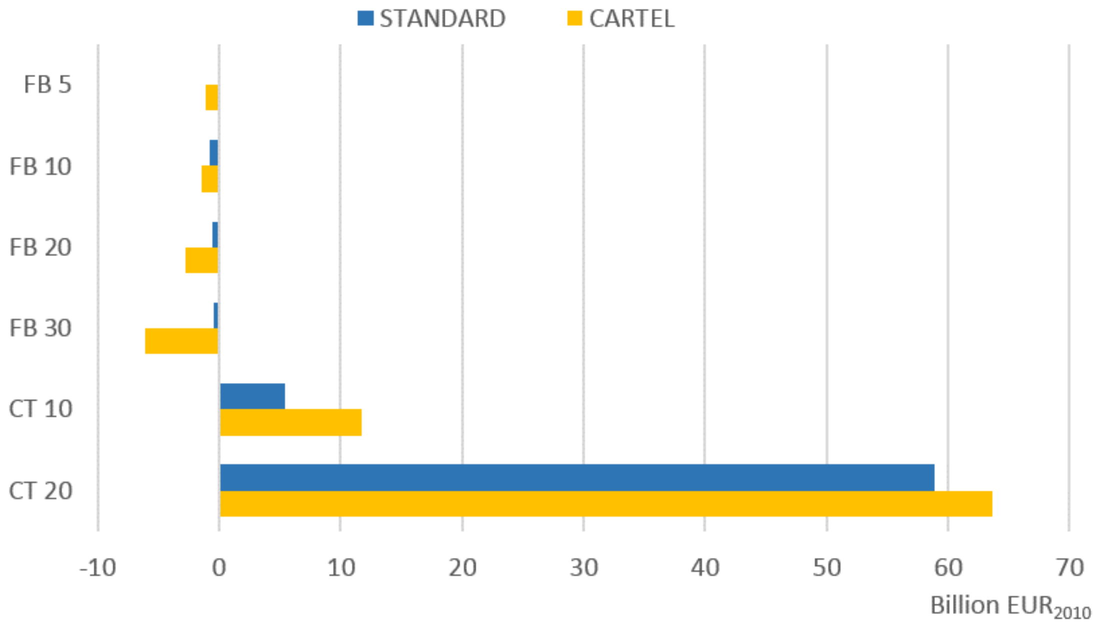

FIGURE 4.12: Effects of Higher Market Power of Gas Suppliers on Power System Costs

4.6 Conclusions

This research has discussed how a coal tax and a fixed bonus RES subsidy in combination with a CO_2 emissions quota affects power system costs. Since climate policies influence gas demand of the power sector and hence, gas prices, this research explicitly accounts for the interactions between the power and the gas market. In a stylized theoretical model using the example of a fixed bonus RES subsidy, I have identified three effects of the subsidy on power system costs. First, a subsidy directly affects power generation by fuel type and therefore system costs (*direct effect*). Second, since the subsidy affects gas prices, it also affects power generation by fuel type via the gas price, an effect referred to as the *indirect quantity effect*. The subsidy affecting gas prices also causes an *indirect price effect*, i.e., changing gas prices affect the purchase costs per unit of natural gas consumed by the power sector.

Applying a numerical simulation model and integrating the power and gas market in a case study for 11 relevant European countries, I draw 4 main findings. First, a coal tax influences gas prices ambiguously, depending on the effect of a coal tax on gas demand elasticity. On the contrary, a fixed bonus RES subsidy decreases gas prices for each of the simulated subsidy levels. Second, a coal tax results in tax distortions, i.e., it increases power system costs even at constant gas prices (direct effect). Since a coal tax affects gas prices ambiguously, the overall power system costs increase, even when accounting for the indirect quantity and price effects. Third, the simulation results reveal that a fixed bonus RES subsidy can decrease overall power system costs: On the one hand, the subsidy increases costs given fixed gas prices (direct effect); yet, on the other hand, the subsidy decreases gas prices such that the indirect quantity and price effects overcompensate the direct effect. Fourth, when a higher level of market power of gas suppliers is assumed, the overall effect of higher market power on power system costs is amplified. Concerning a coal tax, the simulation results show that a higher degree of market power further increases costs, whereas, concerning a RES subsidy, it further decreases costs. The assumed discount rate of future costs has proven to be a crucial parameter, which affects these results quantitatively, however not qualitatively.

This analysis has focused solely on the effects of climate policies on the *power system costs* of 11 select European countries. In particular, decreasing power system costs through a fixed RES bonus do *not* imply that this subsidy makes CO_2 abatement more efficient. The reason for decreasing power system costs are the decreasing expenditures of power utilities for the gas purchased, which come at the disadvantage of gas suppliers, whose revenues decline. In other words, introducing the subsidy redistributes welfare from players in the gas market to players or end consumers in the power market, as well as to suppliers of coal or renewable technologies. Even though the discussed subsidy would cause an inefficient allocation of primary energy use in the power sector and, hence, higher CO_2 abatement costs, European policy makers could have a sound motivation to establish a fixed RES bonus subsidy: in order to redistribute welfare from the most important gas suppliers such as Russia, Norway, Algeria or Qatar to market participants of the European power market, i.e., power producers or end users.

This research has pointed out that the evaluation of climate policies in the power sector should take into account the upstream markets and their market structure. The main focus was a discussion of the power system cost effects of climate policies in due consideration of the interdependencies of the power and gas market. Yet, it is important to stress that this study does not provide a comprehensive assessment of climate policies, for several reasons. First, the sole objective of this study is to determine the minimal power system costs. Regarding the coal tax, the tax could aim at further objectives other than efficient CO_2 abatement. Other policy objectives could justify higher costs from a coal tax. Second, this research only assesses two policies and simulates a setting in which there are no other climate policies in place. In reality, there is a variety of (national) climate policies which could affect gas prices differently or interact with other policies. In particular, the study does *not* say that the current regime of national technology-specific RES subsidies decreases power system costs. Third, even though the study reveals cost reduction potentials of a technology-neutral and location-neutral RES subsidy, it remains an open question whether there may be another policy regime that further decreases gas prices and, therefore, power system costs. As such, an EU energy union is often discussed as a mean to decrease gas purchasing costs. However, the main flaw of such a measure, the threat of downstream cartelization, is avoided by a RES subsidy. Fourth, the dynamic effects of climate policies, such as a higher or lower technological progress because of a subsidy, are not investigated in this research. Fifth, efficiency gains and losses in other related markets such as the gas, coal or renewables market have not been assessed. All of the five outlined aspects could motivate interesting extensions to this paper.

Chapter 5

Greenhouse Gas Abatement Cost Curves of the Residential Heating Market – a Microeconomic Approach

5.1 Introduction

The social costs of greenhouse gas (GHG) emissions as a global externality are more and more spotlighted in the worldwide public discussion. Since the UNCED[53] in Rio de Janeiro 1992, but latest since the Stern Review (Stern, 2007) and the IPCC report on climate change in 2007 (IPCC, 2007), politicians, engineers, ecologists and economists argue about optimal strategies of GHG avoidance. Consequently, national objectives and policies for GHG abatement have been introduced in the last years. Besides the emissions produced by major polluters such as the power sector, a significant part of overall emissions stem from small emittents such as households.

In particular, heat provision in residential buildings can play a major role for GHG abatement. Besides enhancing thermal insulation, the replacement of inefficient and carbon intense heating systems holds a huge potential of GHG emission reduction. However, GHG abatement in the residential sector is challenging as the total GHG emissions is the aggregated result of millions of households' individual decisions on heating systems and building insulation. Each household faces a different investment decision: Monetary

[53] United Nations Conference on Environment and Development

costs of the heating system in terms of initial investment, maintenance or fuel consumption are an important factor, yet not the only one; the household utility from a heating system is driven as well by its habits and preferences. Thus, besides monetary costs there is a variety of non-observable factors which influence the investment decision in a heating system.

In order to incentivize GHG reduction in the residential sector, subsidies and carbon taxes are two prominent policy measures to affect the monetary costs and thus the investment decision of a household. However, these policy measures impose costs: not solely monetary for technical equipment, but also in terms of welfare losses due to tax and subsidy distortions. To quantify total social costs of emission reduction, our paper aims at deducing a welfare-based GHG abatement cost curve of the residential heating sector, thereby accounting for costs, characteristics and preferences of households.

Our methodology comprises three steps: First, we develop DIscHEat, an economic microsimulation model of the German heat market for the years 2010 to 2030. The model is an innovate approach since it combines a dynamic bottom-up model (see, for instance, Stadler et al., 2007) with a discrete choice model. The evolution of heating systems in German residential buildings over time is simulated in a bottom-up model. The bottom-up model itself includes a discrete choice model which derives probabilities for heating system choices of households based on the costs of heat provision and household characteristics. Second, we derive analytically how the adoption of technologies takes place based on heating costs and household characteristics in a theoretical discrete choice framework.[54] We show how this diffusion process is affected by public policies and its impact on GHG abatement. The discrete choice approach further enables us deriving different welfare measures such as the compensating variation and excess burden (Diamond and McFadden, 1974, McFadden, 1999, Small and Rosen, 1981), which we use to develop welfare based GHG abatement curves. Third, we apply DIscHEat to investigate the impact of different GHG abatement policies on newly installed heating systems and GHG abatement until 2030, namely a carbon tax and a subsidy regime. A carbon tax, for example, increases the monetary costs of carbon intense technologies, thereby c.p. reducing their installations and consequently curbing carbon emissions. From that we deduce welfare-based GHG abatement curves of the investigated policies, thereby accounting for household individual characteristics.

To conduct our analysis, we choose Germany as an exemplary case for two reasons: first, the insulation level of domestic buildings is already very high and further insulation is very cost-intense in terms of GHG abatement compared to the installation of new heating

[54]See for example Train (2003) for an overview of discrete choice approaches on which we base our framework.

systems (Buildings Performance Institute Europe (BPIE), 2011, IEA, 2011a). Second, since more than 90% of all residential buildings are heated decentrally, the households' individual heating system decisions have a strong impact on the total GHG emissions. Both aspects underline the importance to account for the household individual decisions on investment in heating systems.[55]

Several studies have already adressed pollution abatement curves based on welfare effects of environmental taxes using a general-equilibrium approach (Ballard and Medema, 1993, Bovenberg and Goulder, 1996). In addition to these studies on the macro-level, among the analyses on the micro-level most studies are mainly technical thereby focusing on the technical equipment costs (Kavgic et al., 2010, Swan and Ugursal, 2009). One example of such technology-based approach is a recently published study by McKinsey & Company, Inc. (2009), which identifies significant energy savings with low costs for society. Huntington (2011) discusses the overestimation of the reduction potential in the McKinsey & Company, Inc. (2009) study, which results from assuming adoption rates of technologies of 100%. In an aggregated approach Huntington (2011) shows that accounting for the households' behavior and their reactions on policy measures would revise the GHG abatement curves downwards as well as by including policy costs. There are microeconomic analyses that investigate the impact of environmental policies: Tra (2010) evaluates the benefits of air quality improvements in a discrete choice locational equilibrium model that accounts for welfare impacts of policy interventions in a microeconomic context. However, to date there are few attempts to derive microeconomic GHG abatement curves that account for household individual investment decisions. Our paper fills this gap.

In the light of current literature, our paper contributes to energy economics and its analytical and numerical literature in two ways: First, it extends earlier work by analytically deriving a GHG abatement cost curve based on household preferences and welfare losses on externalities in a microeconomic setting. Second, the paper extends the literature by developing a numerical microsimulation combining a bottom-up approach with an empirical discrete choice estimation. Our paper thus combines the strengths of analytical and numerical approaches.

Our results, first, confirm the implications of Huntington's paper suggesting that welfare-based GHG abatement curves run above technical cost curves. Thus, accounting for household specific characteristics and their reactions on policy measures implies greater costs for society than pure technical equipment costs. Second, our results suggest that

[55] Because GHG abatement costs for insulation measures are so high in Germany, for simplification, we exclude the households' decisions on thermal insulation from our analysis.

in most cases a carbon tax causes less welfare losses than subsidies on technology investments. However, third, in case that households are not utility maximizers, subsidies on investments might be reasonable.

The paper is organized as follows: The next section provides a brief overview of previous research. In Section 5.3, we present the microsimulation model DIscrHEat. In Section 5.4 we derive microeconomic GHG abatement cost curves in a theoretical approach. Section 5.5 presents our results, first, in Section 5.5.1 on the effects of the policies on GHG abatement and the diffusion of technologies. Second, Section 5.5.2 presents the welfare impacts of the different policies to lastly derive GHG abatement cost curves numerically. Section 5.6 concludes.

5.2 Previous Research

There are two strands of literature which are related to our paper. The first strand is on energy demand modeling in general. There are a variety of studies that model the energy demand of the private sector and that identify drivers of energy consumption and energy efficiency. Swan and Ugursal (2009) and Kavgic et al. (2010) give an overview of different bottom-up models and models to analyze residential energy consumption, i.e. mainly technology-based energy demand modeling approaches. These bottom-up models are based on extensive disaggregated data and components that influence energy demand on an individual detailed level. This model type is often applied to identify cost-efficient technology options for achieving certain GHG emission abatement targets. There are also a variety of top-down models that focus on rather macroeconomic relationships. These models use aggregated empirical data to investigate the interrelation of the energy sector and the economy as a whole by variables like GDP, income, temperature and prices of energy carriers. Mansur et al. (2008) analyze the impact of climate change on energy demand and welfare in the US applying a discrete-continous model of fuel choice and energy consumption. They find a potential increase of American energy expenditures and welfare losses caused by temperature rise. Madlener (1996) provides an overview of the different time-series based methodologies applied to analyze residential energy demand. Rehdanz (2007) examines the determinants of household expenditures on space heating and hot water supply in Germany based on panel data and covers a number of socio-economic characteristics of households along with dwelling characteristics. Braun (2010) examines building, socio-economic and regional characteristics in a discrete choice model focusing on space heating technologies applied by households but not on the heating system choice in terms of new heating system installations. Michelsen and Madlener (2012) conduct a survey about heating system installations to analyze the influence of preferences about residential heating system specific attributes on the adoption decision in a discrete choice estimation.

The second strand of related literature focuses on numerical approaches to the deduction of GHG abatement costs. The literature on GHG abatement modeling can be categorized into general equilibrium modeling approaches and technical models. Bovenberg and Goulder (1996) develop an emission abatement curve based on marginal welfare costs in a general equilibrium setting. Nordhaus (2011) and Pearce (2003) determine different social damage costs of GHG. Morris et al. (2008) apply a general equilibrium model to compute marginal abatement costs and marginal welfare costs for different GHG prices. They argue that the marginal abatement costs in their model reflect the shadow prices on the GHG constraint on certain countries or sectors. This is interpretable as a price that would be obtained under an allowance market that developed under a cap and trade system. They come to the conclusion that these marginal abatement costs are not closely related to the marginal welfare costs. The marginal abatement costs of their model vary over countries and are sometimes above and sometimes below the marginal welfare costs and therefore they conclude that they should not be used to derive estimates of welfare change.

A recent study on GHG abatement curves on the micro-level has been published by McKinsey & Company, Inc. (2009) which establishes a cost-efficient GHG abatement curve for different energy efficiency measures. Huntington (2011) discusses how the McKinsey & Company, Inc. (2009) study might overestimate the reduction potential. According to Huntington (2011), McKinsey & Company, Inc. (2009) neglect the actual investment decisions of private households assuming adoption rates of technologies of 100%. In reality, a new technology might not be cost-efficient for everyone even if it is cost-efficient for the average consumer. In addition, the adoption and diffusion of technologies proceeds slowly in general. Huntington (2011) also mentions the exclusion of the households' reactions to the introduction of policy measures and the exclusion of policy costs in the McKinsey & Company, Inc. (2009) study. Introducing basic assumptions to these additional costs and impacts on the GHG abatement curve, Huntington (2011) revises the curve to highlight implications for policymakers if they base their decisions on a what he calls "out-of-pocket" technology based cost curve.

5.3 DIscrHEat – a Microsimulation of the Heating Market

In the following, we develop DIscrHEat (DIscrete choice HEat market simulation model) which is a dynamic simulation model for the German heat market of private households. It simulates the development of installed heating systems and insulation levels of German dwellings until 2030. This approach contributes to literature by combining a dynamic bottom-up model with a discrete choice approach. The development of residential buildings and their heating systems is modeled in a bottom-up model in discrete time periods (see Section 5.3.1). The change of the heating systems in residential buildings, i.e. the households' choice for a certain heating technology is derived by a discrete choice model (see Section 5.3.2), which has been estimated using a unique dataset (see Section 5.3.3).

5.3.1 A Dynamic Bottom-up Model of the Heating Market

The set of residential buildings, or dwellings, D_y evolves in discrete periods of time y ($y \in \{1, ..., Y\}$). The set of residential buildings comprises a complete-disjunctive subset of dwellings $\tilde{D}_{n,j,y}$ differing by heating technology j ($j \in \{1, ..., J\}$), i.e., oil-, gas-, pellet-heaters and heat pumps, and household categories n ($n \in \{1, ..., N\}$) (e.g., single dwellings built between 1900 and 1920), and:

$$D_y = \bigcup_{n,j,y} \tilde{D}_{n,j,y} \tag{5.1}$$

The number of dwellings being element of $\tilde{D}_{n,j,y}$ is labeled $d_{n,j,y}$. In each period y, some of the $d_{n,j,y}$ dwellings have to modernize their heating system, defined by the exogenous modernization rate $r_{n,y}$. Those dwellings are represented by $d^-_{n,j,y}$, whereas those dwellings, which do not modernize their heating system, are represented by $\hat{d}_{n,j,y}$, i.e.:

$$d^-_{n,j,y} = r_{n,y} * d_{n,j,y} \tag{5.2}$$

and

$$\hat{d}_{n,j,y} = (1 - r_{n,y}) * d_{n,j,y} \tag{5.3}$$

.

The dwellings $d^-_{n,i,y}$, replace their old heating technology i ($i \in \{1, ..., J\}$) by a new technology j according to a dwelling-category specific probability rate $P_{n,j,y}$. E.g., an old gas-heater can be replaced by a new gas-heater or a household may choose a heat pump instead. The probability rate, i.e., the technology choice is derived in a discrete choice model (discussed below). After modernizing, the dwellings are grouped by $d^+_{n,j,y}$, i.e.:

$$d^+_{n,j,y} = P_{n,j,y} * \sum_{i \in J} d^-_{n,i,y} \tag{5.4}$$

Now, we are able to model the process for each dwelling category $d_{n,j,y}$, i.e. the changing of the household/technology stock from y to $y+1$:

$$d_{n,j,y+1} = \hat{d}_{n,j,y} + d^{+}_{n,j,y} - d^{-}_{n,j,y} \tag{5.5}$$

5.3.2 Modeling the Technology Choice

As stated before, the probability $P_{n,j,y}$, i.e. the heating technology choice is derived in a discrete choice approach. The probability $P_{n,j,y}$ is a function of the annual heating system costs $c_{n,j,y}$[56] and some specific characteristics z_n for each household category:

$$P_{n,j,y} = f(c_{n,j,y}, z_n) \tag{5.6}$$

The annual system costs $c_{n,j,y}$ are a function of the investment costs $i_{n,j,y}$, the energy consumption $e_{n,j,y}$, the energy price $p_{j,y}$. All parameters depend on the time period of installation y to account for technological progress affecting investment costs as well as efficiency (i.e., energy consumption). Concerning the energy price, we further assume that each household has no knowledge about future energy prices and expects them to be constant over time.[57] Hence total life-cycle costs $C_{n,j,y}$ (net present value) over the future utilization time periods s of the technology are:

$$C_{n,j,y} = \sum_{s}^{s+l} (i_{n,j,y} * a_{r,l} + e_{n,j,y} * p_{j,y}) \frac{1}{(1+r)^s} \tag{5.7}$$

with $a_{r,l}$ being the annuity factor depending on the discount rate r and the economic lifetime l being identical for each technology.

Investment costs and energy consumption are fixed for the future utilization and future energy prices as households expect them to be constant. Thus, life-cycle costs $C_{n,j,y}$ simplify to:

$$C_{n,j,y} = c_{n,j,y} * l * \sum_{s}^{s+l} \frac{1}{(1+r)^s} \tag{5.8}$$

[56] We do not consider the impact of policy measures on the number of investments, but only on the structure of heating system choices. Therefore, the annual heating system costs, accounting for investment costs and future energy savings, are relevant for the heating system choices. However the split of investment costs and future energy savings is irrelevant. Based on IWU / BEI (2010), we argue that households only change their heating system when it is broken. Finding explanations for this behaviour is open for further research.

[57] We assume households to not have perfect foresight and that they have bounded rationality. Hence, only current energy prices are included in their considerations and future energy price developments are not accounted for.

with $c_{n,j,y} = i_{n,j,y} * a_{r,l} + e_{n,j,y} * p_{j,y}$. Assuming an identical economic lifetime for each technology, the life-cycle cost ratio of two technologies is, hence, fully explained by the ratio of annual heating costs.

For the further analysis, $c_{n,j,y}$ also depends on two policy measures that we model (which are constant over time) – Pigovian carbon taxes T_j, increasing the energy price $p_{j,y}$, and subsidies on the investment S_j, decreasing $i_{n,j,y}$.[58] Thus:

$$c_{n,j,y} = f(i_{n,j,y}, e_{n,j,y}, p_{j,y}, T_j, S_j) \tag{5.9}$$

In the following discussion we leave out the time index y to reduce complexity of notations. However, all decisions modeled depend on the time y when the decision is made.

Based on the alternative-specific conditional logit model, first presented by McFadden (1976, 1974), the indirect utility $U_{n,j}$ of each household of category n that chooses between different technologies j is given by:

$$U_{n,j} = V_{n,j} + \epsilon_{n,j} \tag{5.10}$$

$V_{n,j}$ is the observable utility of a household of category n, which installs technology j, whereas $\epsilon_{n,j}$ captures further factors that influence the utility but are not in $V_{n,j}$. $V_{n,j}$ is:

$$V_{n,j} = \alpha_j + \beta c_{n,j} + \gamma_j z_n \tag{5.11}$$

with α_j being an alternative-specific constant that give an extra value to each technology. β represents the negative total annual system cost impact and γ_j is a vector of technology-specific impacts on the household characteristics. We get:

$$U_{n,j} = \alpha_j + \beta c_{n,j} + \gamma_j z_n + \epsilon_{n,j} \tag{5.12}$$

The choice of a household of category n can be described as a dummy variable $y_{n,j}$:

$$y_{n,j} = \begin{cases} 1, \text{if} \quad U_{n,j} > U_{n,i} \quad \forall i \neq j \\ 0, \text{else} \end{cases} \tag{5.13}$$

[58] For more details, Appendix D.1 shows a more detailed specification of the annual heating costs $c_{n,j,y}$ and the impact of T_j and S_j.

The choice probability that determines the diffusion process of a technology is defined as:

$$\begin{aligned} P_{n,j} &= Prob(y_{n,j} = 1) = Prob(U_{n,j} - U_{n,i} > 0, \quad \forall i \neq j) \\ &= Prob(\epsilon_{n,i} - \epsilon_{n,j} < V_{n,j} - V_{n,i} \quad \forall i \neq j) \end{aligned} \tag{5.14}$$

where $\epsilon_{n,i}, \epsilon_{n,j} \sim \textit{iid extreme value}, \quad \epsilon_{n,i} - \epsilon_{n,j}$ has a logistic distribution[59] and only the difference between two utility levels has an impact on the choice probability and not the absolute utility level.

The probability that a household of category n chooses alternative j is[60]:

$$P_{n,j} = \frac{e^{V_{n,j}}}{\sum_i e^{V_{n,i}}} = \frac{e^{\alpha_j + \beta c_{n,j} + \gamma_j z_n}}{\sum_i e^{\alpha_i + \beta c_{n,i} + \gamma_i z_n}} \tag{5.15}$$

This determines the proportion of installations of technology j among the new systems chosen by household type n.

Own cost changes and those of alternative heating systems affect the choice probabilities of a heating system. These cost impacts on the choice probability of a heating system can be described in terms of elasticities. The elasticity of a household's choice probability with respect to heating costs of the system j that he chooses is given by:

$$\frac{\partial P_{n,j}}{\partial c_{n,j}} \frac{c_{n,j}}{P_{n,j}} = \beta(1 - P_{n,j})c_{n,j} < 0 \tag{5.16}$$

which is negative because of the negative cost impact $\beta < 0$.

The elasticity of a household's choice probability for j with respect to heating costs of an alternative system i is given by:

$$\frac{\partial P_{n,j}}{\partial c_{n,i}} \frac{c_{n,i}}{P_{n,j}} = -\beta P_{n,i} c_{n,i} > 0 \tag{5.17}$$

with $i \neq j$.

The effects of the model are ceteris paribus and allow for the computation of own and cross cost elasticities on the diffusion rates of the different technologies, i.e. the choice probabilities of an alternative, keeping all values fixed. The changes in the total GHG emission level are determined by the diffusion process.

[59]The logit model with its elasticities is a standard approach to model the diffusion of technologies. See for instance Geroski (2000).

[60]For detailed mathematical derivations and explanations of logit and conditional logit models see McFadden (1974) and Train (2003).

The elasticities account for the cost effect β on the technology choice. An advantage of the inclusion of $P_{n,j}$ in the elasticities is that changes of $P_{n,j}$ depend on the current level of $P_{n,j}$.[61] The restricted substitution pattern of the choice probability holds on the individual level and is much more flexibel on the aggregated level over all household types. On the aggregated level, the substitution pattern also accounts for the heterogeneity of households.

5.3.3 Estimating the Discrete Choice Model

Using data on the structure of newly installed heating systems in Germany in 2010, we estimate a discrete choice model to identify the effects of the annual costs and further building characteristics (being a proxy for household income and preferences) that have an impact on the heating choice of a household.

We thus assume that the probability $P_{n,j}$ that a representative household n adopts a heating system characterized by the energy carrier j is a function of the annual heating system costs and some building characteristics z_n: $P_{n,j} = f(c_{n,j}, z_n)$.[62] We additionally define alternative-specific, i.e., energy carrier based variables that could have an impact on the choice of a specific energy carrier based heating system. We assume the probability of installing a specific heating system to be different in single and double than in multiple dwellings and in buildings stemming from different vintage classes[63]. Therefore, we include the dummy variable 'single' $z_{1,n}$, with 1 for single and double and 0 for multiple dwellings and the variable 'heatdemand' $z_{2,n}$, serving as a proxy for the vintage class[64]. α_j are the alternative-specific constants. β represents the impact of total annual heating cost per kilowatt hour (kWh) $c_{n,j}$. $\gamma_{1,j}, \gamma_{2,j}$ identify the effects of the alternative-specific variables.

The indirect utility of household n of the chosen heating system j is:

$$V_{n,j} = \alpha_j + \beta c_{n,j} + \gamma_{1,j} z_{1,n} + \gamma_{2,j} z_{2,n} \tag{5.18}$$

[61] Analyzing the development of the German heat market over the last 60 years indicates that this is a realistic assumption and that changes resulting from the cost advantages of new heating systems take place only inertially and based on the number of heating systems of that type that are already installed BDH (2010), IWU / BEI (2010). The inertia of the heating system stock results from the long life spans of the heating systems and the fact that heaters are only exchanged when they are broken. Adoption rates of heating systems that already have a large market share are much higher. The proportional substitution pattern of conditional logit models is often criticized. In the case of the homogenous good heat, it seems however to be appropriate. See for instance Train (2003) for a detailed discussion of the substitution patterns of logit models.

[62] We use the annual heating costs per unit of heat demand in kilowatt hour (kWh) $c_{n,j}$ because we are interested in a normalized impact of costs on the choice of a heating system irrespective of the different dwellings' total heat demand. As such, we can make them comparable for all buildings. We further assume that all households of category n have the same dwelling characteristics.

[63] See Appendix D.4

[64] By tendency, newer buildings c.p. have a lower heat demand.

with the choice probability being:

$$P_{n,j} = \frac{e^{V_{n,j}}}{\sum_i e^{V_{n,i}}} = \frac{e^{\alpha_j + \beta c_{n,j} + \gamma_{1,j} z_{1,n} + \gamma_{2,j} z_{2,n}}}{\sum_i e^{\alpha_i + \beta c_{n,i} + \gamma_{1,i} z_{1,n} + \gamma_{2,i} z_{2,n}}} \tag{5.19}$$

As only the differences of the utilities are of importance for the estimation of the impacts, we define as base alternative 'gas' for which $\gamma_{1,\text{gas}}, \gamma_{2,\text{gas}} = 0$.

Table 5.1 the results of our discrete choice estimation. The cost impact is significant at a 10%-level and as expected the cost impact is strongly negative. [65] All alternative specific constants are significant at a 1%-level and have a negative impact. Only the biomass constant is not significant. The negative impact of the alternative specific constants indicates that the probability to choose either a heat pump, a biomass or oil heater is less probable than choosing a gas-fueled heating system. This seems realistic because the market share of gas heaters in Germany is above 50% since the last years and households tend to have a preference for well-established systems.

Table 5.1: Estimation Results

Number of observations = 11052 Wald chi2(7) = 303.59
Number of cases = 2763
Log likelihood = -2471.1913 Prob > chi2 = 0.0000

choice	coef.	std. err.	z	P> |z|
heatingsystem				
costs	-26.7651	15.7391	-1.70	0.089
biomass				
single	1.0193	0.4400	2.32	0.021
heatdemand	-0.0167	0.0051	-3.30	0.001
constant	-0.7025	0.7290	-0.96	0.335
gas	(base alternative)			
heatpump				
single	1.9561	0.4129	4.74	0.000
heatdemand	-0.0203	0.0037	-5.44	0.000
constant	-1.3075	0.4355	-3.00	0.003
oil				
single	-0.4750	0.1514	-3.14	0.002
heatdemand	0.0202	0.0028	7.17	0.000
constant	-2.6533	0.6660	-3.98	0.000

Including just dwelling characteristics, we only cover systematic differences of heating system installations in our model, which however mainly explain the diffusion of heating systems (see also Braun, 2010). These serve as proxies for the unobservable costs or

[65] The significance of the cost estimate is only at 10% because the estimation is based on our own dataset including simplified cost assumptions. For some specific households, additional costs apart from heating system costs (e.g. switching costs such as costs for network connections etc.) may be of importance. Data on these costs is not available. Braun (2010) estimates a more detailed discrete choice model for the German heating market, however, only focusing on household characteristics. Our paper's focus is not on the estimation itself. If better data were available, the same approach of deriving marginal CO_2 abatement curves could be implemented based on improved and more detailed choice estimations.

other impacts that vary across dwelling types such as additional switching costs or financing costs[66]. The results in Table 5.1 show that the choice probability of non-fossil heating systems biomass and heat pumps is higher in buildings with better insulation and thus lower heat demand, which usually belong to younger vintage classes. The choice probability of these heating systems is also significantly higher for single and double dwellings than for multiple dwellings.

5.4 Deriving Greenhouse Gas Abatement Curves of Policies

Energy efficiency and GHG abatement policies can have different impacts and purposes. They can either try to influence the number of low emission investments made by trying to incentivize the household to invest earlier or more often; or they try to make the household investing in less greenhouse-gas-intense technologies. For deriving greenhouse gas abatement curves in this research, we focus on the latter. First, we specify the policies analyzed in this study (Section 5.4.1). Second, we derive analytically the welfare effects of a policy in terms of the excess burden (Section 5.4.2) and lastly, we derive analytically the greenhouse gas abatement curves of policies (Section 5.4.3).

5.4.1 Policy Specification

We use the DIscrHEat model (see Section 5.3) to analyze the diffusion process of newly installed heating systems until 2030. We distinguish four technologies, i.e., gas-, oil- and biomass-fired burners as well as heat pumps. Beside a reference case without any policies, we simulate three policies: A carbon tax and two subsidy regimes.

The first policy to investigate is a Pigovian carbon tax.[67] We increase the carbon tax gradually to achieve higher levels of GHG abatement.[68] We consider a carbon tax T_j in EUR/kWh which equals a carbon tax τ in EUR/t of CO_2-equivalents times a technology-specific conversion factor CF_j that converts τ into T_j accounting for the amount of CO_2-equivalents in the different energy carriers. In case of a carbon tax all households of the stock that have a heat pump, a gas- or an oil-fired heater are thus affected by such a tax and not only the households that have to make the decision on their heating system, i.e. have to modernize it. However, our analysis is limited to those

[66]For instance, Dieckhöner (2012a) shows that households with higher income rather live in single dwellings.

[67]The carbon tax is a hypothetical policy which is not implemented currently.

[68]For the assumed emissions of the energy carriers, see Table D.3. We assume that no tax is levied on biomass.

households, which exchange their heating system. Thus, in terms of the welfare changes of a tax only the households who modernize their heating system are relevant.

In addition, we simulate two different subsidy regimes, which both provide subsidies S_j on newly installed heating systems reducing the investment costs of the respective systems. For the first subsidy scenario (subsidy I), we implement a simplified version of the German subsidy system with subsidies on heat pump and biomass heaters. Thereby, subsidies on biomass are significantly larger.

The second subsidy scenario (subsidy II) is a hypothetical policy scenario. It provides the same level of subsidies on heat pumps as on biomass heaters and additionally a low subsidy on gas heating systems. We choose this parametrization subsidizing heat pumps and natural gas heaters relatively more than in the German system because marginal abatement costs of biomass heaters are the highest. Contrarily, biomass heaters are highly subsidized in the German system. Like this we aim to generate a subsidy based GHG abatement curve that generates lower welfare losses for the first major part of abatement units (see Table D.6 for the subsidy levels). For both subsidies we increase these subsidy rates proportionally to effectuate higher GHG abatement.

5.4.2 Welfare Effects of Greenhouse Gas Abatement Policies

The aggregated net utility in our model over all households that change their technology and install a new one in period (year) $y \in 2010, ..., 2030$ is defined as follows:

$$U^{aggr.} = \sum_{n,j=1}^{N,J} d_{n,j} * (C + V_{n,j}) \tag{5.20}$$

C is a constant positive utility level that is assumed to be the same for all household types n and indicates the minimum utility of a new technology. $C \geq |V_{n,j}|$ by definition because a new technology needs to be installed when the old one is broken and thus is assumed to imply a higher utility than costs. The utility $V_{n,j}$ is negative because it indicates the cost impact of the essential new systems on the aggregated utility. As for the welfare analysis only the differences between two aggregated utilities with different policies are of importance, we can neglect the constant C from now on.

When we introduce a carbon tax which increases the costs of greenhouse-gas-intense systems to incentivize investments into the lower-emission technologies, the relative annual costs of the different heating systems change. This leads to different investment decisions. The introduction of such policies, which are not lump-sum, cause welfare losses even if the tax revenues are redistributed lump-sum. The households that have to modernize their systems are elastic but not completely elastic as presented in the previous section. For simplification, we assume that the supply function for heating technologies is completely elastic.[69] Then, the welfare loss, i.e. the excess burden, is the difference between the tax revenue and the aggregated compensating variation over all households. The compensating variation of the introduction of a tax indicates how much the government needs to pay the households to compensate the resulting cost increase and keep their original utility level. For a subsidy, the compensating variation reflects the willingness to pay of the households to keep the subsidy. Therefore, for both cases, the tax revenue, which could be redistributed to the respective households and the subsidy expenditure of the government which could be collected from consumers via a lump-sum tax, must be compared with the respective compensating variation.

The compensating variation CV_n for each household of category n is determined for each period t by an equation based on McFadden (1999) which is a generalization of the compensating variation of logit models introduced by Small and Rosen (1981).[70]

To determine the difference in consumer surpluses of the two scenarios with and without policy measures, we get:

$$\int_{V_{n,j}^{\text{no policy}}}^{V_{n,j}^{\text{policy}}} P_{n,j} dV_{n,j} = \left[\ln \sum_j \frac{e^{\alpha_j + \beta c_{n,j} + \gamma_j z_n}}{\beta} \right]_{V_{n,j}^{\text{no policy}}}^{V_{n,j}^{\text{policy}}} \tag{5.21}$$

The amount of money that is needed to keep the utility level before the policy measures, i.e., the compensating variation CV_n, is then computed as follows:

$$\ln \sum_j \frac{e^{\alpha_j + \beta (c_{n,j}^{\text{policy}} - CV_n) + \gamma_j z_n}}{\beta} = \ln \sum_j \frac{e^{\alpha_i + \beta c_{n,j}^{\text{no policy}} + \gamma_j z_n}}{\beta} \tag{5.22}$$

where $c_{n,j}^{\text{policy}}$ indicates the respective total annual heating costs of a household of category n with heating system j including a tax or subsidy and $c_{n,j}^{\text{no policy}}$ describes these costs without any policy measures.

[69] This assumptions leads to an underestimation of the excess burden. It means that the investment costs of heating systems and energy prices are not influenced by demand changes of the residential heating sector. We assume that the residential sector demand is too small to have an impact on energy prices. The producers of heating systems in Germany sell all types of heaters. Thus, they do not depend on a specific system and would adapt their product composition according to the changing demand conditions.

[70] Tra (2010) provides an application of this discrete choice equilibrium framework to the valuation of environmental changes.

Rearranging with respect to CV_n yields the formula derived by Small and Rosen (1981)[71]:

$$CV_n = \frac{1}{\beta}\left[ln\sum_j exp(V_{n,j}^{\text{policy}}) - ln\sum_j exp(V_{n,j}^{\text{no policy}})\right]$$

We have to account for the number of households belonging to the same group with the same building characteristics ($\sum_j d^-_{n,j,y}$) which have to install a new heating system. Thus, aggregating the compensating variation (net future value) of these households which modernize in period y is:

$$CV = \sum_y^Y \sum_{n,j} d^-_{n,j,y} * CV_{n,y} * (1+r)^{Y-y} \tag{5.23}$$

Finally, we define the overall excess burden EB following Diamond and McFadden (1974):

$$EB^{tax} = CV^{tax} - T \tag{5.24}$$

where T indicates the overall tax income in this period with:

$$T = \sum_y^Y \sum_{n,j} d^-_{n,j,y} * P_{n,j} * T_j * (1+r)^{Y-y} \tag{5.25}$$

We consider a carbon tax T_j which equals a carbon tax τ in Euro per tons greenhouse-gas-equivalent times a conversion factor that converts τ into T_j accounting for the GHG emissions of the different systems.

The excess burden of a subsidy is determined similarly:

$$EB^{sub} = S - CV^{sub} \tag{5.26}$$

[71]See Appendix D.4 for a more detailed derivation. Income effects are not accounted for because Braun (2010) shows that the marginal effects of income are low in the German heating market controlling for further household characteristics. The marginal effects are not even significant for all heating system choices. Moreover, income is highly correlated with the dwelling type. Dieckhöner (2012a) shows that households with higher income rather live in single dwellings than in multiple dwellings. In addition, she shows that households with higher income spend more on insulation and thus live rather in dwellings with lower heat demand. Hence, controlling for the dwelling type approximates the impact of differences in income. This approach assumes a constant marginal utility of income denoted by $\frac{1}{\beta}$. Torres et al. (2011) investigate the sensitivity of mistaken assumptions about the marginal utility of income and their impacts on the welfare measures in Monte Carlo experiments. They find that mistaken assumptions about the marginal utility of income can amplify misspecifications of the utility function. However, throughout all misspecification cases analyzed, they find an underestimation of the compensating variation (referred to as 'compensating surplus' in their paper). Thus, the analysis conducted in this paper assuming a constant marginal utility of income is conservative and might even underestimate the compensating variation (and excess burden).

with

$$S = \sum_{y}^{Y} \sum_{n,j} d^{-}_{n,j,y} * P_{n,j} * S_j * (1+r)^{Y-y} \tag{5.27}$$

The presented welfare analysis is based on the households' utility function that is derived from empirical household choices. Thus, it is assumed that household choices have been utility maximizing. However, there may be reasons for households not to make utility maximizing choices. Households may be faced with financing constraints and do not get a credit. Or they misoptimize because of imperfect information on alternatives or inattention because they are distracted by specific characteristics of the product.[72] In this case, measuring welfare by using the households' utility is an erroneous approach. The real utility cannot be observed. Then, a better approximation of welfare effects may be based on technology costs.[73]

Therefore, we also compute total heating system cost differences that result from the introduction of GHG abatement policies. We take the total heating costs C over all households and heating systems and time periods, discounted to a net future value:

$$C = \sum_{y}^{Y} \sum_{n,j} d^{-}_{n,j,y} * P_{n,j} * c_{n,j} * (1+r)^{Y-y} \tag{5.28}$$

In case of a carbon tax, the total heating system cost differences (CD) are the following:

$$CD^{tax} = (C^{\text{policy}} - C^{\text{no policy}}) - T \tag{5.29}$$

Again, we assume that the tax income is redistributed lump-sum.

For a subsidy we get:

$$CD^{sub} = S - (c^{\text{no policy}} - c^{\text{policy}}) \tag{5.30}$$

5.4.3 Microeconomic Greenhouse Gas Abatement Curves

The excess burden EB changes with different tax rates T_j (equivalentely for changes in the subsidy levels S_j). dEB covers the changes in welfare losses of an additional unit

[72]See Allcott and Greenstone (2012). There are further typical barriers in the heating market that constrain utility maximizing behavior of households such as the landlord-tenant problem.

[73]The utility maximizing approach to model the diffusion process is still appropriate as long as the household choice pattern is not be affected by public policies. However, in case of household misoptimizing the evaluation of the compensating variation does not reflect real consumer losses and society's costs.

increase of the tax rate (or subsidy):

$$dEB^{\text{tax}} = \sum_{n \in N, j \in J} \left[\left(\underbrace{\frac{\partial EB}{\partial CV_n}}_{(+)} \underbrace{\frac{\partial CV_n}{\partial V_{n,j}^{\text{policy}}}}_{(-)} \underbrace{\frac{\partial V_{n,j}^{\text{policy}}}{\partial c_{n,j}}}_{(-)} \underbrace{\frac{\partial c_{n,j}}{\partial T_j}}_{(+)} - \underbrace{\frac{\partial T}{\partial T_j}}_{(+/-)} \right) dT_j \right] \tag{5.31}$$

The signs in brackets below the derivatives indicate their direction such that (+) indicates a positive and (−) a negative derivative.

$$\frac{\partial T}{\partial T_j} = \sum_{n \in N, j \in J} \left[\underbrace{H_n P_{n,j}}_{(+)} + \underbrace{\frac{\partial P_{n,j}}{\partial c_{n,j}} \frac{\partial c_{n,j}}{\partial T_j} H_n T_j}_{(-)} \right] \tag{5.32}$$

The first part of the equation indicates the positive impact of the increasing tax rate on the total tax income T whereas the second part displays the negative impact of the decreasing tax base. Hence, $\frac{\partial T}{\partial t_j}$ is positive for the increasing part of the Laffer curve and decreasing for the decreasing part. $\frac{\partial T}{\partial t_j} < \frac{\partial EB}{\partial CV_n} \frac{\partial CV_n}{\partial V_{n,j}^{\text{policy}}} \frac{\partial V_{n,j}^{\text{policy}}}{\partial c_{n,j}} \frac{\partial c_{n,j}}{\partial t_j}$ (see Auerbach, 1985). Thus, $dEB > 0$ when the tax rates are increasing ($dt_j > 0$).

For the change of total subsidy spending in S_j, we would have:

$$\frac{\partial S}{\partial S_j} = \sum_{n \in N, j \in J} \left[\underbrace{H_n P_{n,j}}_{(+)} + \underbrace{\frac{\partial P_{n,j}}{\partial c_{n,j}} \frac{\partial c_{n,j}}{\partial S_j} H_n S_j}_{(+)} \right] \tag{5.33}$$

as the subsidy increases the costs decrease ($\frac{\partial c_{n,j}}{\partial s_j} < 0$) and the installation rate $P_{n,j}$ of the technology j increases through decreasing costs. Adapting Equation 5.31 accounting for Equation 5.26 we would get $dEB^{\text{sub}} > 0$ for $dS_j > 0$.

In the case that households are not utility maximizing, the changes in the total annual heating costs might be more appropriate to be considered than dEB:

$$dCD^{\text{tax}} = \sum_{n \in N, j \in J} \left[\left(\underbrace{\frac{\partial c_{n,j}}{\partial t_j}}_{(+)} - \underbrace{\frac{\partial T}{\partial T_j}}_{(+/-)} \right) dt_j \right] \tag{5.34}$$

The amount of GHG emissions $CO2_{n,j}$ that is consumed by household n who installs a new technology is determined by the proportion of installations $P_{n,j}$.

$$CO2_{n,j} = f_j(P_{n,j}) \tag{5.35}$$

where $f(P_{n,j})$ is a linear function that transfers the energy consumed by the chosen technology into GHG emissions. Besides the new technologies, the technology stock (i.e. the currently installed heating systems) ST also emitts GHG. Thus, the aggregated GHG emissions over all households sum up to:

$$CO2 = \sum_{n,j} f_j(P_{n,j}) + ST \tag{5.36}$$

We analyze the impact of a carbon tax and investment subsidies on the diffusion process and on GHG abatement. We assume that the emissions of the stock are not targeted by the policies. Introducing a new policy $T_j, T_i \quad \forall i \neq j$ (or $S_j, S_i \quad \forall i \neq j$) thus leads to the following change of total GHG emissions:

$$dCO2 = \sum_{n,j} \left[\left(\underbrace{\frac{\partial f_j(P_{n,j})}{\partial P_{n,j}}}_{(+)} \underbrace{\frac{\partial P_{n,j}}{\partial c_{n,j}}}_{(-)} \underbrace{\frac{\partial c_{n,j}}{\partial T_j}}_{(+)} \right) dT_j + \sum_i \left(\underbrace{\frac{\partial f_j(P_{n,j})}{\partial P_{n,j}}}_{(+)} \underbrace{\frac{\partial P_{n,j}}{\partial c_{n,i}}}_{(+)} \underbrace{\frac{\partial c_{n,i}}{\partial T_i}}_{(+)} \right) dT_i \right] \tag{5.37}$$

and equivalently for S_j, S_i with $\frac{\partial c_{n,j}}{\partial S_j} < 0$ and $\frac{\partial c_{n,i}}{\partial S_i} < 0 \quad \forall i \neq j$.

The marginal GHG abatement $dX = -dCO2$ is positive for an increasing tax rate $dT_j > 0$ (or with a decreasing subsidy $dS_j < 0$) of the carbon-intense system j. The marginal GHG abatement dX is negative with the increasing tax rates $dT_i > 0$ (or the decreasing subsidy $dS_i < 0$) of the alternatives i. Setting a Pigovian tax τ with $\frac{dT_i}{dT_j}$ being constant would therefore lead to $dX < 0$.

$\frac{\partial f(P_{n,j})}{\partial P_{n,j}}$, $\frac{\partial c_{n,j}}{\partial T_j}$ and $\frac{\partial c_{n,i}}{\partial T_i}$ are constants due to the respective linear relations. Thus, the changes in the total GHG emission level are determined by the impact of the cost changes on the diffusion of technologies $\frac{\partial P_{n,j}}{\partial c_{n,j}} < 0$ and $\frac{\partial P_{n,j}}{\partial c_{n,i}} > 0$.

Finally, we are able to derive the marginal GHG abatement cost curve $g(X)$ that accounts for the reaction of households and the resulting diffusion process of technologies as well as marginal welfare losses. We define the marginal GHG abatement cost curve as:

$$g(X) = \frac{dEB}{dX} \tag{5.38}$$

In the case that households are not maximizing utility dCD might be considered instead of dEB.

5.5 Results of the numerical analysis

5.5.1 Greenhouse Gas Abatement Policies and Diffusion of Heating Systems

To evaluate the three policy scenarios, we first investigate the diffusion process of the newly installed heating systems in this section. Figure 5.1 presents the relationship between a carbon tax and the total GHG emissions. This underlines how the DIscrHEat model works. Higher taxes increase heating costs of carbon-intensive technologies, implying lower diffusion rates of these technologies and more GHG abatement.

We accumulate GHG abatement until 2030 and see that about 300 million tons of GHG abatement are already achieved in the reference scenario at a tax of zero. This amount of GHG reduction corresponds to a decrease from an annual 134 to an annual 105 million tons of GHG emissions between 2010 and 2030 in the reference scenario without policy measures. These reductions are achieved because of the assumed increases in annual use efficiencies of the heating systems over time, the diffusion of the recent non-fossile heating technologies heat pump and biomass, the demolition of old insufficiently insulated buildings and the construction of well-insulated new buildings.

Additional GHG abatement then requires policy intervention. The additional GHG avoidance achieved by a carbon tax is slightly increasing with the proportional increase of the tax rate. At levels between 700 and 800 million tons of accumulated CO_2-equivalent (CO_2-eq.) additional abatement of GHG requires a steep increase of taxes.

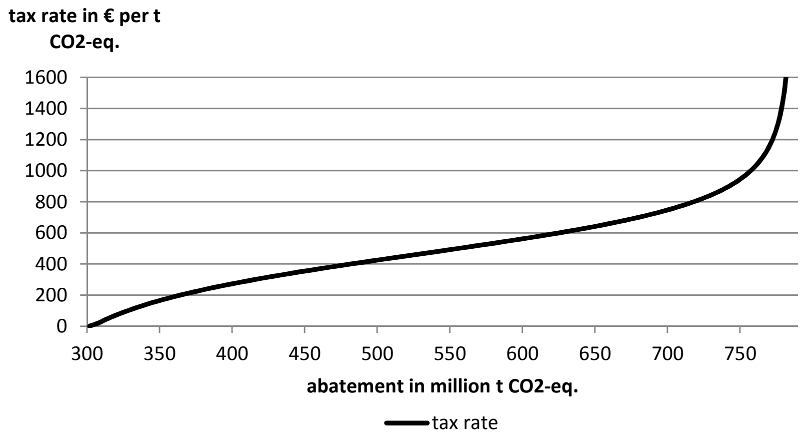

FIGURE 5.1: Tax Rate and Resulting GHG Abatement

Figure 5.2 presents the effects on the government's budget of introducing introducing each of the three individual policies separately. For abatement levels above 500 million tons of accumulated CO_2-eq. expenses for the subsidies increase overproportionally and are significantly higher than the tax revenue that is generated by a carbon tax. At about the same abatement level, the tax revenue starts to decrease indicating the falling part of the Laffer curve. This is where the shrinking tax base, i.e. mainly fossile heating systems disappearing in the building stock, reduces the revenue more than the increasing tax rate adds to the revenue.

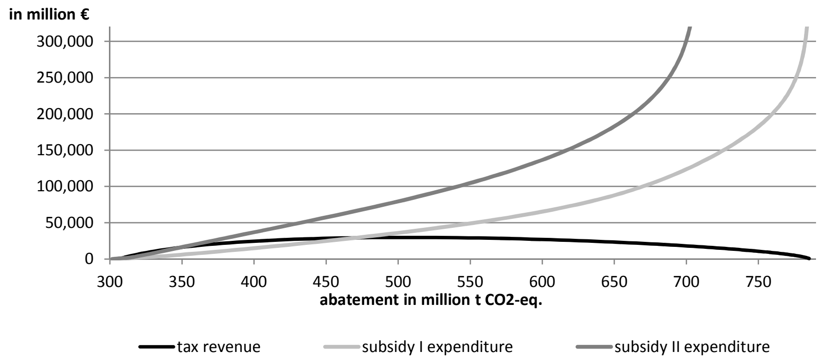

FIGURE 5.2: Tax Revenue and Subsidy Expenditure

The diffusion of heating systems and the resulting accumulated amounts of GHG abatement until 2030 in the three policy scenarios are illustrated in Figure 5.3. We observe the intuitive result that both a carbon tax and subsidies on biomass heaters and heat pumps decrease the installation of oil- and gas-fired heaters. The diffusion of biomass heaters and heat pumps varies in both subsidy scenarios. In subsidy I, subsidies on biomass heaters are remarkably higher than subsidies on heat pumps. Therefore, installation rates of heat pumps in the subsidy I are very low. The subsidy II scenario assumes a constant relative subsidy level for heat pumps and biomass heaters. In this scenario diffusion of heat pumps is higher than for biomass heaters. For all of the three scenarios, we observe that subsidies and carbon taxes decrease the market share of oil- and gas-fired heaters, implying GHG abatement.

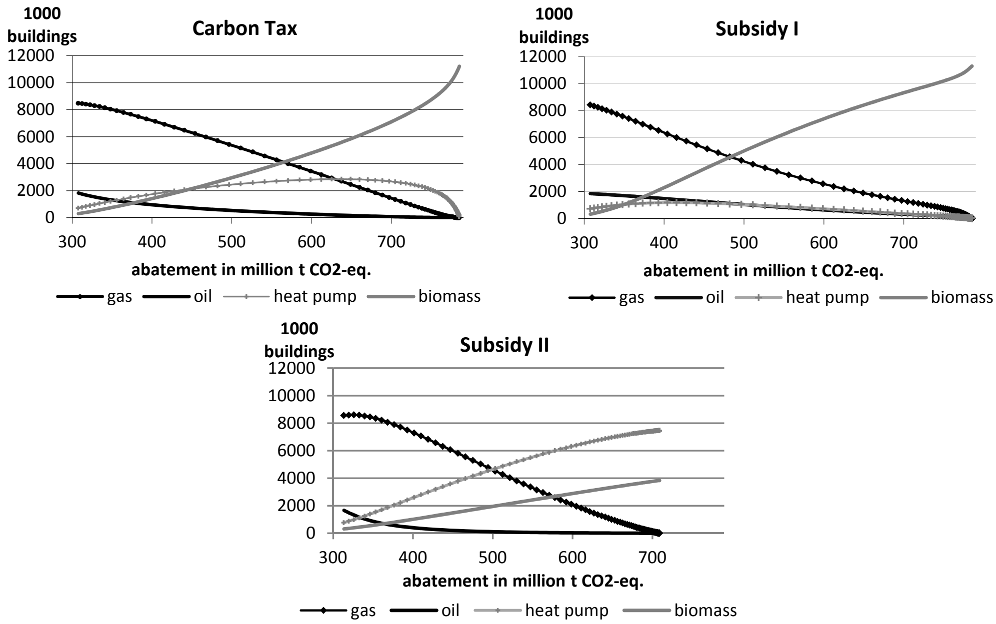

Figure 5.3: Installed Heating Systems in 2030 Depending on GHG Reduction and Policy Measures

5.5.2 Welfare Analysis

In this section, we compare different welfare measures of the three policies in relation to the accumulated GHG abatement. We compute the excess burden and heating system cost differences accumulated for the years 2010 to 2030, i.e. their net future values, given a discount rate of 6%.[74]

Figure 5.4 presents two different welfare measures, i.e., the excess burden and (total) heating system cost differences of the three policy measures. The excess burden is on a significantly higher level than the heating system cost difference and the increase of the excess burden is steeper.

The carbon tax implies a significantly lower excess burden for all levels of GHG reduction than the subsidies on investments and is therefore the more efficient policy. If we cannot observe all costs and impacts determining the heating system choice of households, the determination of an investment subsidy that is equivalent to a Pigovian carbon tax is impossible and thus always leads to larger distortions on the household choice. Thus, a subsidy on the heating investment causes a higher excess burden than a carbon tax as it affects the price of emitting GHG directly. We could therefore identify the first best

[74]In Appendix D.3, we provide a sensitivity analysis assuming a discount rate of 3%.

carbon tax as the lower bound for CO_2 abatement costs. Assuming that administration costs would be the same or even higher, other policy measures would lead to higher distortions and welfare costs. However, in case of an energy efficiency gap, Allcott and Greenstone (2012) point out that if investment inefficiencies exist, subsidies for energy efficient capital stock might have greater benefits than costs. Applied to GHG abatement in our case, this could mean that in case of financing constraints, a subsidy as a second best policy could help to reduce this problem and incentivize households to invest in less CO_2-intense heating systems. Thus, in reality welfare losses of optimal GHG abatement policies might lay somewhere between the first best Pigovian tax and the subsidy curve.

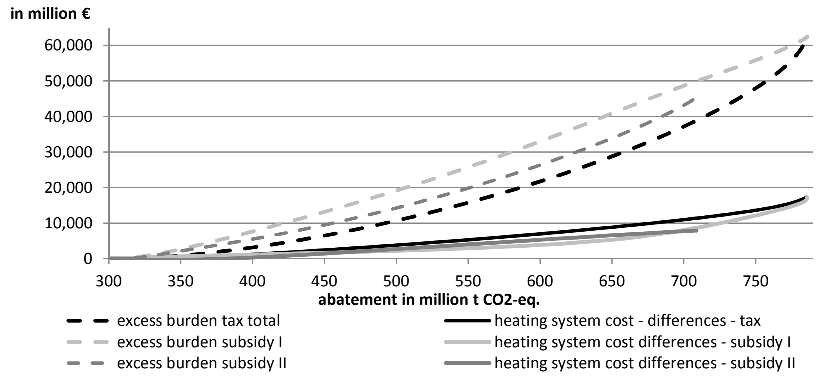

Figure 5.4: Excess Burden of Different Scenarios Depending on GHG Reduction

The curves representing heating system cost differences are significantly lower than those representing the excess burden. Note, that the curves on heating system cost differences are based on the same diffusion process of the heating systems as before. However, they neglect the losses in consumer utility and focus on pure heating system costs spent.[75] A comparison of the curves in Figure 5.4 suggests, that a plain heating system cost consideration underestimates costs that incur for households and thus society. The cost differences caused by the subsidies are even below those of the carbon tax.

We further analyze different welfare measures relative to the GHG abatement level achieved by a Pigovian carbon tax and subsidies on heating system investments to investigate the marginal costs of GHG abatement. We define the following measures based on Auerbach (1985), Baumol (1972), Mayshar (1990):

- The average costs of public funds in Figure 5.5 equal the compensating variation of a policy measure relative to the tax revenue T generated: $ACPF = \frac{CV}{T}$. $1-ACPF$ thus indicates the level of excess burden caused in percent of tax revenue.
- The marginal costs of public funds are the marginal compensating variation per marginal additional tax revenue T generated: $MCPF = \frac{\Delta CV}{\Delta T}$. $MCPF$ measures

[75]Technology based approaches to determine GHG abatement curves would imply even lower costs since they neglect household characteristics and therefore household preferences.

the additional welfare loss in raising the total tax income. $1-MCPF$ thus indicates the marginal level of excess burden caused in percent of an additional tax revenue unit. The different levels of $MCPF$ for different CO_2 abatement levels are shown in Figure 5.5.

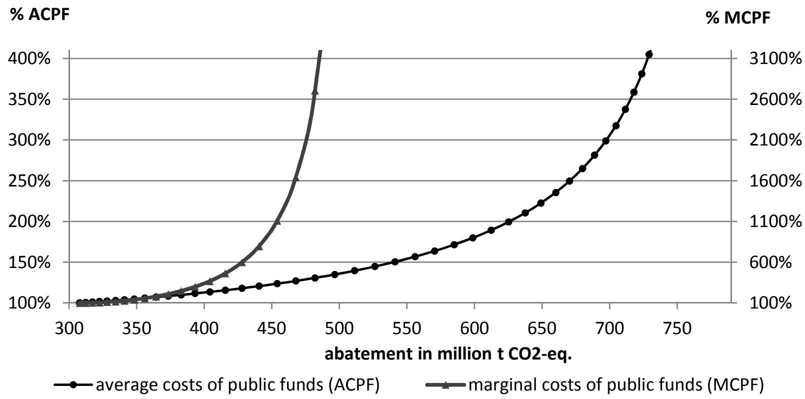

FIGURE 5.5: Marginal and Average Cost of Public Funds Depending on GHG Reduction

The ACPF are increasing slighty whereas the MCPF first increase slowly, but getting closer to an abatement level of 450 million t CO_2-eq., the MCPF increases significantly. At this abatement level, the slope of the tax revenue curve is already close to zero in Figure 5.4 indicating that the tax base, i.e. mainly the oil and gas heaters, is decreasing significantly. This is also shown in Figure 5.3. Further GHG abatement is thus very costly for society because large amounts have already been reduced and additional welfare losses are comparetively high relative to the additional tax revenue generated. Up to a level of 430 million t of accumulated CO_2-eq. abatement, the MCPF remains below 1500% and the ACPF below approximately 120%. Thus, at this point the excess burden of an additional accumulated GHG reduction of 130 million t CO_2-eq. amounts to approximately 20% of the total tax revenue generated and the generation of a marginal tax income unit causes additional welfare losses of 1500% of the additional tax revenue generated. In summary, accounting for the quantity effects or the decreasing tax base of the carbon tax, i.e. the decreasing number of oil and gas heaters, the MCPF indicate that the additional welfare losses relative to tax revenue generated increase significantly for accumulated abatement levels of 450 t CO_2-eq. until 2030 or total annual GHG emissions of 92 million tons in 2030. Hence, referring to Figue 5.1 we can conclude that tax rates above 350 per t CO_2-eq. cause immense marginal costs of public funds and thus seem politically rather unrealistic.

5.5.3 Welfare-based Greenhouse Gas Abatement Curves

As stated in Section 5.4.3, we use the marginal excess burden to derive GHG abatement curves. The results are presented in Figure 5.6. To derive a GHG abatement curve based on welfare losses in our partial analysis, we compute the marginal excess burden per additional unit of GHG reduction X as derived in Section 5.4.3: $MEB = g(X) = \frac{dEB}{dX}$. The marginal excess burden of the carbon tax is significantly lower than the marginal excess burden of the subsidy throughout all realistic abatement levels up to 450 million t CO_2-eq.[76] The MEB of subsidy I is decreasing at very high abatement levels because multiple dwellings mainly start switching their heating systems at very high subsidy levels in this policy regime.

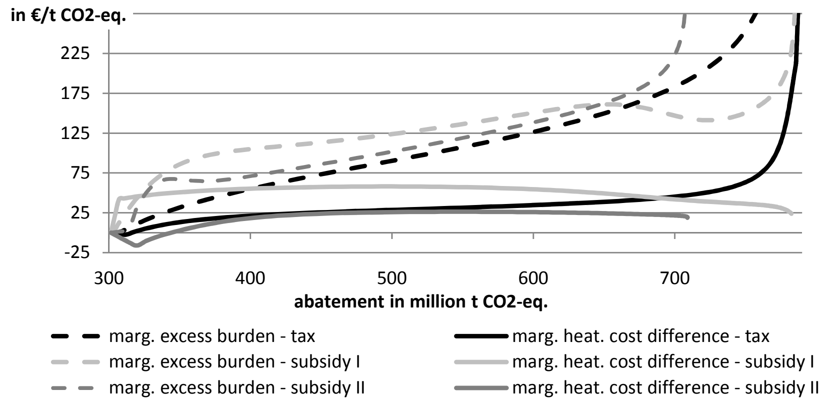

FIGURE 5.6: Marginal Excess Burden of Greenhouse Gas Reduction

The marginal cost difference curves ($MCD = \frac{dCD}{dX}$), which include solely the monetary heating system costs instead of the utility, are also displayed in Figure 5.6. These marginal cost difference curves reflect the additional heating system costs of a unit of GHG reduction at the different abatement levels already achieved. The curves indicate that the cost based curves are again significantly below the welfare loss based curves. The marginal heating system cost differences of subsidy I are also significantly higher than those of a carbon tax (for abatement levels up to 700 million t CO_2-eq.). Contrarily, the marginal cost difference of subsidy II are lower indicating, that in cases for which a utility-based measure is not appropriate, subsidies can in general be effective. However, Figure 5.2 indicates that such a policy requires a large budget to finance the subsidy expenses. A policy that changes household behavior could then be more appropriate.

In general, the welfare based GHG abatement curve might overestimate the abatement costs assuming that households do not change their behavioral patterns until 2030. If one assumes that the households' cost elasticities might change over time and that more

[76]The paper's results to be underestimates of the true efficiency gains from using a carbon tax. In reality, households are more heterogeneous than in the presented simplified approach.

households might switch to a less carbon intense heating system over time, thereby bearing less non-observed costs, the abatement curve might be somewhere between the cost-based and utility-based abatement curves. However, in comparison to pure technology based curves, these curves account for households' reactions to policy measures and policy costs that society would have to bear.

5.6 Conclusions

Analytically, we derive a welfare based GHG abatement curve, thereby taking into account household investment decisions and cost effects of policy measures. We implement the theory into the micro-simulation heat market model DIscrHEat. The model is an innovate approach since it combines a bottom-up model with a discrete choice model. The bottom-up model projects the evolution of heating systems in German residential buildings up to 2030. The bottom-up model includes a discrete choice model which determines the heating system choices of households based on the costs of heat provision.

We apply DIscrHEat to derive an abatement curve based on household preferences and welfare losses for the German residential heating market: we simulate the diffusion of heating systems until 2030 with and without policy measures to finally derive the compensating variation, excess burden and heating system cost differences in relation to GHG abatement. In comparison to technology-based abatement curves, this approach takes household investment in heating technologies into account as well as welfare costs of policy measures.

Our microeconomic analysis provides a partial analysis of welfare based GHG abatement costs in the context of optimal abatement strategies. Analyzing these costs and options of GHG abatement is of major importance in the residential heat market and also holds for other sectors, where the individual decisions of economic agents affect the GHG reduction potential and the implied welfare costs. Implementing certain policies to provide incentives for GHG reduction needs to account for the individual decisions of economic agents. Their elasticities determine the welfare costs and thus the costs that society would have to bear in order to achieve certain abatement objectives.

Based on our model results for the German residential heating market we conclude that a carbon tax is more efficient than subsidies on heating system investments in most cases. A subsidy on investments may cause lower abatement costs if assuming that households do not maximize utility. However, this policy requires very high subsidies (and lump-sum taxes) and precise information on household investment decisions into heating systems. Hence, such a policy seems rather not implementable in reality. The subsidy regime currently implemented by the German government subsidizes expensive biomass heaters to a large extent and reflects a suboptimal design: For the first, i.e., affordable section of GHG abatement units, the cost curves of this policy regime run above those of a carbon tax and those of an alternative subsidy regime. The alternative subsidy regime promotes heat pumps and natural gas systems more than the German regime. In summary, regarding policies, which change heating system choices through relative costs, a carbon tax is optimal. However, if financing constraints for households exist, subsidies on new heating system installations might be reasonable. Our paper gives rise to several interesting research sequels. First of all, a discrete choice estimation on the heating system choice enriched with household income data would strengthen the quality of the simulation model. Further, in our model, household preferences and cost elasticities remain constant over time and the policy measures, which we introduce are assumed to not affect the preferences. There are alternative policy measures, which might change the household decisions over time and might impact abatement curves. These could be information campaigns for households that compare their energy behavior with others. The evaluation of the GHG abatement potential and costs of such policy measures remains open for further research as well. The partial analysis of the paper does not cover additional welfare effects of the policy measures caused by cutting other taxes at the same time (see the analyses of the double dividend hypothesis for Bovenberg and de Mooij, 1994, Goulder, 1995 and Fullerton and Metcalf, 1998). In addition, environmental policies might have redistributive effects which might need to be included in the welfare analysis of different policy measures if equity or equality are highly valued by society. (See Cremer et al., 2003 and Llavador et al., 2011). This type of analyses are beyond the scope of our paper and are as well open for further reasearch.

The results of our paper have implications to policy makers: Understanding how households react to different policies to derive micro-economic GHG abatement curves is crucial for developing targeted policies and for achieving abatement objectives.

Appendix A

Supplementary Material for Chapter 2

A.1 Details of the Model

The model's spatial structure is formulated as a directed graph consisting of a set N of vertices and a set $A \subset N \times N$ of edges. The set of vertices can be subdivided into sources and sinks, where gas production facilities are modeled as sources and importing regions as sinks. The model's time structure is represented by a set $T \subset \mathbb{N}$ of points in time (months). This time structure is flexible and can be customized by the user, which means any year (y) until 2050 can be simulated with up to 12 months per year. An overview of all sets, decision variables and parameters can be found in Table A.1.

Table A.1: Model Sets, Variables and Parameters

Sets	
$n \in N$	all model nodes
$t \in T$	months
$y \in Y$	years
$p \in P \in N$	producer / production regions
$e \in E \in N$	exporter / trader
$d \in D \in N$	final customer / importing regions
$r \in R \in N$	regasifiers
$l \in L \in N$	liquefiers
$s \in S \in N$	storage operators
Primal Variables	
$pr_{e,p,t}$	produced gas volumes
$fl_{e,n,n1,t}$	physical gas flows
$tr_{e,d,t}$	traded gas volumes
$st_{s,t}$	gas stock in storage
$si_{s,t}$	injected gas volumes
$sd_{s,t}$	depleted gas volumes
Dual Variables	
$\lambda_{e,n,t}$	marginal costs of physical gas supply by exporter e to node n in time period t
$\sigma_{s,t}$	(intertemporal) marginal costs of storage injection
$\beta_{d,t}$	marginal costs / price in node n in time period t
$\mu_{e,p,t}$	marginal benefit of an additional unit of production capacity
$\phi_{n,n1,t}$	marginal benefit of an additional unit of pipeline capacity
$\epsilon_{s,t}$	marginal benefit of an additional unit of storage capacity
$\rho_{s,t}$	marginal benefit of an additional unit of storage injection capacity
$\theta_{s,t}$	marginal benefit of an additional unit of storage depletion capacity
ι_t	marginal benefit of an additional unit of LNG transport capacity
$\gamma_{r,t}$	marginal benefit of an additional unit of regasification capacity
$\zeta_{l,t}$	marginal benefit of an additional unit of liquefaction capacity
$\chi_{e,n,y}$	marginal costs of delivery obligation
Parameter	
$cap_{n,t/n,n1,t}$	monthly infrastructure capacity
$trc_{n,n1,t}$	transport costs
$(m)prc_{n,t}$	(marginal) production costs
$opc_{n,t}$	operating costs
$mdo_{e,n,t}$	minimal delivery obligation of exporter e
$dist_{n,n1}$	distance between node n and node $n1$ in km
$LNGcap$	initial LNG capacity
$speed$	speed of LNG tankers in km/h
cf_s	conversion factor used for storage injection & depletion capacity

A.1.1 Remaining Capacity Constraints

In Section 2.2.2, we skipped a few capacity constraints in order to keep the description of our model as brief as possible. These are listed in the following. Along the lines of Inequality 2.17, Inequality A.1 states that the sum over all transport flows (decided on by the traders) through the liquefaction terminal, i.e., all natural gas that is liquefied, has to be lower than the respective liquefaction capacity.

$$cap_{l,t} - \sum_{e \in E} \sum_{n \in A_{\cdot,l}} fl_{e,n,l,t} \geq 0 \quad \forall l, t \qquad (\zeta_{l,t}). \tag{A.1}$$

The same holds true for the restriction of gas volumes that are regasified and then transported to a demand node d in month t:

$$cap_{r,t} - \sum_{e \in E} \sum_{d \in A_{r,\cdot}} fl_{e,r,d,t} \geq 0 \quad \forall r, t \qquad (\gamma_{r,t}). \tag{A.2}$$

Finally, we account for a limitation of available LNG tankers. Hence, the sum of all gas volumes transported between liquefaction terminal l and regasification terminal r in month t is restricted by the available LNG transport capacity:

$$(LNGcap) * 8760/12 * speed - \sum_{e \in E} \sum_{l \in L} \sum_{r \in R} 2 * (fl_{e,l,r,t} * dist_{n,n1}) \geq 0 \quad \forall t \qquad (\iota_t) \tag{A.3}$$

where *speed* is defined as the average speed of a LNG tanker (km/h), $dist_{n,n1}$ as the distance in km between node n and node $n1$ and *LNGcap* as the number of existing LNG tankers times their average size in the initial model year. By using Inequality A.3, we take into account that each LNG tanker that delivers gas to a regasification terminal has to drive back to a liquefaction terminal in order to load new LNG volumes. Therefore, we simplify the model by assuming that each imaginary LNG tanker drives back to the liquefaction terminal from where it started.

A.1.2 First-order Conditions of the Model

A.1.2.1 Physical flows

Taking the first partial derivative of Equation 2.16 with respect to $fl_{e,n,n1,t}$ and accounting for the Inequalities (capacity constraints) 2.17, A.1, A.2 and A.3 results in:

$$\begin{aligned}\frac{\partial L_{eII}}{\partial fl_{e,n,n1,t}} = -\lambda_{e,n1,t} + \lambda_{e,n,t} + trc_{n,n1,t} + opc_{n,t} \\ + \phi_{n,n1,t} + \zeta_{l,t} + \gamma_{r,t} \\ + \iota_t * 2 * dist_{l,r} \geq 0 \quad \perp \quad fl_{e,n,n1,t} \geq 0 \qquad \forall e, n, n1, t. \end{aligned} \tag{A.4}$$

A.1.2.2 Production

The first-order condition for production is derived from the payoff function $\Pi_p(pr_{e,p,t})$ defined as

$$\max_{pr_{e,p,t}} \Pi_p(pr_{e,p,t}) = \sum_{t \in T} (\lambda_{e,p,t} * pr_{e,p,t} - prc_{e,p,t}(pr_{e,p,t})) \tag{A.5}$$

where $pr_{e,p,t}$ is the corresponding decision vector of p. The set of feasible solutions for $pr_{e,p,t}$ is restricted by the non-negativity constraint $pr_{e,p,t} \geq 0$. The first-order conditions of the producer's problem consists of Constraint 2.15 as well as the following partial derivative of the Lagrangian L_p:

$$\frac{\partial L_p}{\partial pr_{e,p,t}} = -\lambda_{e,p,t} + mprc_{e,p,t}(pr_{e,p,t}) + \mu_{e,p,t} \geq 0 \quad \perp \quad pr_{e,p,t} \geq 0 \qquad \forall p, t \tag{A.6}$$

A.1.2.3 Storage utilization

The following derivatives derived from Equations 2.18 and 2.19 (as well as the respective capacity constraints) constitute the first-order conditions of the storage operator's optimization problem:

$$\frac{\partial H_s}{\partial sd_{s,t}} = -\beta_{d,t} + \sigma_{s,t} + \theta_{s,t} \geq 0 \quad \perp \quad sd_{s,t} \geq 0 \qquad \forall s, t \tag{A.7}$$

$$\frac{\partial H_s}{\partial si_{s,t}} = -\sigma_{s,t} + \beta_{d,t} + \rho_{s,t} \geq 0 \quad \perp \quad si_{s,t} \geq 0 \qquad \forall s, t \tag{A.8}$$

$$-\frac{\partial H_s}{\partial st_{s,t}} = \epsilon_{s,t} = \Delta\sigma_{s,t} = \sigma_{s,t+1} - \sigma_{s,t} \leq 0 \quad \perp \quad st_{s,t} \leq 0 \qquad \forall s, t. \tag{A.9}$$

A.2 Data

TABLE A.2: Nodes in the Model

	Total number of nodes	**Number of countries**	**Countries with more than one node**	**Countries aggregated to one node**
Demand	84	87	Russia and the USA	Baltic countries and former Yugoslavian republics
Production	43	36	China, Norway, Russia and the USA	-
Liquefaction	24	24	-	-
Regasification	27	25	-	-
Storages	37	37	-	-

A.2.1 Production

For the majority of nodes, see Table A.2, we model gas production endogenously. Only for very small gas producing countries and those with little exports do we fix production volumes to limit model complexity. Concerning endogenous production, we face the problem that there are only sources with data on historical production (i.e., IEA (2011c) but no single source that provides information about historical or current production capacities. We collect information from various sources listed in Table A.3. For the major LNG exporters (Qatar and Australia), we derive possible production capacities from the domestic demand assumptions and liquefaction capacities. In total, we assume a global production capacity of 3542 bcm in 2010 and 3744 bcm in 2012. Of that capacity, 12-13% is assumed to be fixed production. The usage of the remaining production capacity (87%) is optimized within the model.

TABLE A.3: Assumptions and Data Sources for Production

	Assumptions	**Sources**
Production	Exogenous production of small countries in 2010	IEA (2011c)
	Forecast on exogenous production of small-scale producing countries	ENTSOG (2011), IEA (2011c,d)
	Estimates of future production capacity in the USA	IEA (2011b)
	Development of production capacities in Norway and Russia	Söderbergh et al. (2009, 2010)
	Forecasts for Saudi-Arabia, China, India, Qatar and Iran	IEA (2011c)
	Information which allow us to get an idea of production capacities in Africa, Malaysia, Indonesia and Argentina	IEA (2011d)

Concerning production costs, we follow an approach used in Golombek et al. (1995, 1998).[77] For the exporting countries, we estimate Golombek production functions by OLS regression, using various data sources such as Seeliger (2006) and OME (2001), or information on costs published in the *Oil and Gas Journal*.

A.2.2 Infrastructure

We consider the global gas infrastructure data aggregated on a country level. To reduce complexity, we bundle LNG capacities to one representative LNG hub per country. The same applies for storages and pipelines, although, e.g., Russia and the Ukraine are connected via multiple pipelines in reality, we bundle pipeline capacity into one large pipeline "Russia-Ukraine". The Institute of Energy Economics at the University of Cologne (EWI) has its own extensive pipeline database that serves as the major source for current pipeline capacities and distances. New pipeline projects between 2010 and 2012 are based on publicly available data. The distances of the 196 LNG routes were measured using a port to port distance calculator[78].

Table A.4: Assumptions and Data Sources for Infrastructure

	Assumptions	**Sources**
Infrastructure	Current and future capacities of LNG terminals	GIIGNL (2010), IEA (2011d)
	National storage capacities (yearly working gas volumes)	Benquey and Lecarpentier (2010), IEA (2011c)
	Underground storage capacities of China, Japan and South Korea	IGU (2003), Yoshizaki et al. (2009), Yuwen (2009)
	Onshore/offshore pipelines transportation costs (US$16/kcm/1000 km and US$26/kcm/1000 km)	Jensen (2004), Rempel (2002), Van Oostvoorn et al. (2003)
	LNG liquefaction and regasification costs add up to US$59/kcm	Jensen (2004)
	Variable operating costs for storage injection of US$13/kcm	CIEP (2008)

We account for LNG transport distances by LNG tanker freight rates of US$78000/day (Jensen, 2004). Based on our costs assumptions shown in Table A.4, the break-even

[77]Please refer to Section 2.2.2 for more details on the Golombek production function, in particular on the marginal cost function (its first derivative) that is used in our model.

[78]Please refer to http://www.searates.com/reference/portdistance/

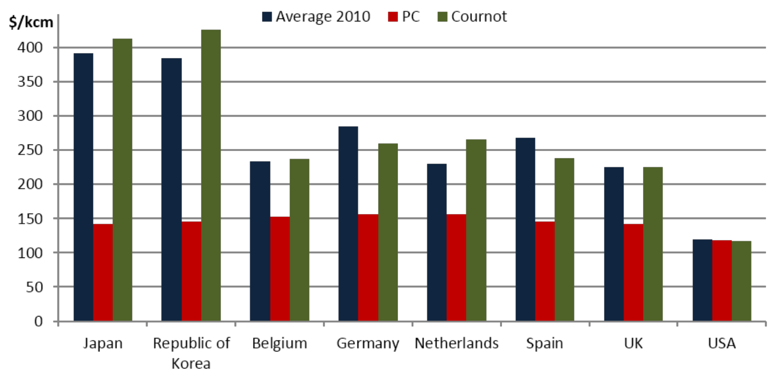

FIGURE A.1: Actual and Simulated Average Prices (in US$/kcm)

distance between onshore pipelines and LNG transport is 4000 km, and around 2400 km for offshore pipelines[79]. This is in line with Jensen (2004) and Rempel (2002).

A.3 Cournot Setting vs. Perfect Competition

The objective of this section is to justify our decision to model the gas market as an oligopoly. Therefore, we compare two market settings – perfect competition and Cournot competition with a competitive fringe – with respect to how well these simulations fit to the actual market outcomes in 2010. These two settings were chosen because, on the one hand, global gas markets are characterized by a relatively high concentration on the supply side, while on the other, because of cost decreases in the LNG value chain, regional arbitrage has become a viable option, thereby potentially constraining the exercise of market power.

We start out by analyzing the model outcomes of the perfect competition scenario. Figure A.1 compares the observed average prices in US$/kcm with the resulting average market clearing prices in the different market settings. Simulated prices in the perfect competition scenario are significantly lower than the actual prices in 2010 in almost every country depicted in Figure A.1, except for the USA.

Figure A.2 displays the deviation of simulated total demand from actual demand realized in 2010 for the two different model settings. The deviation is shown as a percentage of the actual demand figures in 2010. Figure A.2 shows that endogenous demand in the perfect competition scenario strongly deviates from reality. The largest deviations were observed for Asia/Oceania and Europe, where the modeled demand exceeds the actual realized demand in 2010 by 3.7% and 9.7%, respectively. In contrast, simulated demand in North America resembles the actual demand quite well.

[79]We assume that the average speed of a typical LNG vessel amounts to 19 knots and that the average capacity lies at *ca* 145000 cbm.

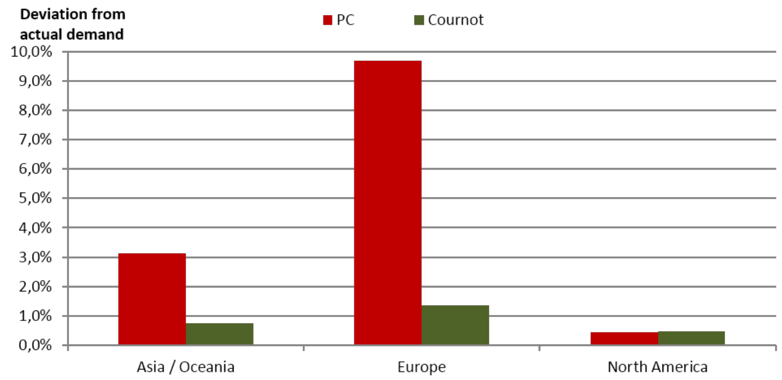

FIGURE A.2: Deviation of Demand under Different Settings (in % of actual demand in 2010)

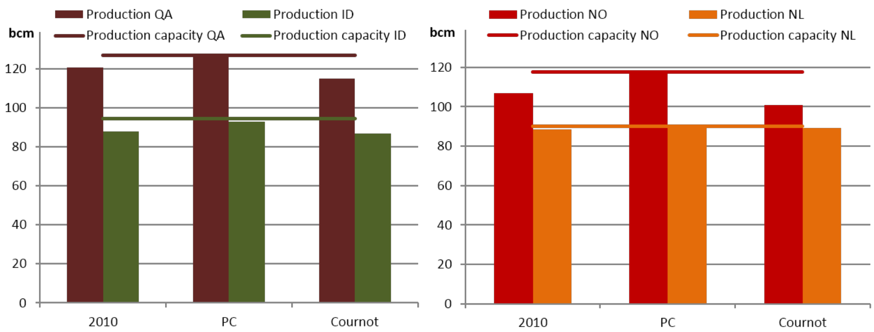

FIGURE A.3: Annual Production and Capacities in Four Selected Countries in the Different Market Settings (in bcm)

Figures A.3 and A.4 display production capacity (indicated by the bars), simulated production volumes and actual production in 2010 for five selected countries. Concerning the perfect competition case, the simulated production of the five producing countries exceeds production volumes observed in 2010 (see Figures A.3 and A.4). From Figures A.1 to A.4, we conclude, that except for the North American natural gas market, the assumption of perfect competition does not fit well with actual market data. Therefore, we model the eight most important LNG exporting countries and the three most important pipeline exporters as Cournot players, thus allowing them to exercise market power by means of production withholding. All countries have almost all of their exports coordinated by one firm or consortium, e.g., Gazprom (Russia), Statoil (Norway) or Sonatrach (Algeria).

In comparison with the perfect competition setting, model results in the Cournot setting (i.e., demand, production and prices) seem to represent reality more accurately. Because the Cournot setting with a competitve fringe provides the closer fit to actual production, demand and price data such a setting is used for our analysis presented in Section 3.4.

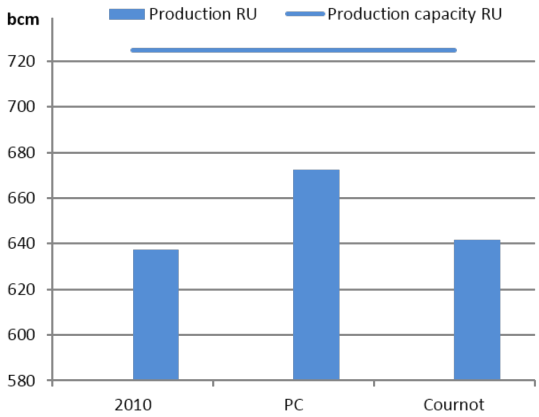

FIGURE A.4: Annual Russian Production and Capacities in the Different Market Settings (in bcm)

A.4 Sensitivity Analysis

We analyze three alternative settings for the IP sector's demand elasticity, since this elasticity assumption is most important in determining overall demand elasticity in almost all countries. For example, we conduct one sensitivity analysis in which the elasticity in all countries is 50% higher (labeled "High"), i.e., -0.15 and -0.6 respectively, one in which it is 50% lower ("Low") and one in which the IP sector's demand elasticity is -0.4 in all countries ("Same").

We find that elasticity assumptions ("Basic") used in our analysis provide the best fit with actual data. While prices in the sensitivity scenario "Low" substantially exceed actual prices (see Figure A.5, in particular in Japan and Korea), prices in the sensitivity scenario "High" undershoot prices in almost all countries (with the exceptions of Korea and the Netherlands). If we take a closer look at the scenario "Same" (Figure A.6), we see that by assuming the same demand elasticity in all countries, regional price differences are much lower than in reality (or in the scenario "Basic"). Therefore, given

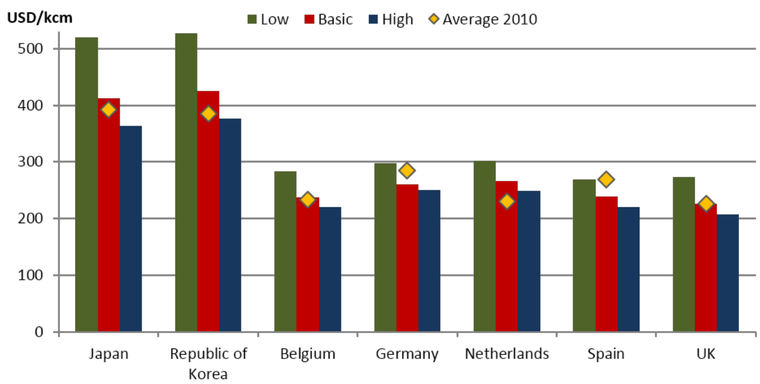

FIGURE A.5: Sensitivity Analysis I: Comparison of Prices in Selected Countries with Varying Elasticity Assumptions

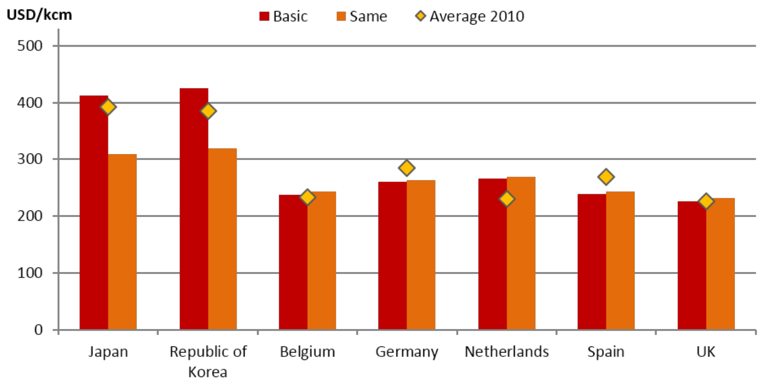

FIGURE A.6: Sensitivity Analysis II: Comparison of Prices in Selected Countries with Varying Elasticity Assumptions

the elasticity assumptions used in this paper, we are able to obtain a reasonably good fit to the actual prices in 2010 and conclude that no other combination of elasticities could improve the accuracy of our model.

Appendix B

Supplementary Material for Chapter 3

B.1 Oligopolistic Market with a Binding Capacity Constraint on one Firm's Output

We are interested in a setting where the integrated firm optimizes output on a division-level. However, this time we introduce a binding capacity constraint on one of the division's output, e.g., $\mathring{x}_i^1$. The first-order conditions of the divisions with no capacity limit are equivalent to Equation 3.5. Using the first-order conditions and inserting them in the price formulas yields:

$$\begin{aligned} p_c &= a - bx_c^1 - bx_c^2 - p_i = a - p_c - p_c - p_i \\ \Leftrightarrow p_c &= \frac{a - p_i}{3} \end{aligned} \tag{B.1}$$

and

$$\begin{aligned} p_i &= a - b\mathring{x}_i^1 - bx_2^1 - p_c = a - b\mathring{x}_i^1 - p_i - p_c \\ \Leftrightarrow p_i &= \frac{a - b\mathring{x}_i^1 - p_c}{2}. \end{aligned} \tag{B.2}$$

Using Equations B.1 and B.2 yields:

$$\begin{aligned} p_i &= \frac{3a - 3b\mathring{x}_i^1 - a + p_i}{6} \\ \Leftrightarrow p_i &= \frac{2a - 3b\mathring{x}_i^1}{5} \end{aligned} \tag{B.3}$$

and

$$p_c = \frac{a}{3} - \frac{2a - 3b\mathring{x}_i^1}{15} = \frac{a + b\mathring{x}_i^1}{5} \tag{B.4}$$

as well as

$$\begin{aligned} bx_c^n &= \frac{a + b\mathring{x}_i^1}{5} \\ \Leftrightarrow x_c^n &= \frac{a}{5b} + \frac{\mathring{x}_i^1}{5}. \end{aligned} \tag{B.5}$$

This allows us to derive the profit of the integrated firm optimising output division-by-division (i_1 and c_1) and one division has a binding capacity constraint, contingent on $\mathring{x}_i^1$:

$$\begin{aligned} \pi^{i_1+c_1} &= \mathring{x}_i^1 \left(\frac{2a - 3b\mathring{x}_i^1}{5} \right) + \left(\frac{a}{5b} + \frac{\mathring{x}_i^1}{5} \right) \left(\frac{a + b\mathring{x}_i^1}{5} \right) \\ &= \frac{2a\mathring{x}_i^1 - 3b\left(\mathring{x}_i^1\right)^2}{5} + \frac{a^2 + ab\mathring{x}_i^1}{25b} + \frac{a\mathring{x}_i^1 + b\left(\mathring{x}_i^1\right)^2}{25} \\ &= \frac{10ab\mathring{x}_i^1 + ab\mathring{x}_i^1 - 15b^2\left(\mathring{x}_i^1\right)^2 + b^2\left(\mathring{x}_i^1\right)^2 + a^2 + ab\mathring{x}_i^1}{25b} \\ &= \frac{a^2 + 12ab\mathring{x}_i^1 - 14b^2\left(\mathring{x}_i^1\right)^2}{25b}. \end{aligned} \tag{B.6}$$

Therefore, the profit of division-level optimization is identical the profit of firm-level optimization form Equation 3.18.

B.2 Model Overview

Table B.1: Model Sets, Variables and Parameters

Sets	
$y \in Y$	years
$f \in F$	factor inputs
$n \in N$	mining companies
$m \in M \in N$	mines
$d \in D \in N$	importing regions
Variables	
$pi_{d,y}$	pig iron demand / production in import region d
$tr_{n,f,m,d,y}$	transport of input f from mine m to import region d
$sa_{n,f,d,y}$	sales of input f to import region d
$sa^{b}_{n,d,y}$	sales of a bundle of inputs to import region d
$\lambda_{d,y}$	price of pig iron in import region d
$\rho_{f,d,y}$	price of factor input f in import region d
$\upsilon_{n,f,d,y}$	physical value of input f for company n to produce and to transport in import region d
$\mu_{n,f,m,y}$	marginal benefit of an additional unit of production capacity of input f at mine m
Parameter	
$cap_{n,f,m,y}$	annual production capacity of input f at mine m
$fin_{f,d,y}$	factor intensity of input f in crude steel production in import region d
$pco_{f,m,y}$	free-on-board costs of input f produced in mine m
$tco_{f,m,d,y}$	seaborne transport costs of input f (produced in mine m) to import region d
$cva_{n,y}$	company n's conjectural variation
$slo_{d,y}$	slope of linear pig iron demand function
$int_{d,y}$	intercept of linear pig iron demand function
sim_{n}	binary parameter indicating whether integrated company n optimizes on a firm-level

B.3 Statistical Measures

In order to assess the accuracy of our model, we compare market outcomes, such as production, prices and trade flows, to our model results. In comparing trade flows, we follow, for example, Kolstad and Abbey (1984), Bushnell et al. (2008) and more recently Trüby (2013) by applying three different statistical measures: a linear hypothesis test, the Spearman rank correlation coefficient and Theil's inequality coefficient. In the following, we briefly discuss the setup as well as some of the potential weakness of each of the three tests.

Starting with the linear hypothesis test, the intuition behind the test is that in case actual and model trade flows had a perfect fit the dots in a scatter plot of the two data sets would be a aligned along a line starting at zero and having a slope equal to one. Therefore, we test model accuracy by regressing actual trade flows A_t on the trade flows of our model M_t, with t representing the trade flow between exporting country $e \in E$ and importing region $d \in D$, as data on trade flows is available only on a country level (see Subsection 3.3.3.3). Using ordinary least squares (OLS), we estimate the following linear equation:

$$A_t = \beta_0 + \beta_1 * M_t + \epsilon_t. \tag{B.7}$$

Modeled trade flows have a bad fit with actual data if the joint null hypothesis of $\beta_0 = 0$ and $\beta_1 = 1$ can be rejected on typical significance levels. One of the reasons why this test is applied in various studies is that it allows hypothesis testing, while the other two tests used in this paper are distribution-free and thus do not allow such testing. However, there is a drawback to this test as well, since the results of the test are very sensitive to how good the model is able to simulate outliers. To improve the evaluation of the model accuracy regarding the trade flows we apply two more tests.

The second test we employ is the Spearman's rank correlation coefficient, which, as already indicated by its name, can be used to compare the rank by volume of the trade flow t in reality to the rank in modeled trade flows. Spearman's rank correlation coefficient, also referred to as Spearman's rho, is defined as follows:

$$rho = 1 - \sum_{t}^{T} g_t^2/(n^3 - n) \tag{B.8}$$

with g being the difference in the ranks of the modeled and the actual trade flows and T being the total number of trade flows. Since Spearman's rho is not based on a distribution hypothesis testing is not applicable, but instead one looks for a large value of rho. However, Spearman's rank correlation coefficient does not tell you anything about how well the predicted trade flows compare volumewise to the actual trade flow volumes, since it could be equal to one despite total trade volume being ten times higher in reality as long as the market shares of the trade flows match.

Finally, we apply the normed-version of Theil's inequality coefficient U, which lies between 0 and 1, to analyse the differences between actual and modeled trade flows. A U of 0 indicates that modeled trade flows perfectly match actual trade flow, while a large U hints at a large difference between the two data sets. Theil's inequality coefficient is defined as:

$$U = \frac{\sqrt{\sum_t^T (M_t - A_t)}}{\sqrt{\sum_t^T M_t^2} + \sqrt{\sum_t^T A_t^2}} \tag{B.9}$$

Appendix C

Supplementary Material for Chapter 4

C.1 Convergence of the Power and the Gas Market Model

In order to assess the convergence of the power market model and the gas market model, equilibrium gas prices and gas demand of both models are compared in this section. Since the equilibrium gas prices of the gas market model are used as an input to the power market model, gas prices are identical in both models. Therefore, the convergence of both models is assessed by comparing the equilibrium gas demand of the power market model and the gas market model.

Table C.1 lists the deviation of gas demands of both models for different scenarios. The deviation d is derived as follows: $d = \frac{x_{dim}}{x_{col}} - 1$, with x_{dim} being the equilibrium gas demand derived by the DIMENSION model and x_{col} being the equilibrium gas demand derived by the COLUMBUS model. The worst convergence of both models is observed for the years 2015 and 2020 and the scenarios FB20 and FB30 with deviations of up to 10%.

One approach to improve the consistency of both models could be to use a different functional shape of the inverse demand function for a certain year, e.g., a hyperbolic function. Another approach could be to focus the range of gas price samples to a smaller interval, i.e., increasing the fit in the region of prices that were relevant during the gas price simulation. Consequently, instead of sampling gas prices between 15 and 50 $\text{EUR}_{2010}/\text{MWh}_{\text{th}}$ for all years, I limit the price range to 15 to 25 $\text{EUR}_{2010}/\text{MWh}_{\text{th}}$ for the year 2015, to 20 to 30 $\text{EUR}_{2010}/\text{MWh}_{\text{th}}$ for the year 2020 and to 25 to 40 $\text{EUR}_{2010}/\text{MWh}_{\text{th}}$ for the years 2030 and 2040. The gas demand function is estimated

TABLE C.1: Deviation of Gas Demands between Power Market Model and Gas Market Model

Scenario	**2015**	**2020**	**2030**	**2040**
REF	5%	-2%	-1%	0%
FB5	3%	-1%	-2%	1%
FB10	0%	-1%	-2%	1%
FB20	-5%	-3%	-4%	1%
FB30	-5%	-10%	-7%	3%
CT10	5%	-2%	3%	1%
CT20	5%	2%	1%	-1%

once more based on the restricted set of samples, and new equilibria of both models are derived. Table C.2 lists the resulting gas demand deviations between both models. The results reveal that the outlined approach has improved the convergence of both models. The results of the numerical analysis change slightly, but are generally robust to this approach. In particular, none of the main messages of this study is affected qualitatively.

TABLE C.2: Deviation of Gas Demands between Power Market Model and Gas Market Model with a Focused Price Range

Scenario	**2015**	**2020**	**2030**	**2040**
REF	0%	-2%	-1%	0%
FB5	-1%	0%	-1%	0%
FB10	-3%	0%	0%	-2%
FB20	-2%	1%	-2%	-2%
FB30	-2%	-2%	-3%	1%
CT10	-1%	0%	2%	-1%
CT20	2%	1%	0%	-1%

C.2 Sensitivity Analysis of the Discount Rate

The following section of the Appendix analyzes, how a discount rate of 3% instead of 10% affects the model results. First, Figure C.1 illustrates the gas price/demand samples for two Fixed Bonus scenarios given a 3% discount rate. Note that the samples spread out more than the samples for which a 10% discount rate is assumed (see Figure 4.6). Thus, the inter-temporal components of the demand function have a higher relevance the lower the discount rate gets. This finding does not surprise, since future costs have a higher weight if a lower discount rate is assumed. This also explains why gas prices and gas demand are c.p. lower given a 3% discount rate instead of a 10% discount rate. Assuming a lower discount rate lets renewables become more competitive since future fuel costs of, e.g., natural gas have a higher impact on generation costs.

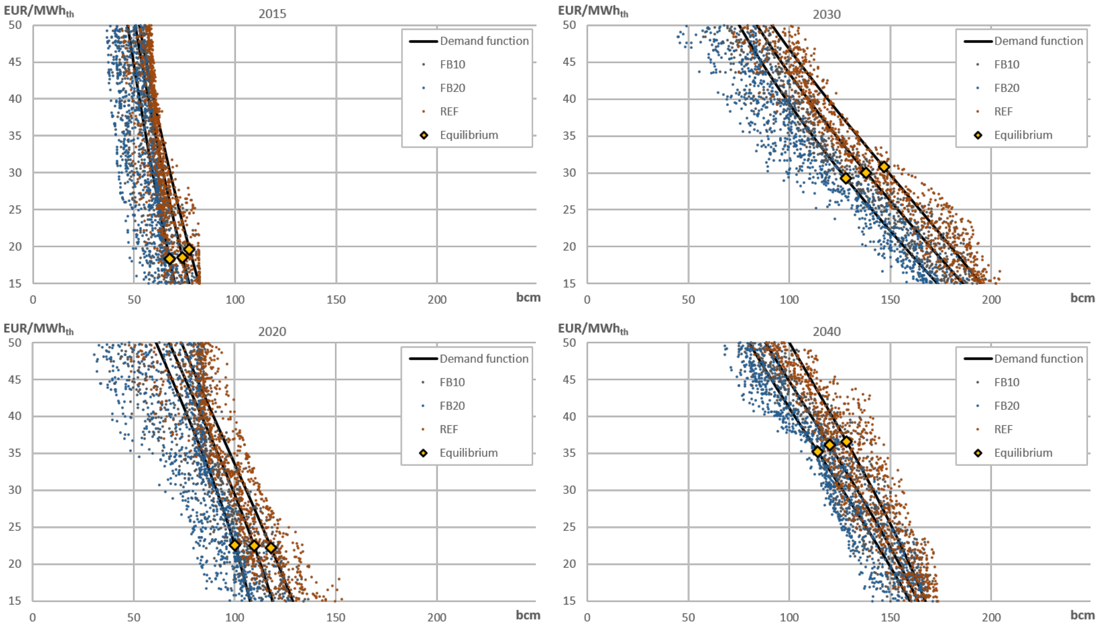

FIGURE C.1: Gas Price/Demand Samples, Demand Curves and Gas Market Equilibria for the Fixed Bonus Scenarios at a Discount Rate of 3%

Figure C.2 depicts the cost effects of the Fixed Bonus and Coal Tax scenarios when assuming a discount rate 3%. Similar effects as in the 10% discount rate case can be observed, i.e., the overall cost effect of a coal tax is positive and (except for the FB30 scenario) it is negative for the Fixed Bonus scenarios. However, effects strongly differ in magnitude due to the lower discount rate of 3%.

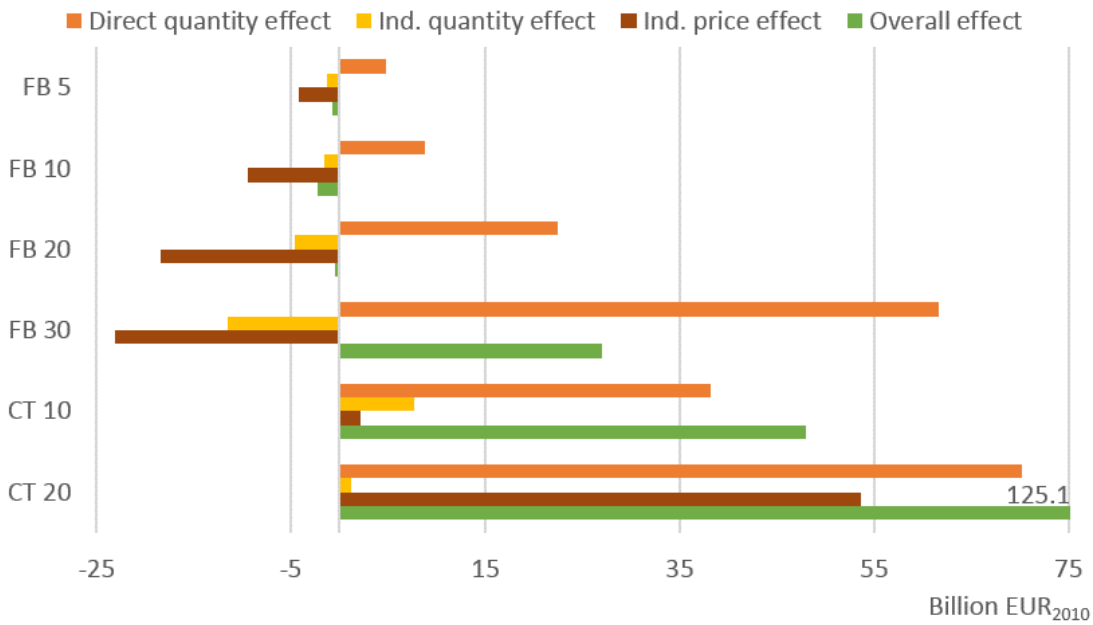

FIGURE C.2: Power System Cost Effects of Different Levels of Coal Taxes and RES Subsidies at a Discount Rate of 3%

C.3 Data

Table C.3: Fuel Costs for Power Generation

EUR_{2010}/MWh_{th}	**2015**	**2020**	**2030**	**2040**
Nuclear	3.5	3.3	3.3	3.3
Lignite	1.4	1.4	2.7	2.7
Coal	9.1	10.1	10.9	11.9
Oil	42.5	47.6	58.0	69.0

Table C.4: Gross Electricity Demand

TWh_{el}	**2015**	**2020**	**2030**	**2040**	**CAGR 2015-40**
AT+CH	131.8	140.0	149.4	158.1	0.7%
BE+NL	212.9	226.3	241.7	255.9	0.7%
DK	40.6	43.1	46.0	48.7	0.7%
FR	493.6	523.6	558.3	590.0	0.7%
DE	598.8	618.8	636.5	637.0	0.2%
GB	395.2	419.4	447.4	473.0	0.7%
IT	354.8	387.4	443.6	506.1	1.4%
CZ+PL	214.6	233.9	260.5	289.1	1.2%

Table C.5: Power Plant Parameters

	Fixed Operation and Maintenance costs (EUR_{2010}/kW)	**Generating efficiency [%]**	**Own consumption [%]**
CCGT	23-28	48-60	3
Coal	36-55	37-50	8
Lignite	43-70	35-46,5	6
Gas turbine	17	35-40	3
Oil turbine	27	35-40	5
Wind onshore	13	100	
Wind offshore	93	100	
PV roof	17	100	
PV base	15	100	
Biomass solid	165	30	
Biomass gas	120	40	
Coal CHP	55	23	8
Gas CHP	40	36	2
Lignite CHP	45	23	6
Biomass solid CHP	175	25	
Biomass gas CHP	130	27	

Table C.6: Investment Costs of New Power Plant Capacity

EUR_{2010}/kW	**2015**	**2020**	**2030**	**2040**
CCGT	675-725	675-725	675-725	675-725
Coal	1500-2350	1500-2250	1500-2000	1500-1850
Lignite	1500-2000	1500-1950	1500-1900	1500-1850
Gas turbine	375	375	375	375
Oil turbine	450	450	450	450
Wind onshore	1250-1290	1200-1255	1150-1190	1100-1130
Wind offshore	3500-3850	3200-3520	2800-3080	2650-2915
PV	1600-1700	1600-1650	1500-1550	1400-1450
Biomass solid	3300	3300	3300	3300
Biomass gas	2400	2400	2400	2400
Hydro storage	2300	2300	2300	2300
Pump storage	1200	1200	1200	1200

Table C.7: CO_2 Cap of the 11 European Countries

	2012	**2015**	**2020**	**2030**	**2040**	**2050**
Million tons of CO_2	945.3	886.5	788.5	592.5	396.5	200.4

Table C.8: CO_2 Factors of Primary Energy Combustion

tCO_2/MWh_{th}	
Lignite	0.399
Coal	0.339
Oil	0.266
Gas	0.201

Appendix D

Supplementary Material for Chapter 5

D.1 Specification of Annual Heating Costs and Cost Implications of Policies

As stated in Section 5.3.2, annual heating costs of a household of category n and a technology j, modernized in period y are a function of the investment costs $i_{n,j,y}$, the energy consumption $e_{n,j,y}$, the energy price $p_{j,y}$, plus, in the case of policies being introduced, a tax payment T_j or a lump-sum subsidy S_j:

$$c_{n,j,y} = f(i_{n,j,y}, e_{n,j,y}, p_{j,y}, T_j, S_j) \tag{D.1}$$

The total annual heating costs are derived as follows,:

$$c_{n,j,y} = (i_{n,j,y} - S_j) * a_{r,l} + o_{n,j,y} + e_{n,j,y} * (p_{j,y} + T_j) \tag{D.2}$$

with $o_{n,j,y}$ being the fixed operation and maintenance costs of a technology and $a_{r,l}$ being the annuity factor.

Thus, a lump-sum subsidy $S_j > 0$ decreases annual heating costs $c_{n,j,y}$ by decreasing the costs of the initial investment. A tax payment $T_j > 0$ for each unit of consumed energy increases annual heating costs. The tax payment per unit of energy consumed T_j is derived from the carbon tax τ times technology-specific conversion factor CF_j, i.e., $T_j = \tau * CF_j$.

The energy consumption $e_{n,j,y}$, e.g. gas consumption, is derived from the heating demand H_n, which varies by household category, and the technology specific use efficiency $\epsilon_{n,j,y}$. The use efficiency depends on technology j, the household category n and the time of installation y (to account for technological progress). Thus:

$$e_{n,j,y} = \frac{H_n}{\epsilon_{n,j,y}} \tag{D.3}$$

Therefore, the lower the efficiency and the higher the heating demand, the higher is the energy consumption.

D.2 Assumptions and Data

Starting point of the model calculations in DIscrHEat is a detailed overview of the current German building stock of private households in 2010. We distinguish single and multiple dwellings and six vintage classes. Each of those building classes has an average net dwelling area and a specific heat energy demand (kWh/m^2a). Additionally, we include data on the distribution of heating systems in each building class.

To simulate the future development of the German building stock (i.e. the installed heating technologies and the buildings' insulation level), DIscrHEat accounts for new buildings and demolitions. Furthermore, we assume that a certain percentage of buildings has to install a new heating system. Those modernization rates are given exogenously. IWU / BEI (2010) show that in Germany, investments into new heaters mostly take place when mendings or replacements need to be done. Therefore, we assume that heater replacements only take place according to empirical rates of the last years based on IWU / BEI (2010).

The estimation of the discrete choice model is based on data on the distribution of energy carriers chosen by a number of building type categories in 2010, characteristics of these building types and the heating system costs. The dwelling stock comprises six different vintage classes, differentiates between single/double and multiple dwellings and three different insulation levels (heat demand levels) per house type vintage class combination. Due to a lack of data for the diffusion of energy carriers per insulation level, we include the average heat demand per dwelling category in our discrete choice estimation. However, we account for the different insulations in our simulation model. Thus, our data comprises twelve different representative dwelling types with different heat demand, heating system costs and distributions of heating systems chosen in 2010. Out of this aggregated data, we generate our data set which represents the number of buildings that changed their heating system in 2010 differentiated by dwelling type with the respective characteristics. Heating system costs are derived using the data listed in the tables below. Additionally, a fixed interest rate of 6% and an assumed household's planning horizon of 15 years determine the annuity factor.[80] An overview of all data sources is provided in Table D.1.

TABLE D.1: Data and Sources

Input data	Specification of parameters	Sources
dwelling stock	in 2005	Destatis (2008),Destatis (2010b)
	extrapolation until 2010	IWU / BEI (2010)
	new buildings and demolitions	Destatis (2010c),Destatis (2010a)
costs	capital costs	
	except for micro chp	IE Leipzig (2009)
	micro chp	own assumptions
distribution of new heaters installed in 2010	distribution of decentral heating systems	BDH (2010)
	distribution in new buildings	Destatis (2010b)
	distribution in buildings with different construction years	IWU / BEI (2010)
greenhouse gas emissions	emissions of different energy carriers	Öko-Institut e.V. (2011)
modernization rates for heating systems and insulation	rates for dwellings with different construction years	IWU / BEI (2010)

TABLE D.2: Energy Prices

Euro/kWh	**2010**	**2015**	**2020**	**2025**	**2030**
biomass	0.05	0.05	0.06	0.07	0.07
natural gas	0.06	0.07	0.07	0.08	0.09
heating oil	0.08	0.09	0.10	0.11	0.12
electricity	0.20	0.22	0.23	0.23	0.23

Own assumptions.
In addition, an annual fixed charge of 120 Euro has to be paid for natural gas.

TABLE D.3: CO_2 Emissions of Energy Carriers

Energy carrier	**g CO_2-eq./kWh**
biomass	26
natural gas	242
heating oil	324
electricity	350

Based on Öko-Institut e.V. (2011).

[80]In Appendix D.3, we provide a sensitivity analysis assuming a discount rate of 3%.

TABLE D.4: Dwelling Stock

dwelling type	construction year	average dwelling area (m^2)	number of buildings (1000)	heating systems: district heating	gas	electricity	heating oil	biomass	heat pump	total	insulation level: no	low	average	total
single	1900 - 1918	135	1988	39	935	144	618	146	106	1988	60	1272	656	1988
single	1919 - 1948	129	1960	45	1062	96	618	78	60	1960	39	1313	608	1960
single	1949 - 1978	141	5522	157	2169	223	2670	169	134	5522	359	4072	1090	5522
single	1979 - 1990	151	1939	43	934	75	763	66	58	1939	738	1073	128	1939
single	1991 - 1995	149	592	18	364	1	185	12	12	592	473	104	15	592
single	1996 - 2000	147	926	43	639	9	196	23	16	926	787	139	0	926
single	2001 - 2004	148	593	30	420	8	85	30	20	593	545	48	0	593
single	2005 - 2010	144	516	24	396	7	47	39	4	516	490	26	0	516
multi	1900 - 1918	430	399	41	269	13	62	8	6	399	8	243	148	399
multi	1919 - 1948	430	353	56	225	11	51	6	4	353	7	236	109	353
multi	1949 - 1978	430	1537	377	709	37	382	17	15	1537	85	1062	390	1537
multi	1979 - 1990	430	402	138	176	11	71	3	4	402	171	193	38	402
multi	1991 - 1995	430	137	18	93	0	24	0	1	137	109	23	5	137
multi	1996 - 2000	430	149	26	101	0	21	0	0	149	131	18	0	149
multi	2001 - 2004	430	60	10	46	0	5	0	0	60	56	4	0	60
multi	2005 - 2010	430	46	6	37	0	3	0	0	46	45	1	0	46

Based on ARGE Kiel (2010), Destatis (2008, 2010b).

Table D.5: Cost Assumptions

		investment costs (Euro)					operating costs (Euro/a)	annual use efficiency				
		2010	**2015**	**2020**	**2025**	**2030**	**2010 to 2030**	**2010**	**2015**	**2020**	**2025**	**2030**
energy carrier i	**single dwelling (stock) [142 m^2]**											
gas	gas condensing boiler	6426	6426	6426	6426	6426	117	0.95	0.95	0.95	0.95	0.95
oil	oil condensing boiler	8806	8806	8806	8806	8806	205	0.98	0.98	0.98	0.98	0.98
pellet	pellet heater	17017	17017	17017	17017	17017	340	0.95	0.95	0.95	0.95	0.95
heat pump	air water heat-pump	13195	13195	13063	12932	12803	50	3.7	3.75	3.80	3.85	3.90
	single dwelling (new) [144 m^2]											
gas	gas condensing boiler	9817.5	9621	9429	9240	9055	147	0.95	0.95	0.95	0.95	0.95
oil	oil condensing boiler	12197.5	11954	11714	11480	11251	235	0.98	0.98	0.98	0.98	0.98
pellet	pellet heater	17017	17017	17017	17017	17017	340	0.95	0.95	0.95	0.95	0.95
heat pump	air water heat-pump	13195	13195	13063	12932	12803	50	3.7	3.75	3.80	3.85	3.90
	multi dwelling (stock) [430 m^2]											
gas	gas condensing boiler	9520	9520	9520	9520	9520	120	0.95	0.95	0.95	0.95	0.95
oil	oil condensing boiler	15232	15232	15232	15232	15232	210	0.98	0.98	0.98	0.98	0.98
pellet	pellet heater	24514	24514	24514	24514	24514	400	0.95	0.95	0.95	0.95	0.95
heat pump	air water heat-pump	25130	25130	25130	25130	25130	50	3.7	3.75	3.80	3.85	3.90
	multi dwelling (new) [430 m^2]											
gas	gas condensing boiler	15351	15044	14743	14448	14159	120	0.95	0.95	0.95	0.95	0.95
oil	oil condensing boiler	21063	20642	20229	19824	19428	240	0.98	0.98	0.98	0.98	0.98
pellet	pellet heater	24514	24514	24514	24514	24514	400	0.95	0.95	0.95	0.95	0.95
heat pump	air water heat-pump	25130	34165	33823	33485	33150	50	3.7	3.75	3.80	3.85	3.90

Based on IE Leipzig (2009).

Table D.6: Subsidies on Heating System Investment

Heating system	**single dwelling (Euro)**	**multi dwelling (Euro)**
	subsidy I	subsidy I
biomass	2500	2500
heat pump	900	1200
	subsidy II	subsidy II
gas	500	500
biomass	900	1200
heat pump	900	1200

Table D.7: Heat Demand per Insulation Level

in (kWh/m^{2}a)		**no**	**low**	**average**
single	1900 - 1918	227	197	167
single	1919 - 1948	238	209	175
single	1949 - 1978	222	200	166
single	1979 - 1990	161	152	125
single	1991 - 1995	132	123	111
single	1996 - 2000	116	106	
single	2001 - 2004	99	97	
single	2005 - 2010	92	85	
multi	1900 - 1918	189	163	140
multi	1919 - 1948	194	166	143
multi	1949 - 1978	178	157	138
multi	1979 - 1990	136	125	110
multi	1991 - 1995	121	113	104
multi	1996 - 2000	116	108	
multi	2001 - 2004	105	104	
multi	2005 - 2010	96	90	

Table D.8: Modernization Rates

dwelling construction year	**2010**	**2015**	**2020**	**2025**	**2030**
1900 - 1918	3.3%	3.3%	3.3%	3.3%	3.3%
1919 - 1948	3.3%	3.3%	3.3%	3.3%	3.3%
1949 - 1978	3.3%	3.3%	3.3%	3.3%	3.3%
1979 - 1990	2.3%	2.3%	2.3%	2.3%	2.3%
1991 - 1995	2.3%	2.3%	2.3%	2.3%	2.3%
1996 - 2000	0.0%	2.3%	2.3%	2.3%	2.3%
2001 - 2004	0.0%	0.0%	2.3%	2.3%	2.3%
2005 - 2010	0.0%	0.0%	0.0%	2.3%	2.3%

Based on IWU / BEI (2010).

Table D.9: Distribution of New Heaters Installed in 2010

	gas	**oil**	**biomass**	**heatpump**
single dwelling				
year of construction				
until 1918	7.9308%	2.6599%	0.5342%	0.6976%
1919 - 1948	7.7124%	2.5866%	0.5194%	0.6784%
1949 - 1978	21.3081%	7.1464%	1.4351%	1.8744%
1979 - 1990	5.6628%	1.1024%	0.2410%	0.8156%
1991 - 1995	1.7252%	0.3359%	0.0734%	0.2485%
new building (since 2005)	9.9751%	0.6252%	1.4881%	5.7876%
multi dwelling				
year of construction				
until 1918	1.6996%	0.5256%	0.1056%	0.0055%
1919 - 1948	1.4807%	0.4579%	0.0920%	0.0048%
1949 - 1978	6.4123%	1.9832%	0.3983%	0.0209%
1979 - 1990	1.3330%	0.2280%	0.0498%	0.0068%
1991 - 1995	0.4531%	0.0775%	0.0169%	0.0023%
new building (since 2005)	1.0790%	0.0418%	0.1242%	0.2372%

Based on BDH (2010),Destatis (2010b),IWU / BEI (2010)

D.3 Sensitivity Analysis of the Assumed Interest Rate

In the following, we provide a sensitivity analysis assuming an interest rate of 3%. Figure D.1 illustrates the welfare-based GHG abatement cost curves (i.e., based on the excess burden) for each of the three policies for an interest rate of 3% (dashed lines) and 6% (solid lines). Interestingly, the welfare-based GHG abatement costs decrease for a lower interest rate. The explanation is that less carbon intensive, but capital-intensive technologies such as heat pumps or biomass heaters become relatively cheaper compared to, e.g., gas-fired heaters. Therefore, abatement costs decrease. However, in the case of a subsidy, the opposite holds. This reason is that the subsidy, which is paid lump-sum when the investment is made becomes less valuable since the interest rate is lower.

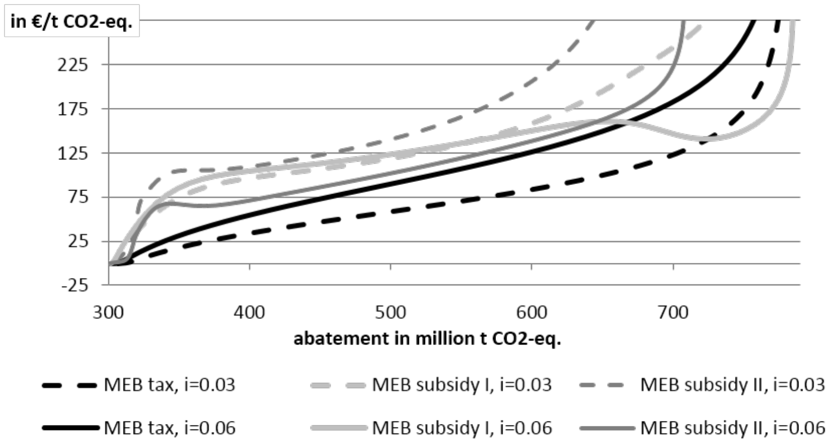

Figure D.1: Marginal Excess Burden of GHG Abatement for Different Interest Rates

D.4 Discrete Choice Model - Statistics, Welfare Measurement and Tests

Figure D.2 presents the structure of newly installed heating systems in Germany in 2010 across different dwelling types and their total annual heating costs in Euro. The groups contain dwellings of the same type with the same year of construction, housetype (single/double or multiple and average insulation status/heat demand). The frequency of each group in the sample is indicated by the area of the circles[81]. Analyzing these heating system choices leads to the assumptions that the annual costs of a heating system might have an impact on the households' heating system choices. Yet, costs are

[81]Please note that the group with the construction period 1949 – 1978 includes so many buildings because it covers the longest time period. There was no further differentiation of construction periods in the data. In the two vintage classes 1996 – 2000 and 2001 – 2004 there were almost no newly installed heating systems in 2010 because of the 15-year lifetime of heating systems on average in Germany.

not the only driver. In addition, the heating system choice differs systematically across the different dwelling types and the buildings' vintage class.

FIGURE D.2: Costs and Frequency of Energy Carriers Installed in Different Dwellings in 2010

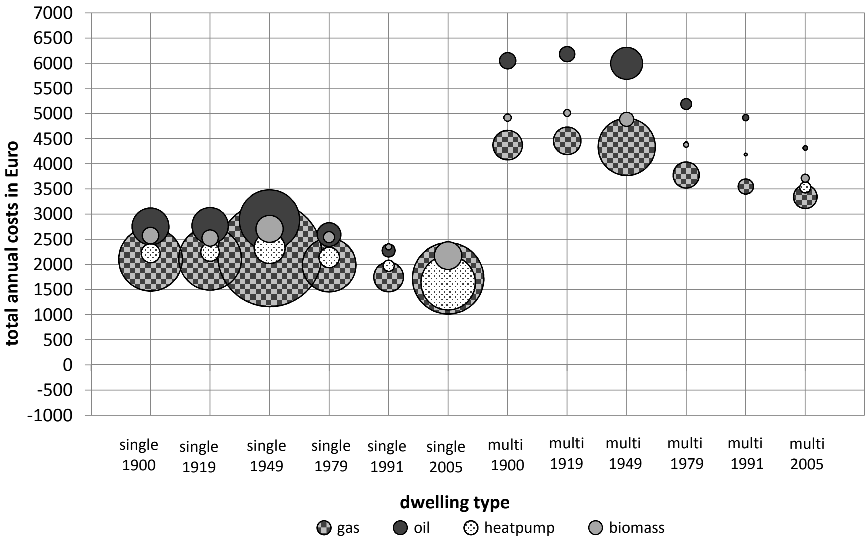

Table D.10 presents the summary statistics of our discrete choice estimation.

TABLE D.10: Summary Statistics

		mean	std. dev.	min	max
choice					
	biomass	0.0507	0.2194	0	1
	heatpump	0.1042	0.3056	0	1
	gas	0.6681	0.4710	0	1
	oil	0.1770	0.3817	0	1
costs	over all alternatives	0.1336	0.0315	0.0870	0.2155
	biomass	0.1437	0.0362	0.0977	0.2155
	heatpump	0.1222	0.0200	0.0985	0.1624
	gas	0.1172	0.0264	0.0870	0.1711
	oil	0.1514	0.0273	0.1206	0.2072
single		0.8313	0.3745	0	1
heatdemand		122.3183	29.5189	70	149.2417

Later works on random utility models of discrete choice or mixed logit models (McFadden and Train, 2000, Train, 2003) or the approach presented by Berry (1994), Berry et al. (1995) and others point out that the approaches presented in McFadden (1976, 1974) neglect product heterogenity. We assume, that this might be true for products such as cars but is not valid in the case of heating systems installations since the product heat energy is a rather homogenous good. In addition, especially the approach of Berry et al. (1995) accounts for price endogeneity and price formation on the market level by demand and supply. Our analysis sets its focus on energy consumption neglecting supply and is thus a partial analysis of the residential heat market. Further, we do not deal with price endogeneity as we assume that energy prices are not determined by the residential energy demand: the price of oil and gas is influenced by global supply and demand effects and other sectors such as power generation, transport or industry sectors rather than private households' heat demand. We also assume the price of biomass to be exogenous because the final biomass consumption of the residential sector accounted for 16% of German and only 3% of the European primary biomass production and there is still a significant unused biomass potential (European Commission, 2007, Eurostat, 2011. Another often mentioned problem with the presented approach is the Independence of Irrelevant Alternatives (IIA) assumption, which we test for (see the last section of this Appendix).

Computation of the compensating variation

Small and Rosen (1981) introduce a methodology to determine the aggregated compensating variation for discrete choice models and overcome the difficulty of the demand function aggregation and the discontinuity of the demand functions. We apply a generalization of this apporoach to determine the compensating variation CV_n of the representative household n based on McFadden (1999) associated with a changing of $V_{n,j}$ resulting from introducing a policy.

We have the distribution of the energy carriers j chosen based on the following:

$$P_{n,j} = \frac{e^{V_{n,j}}}{\sum_i e^{V_{n,i}}} \tag{D.4}$$

To compute the consumer surplus based on the utility in the no-policy case and the policy case we get:

$$\int_0^{V_{n,j}^{\text{no policy}}} P_{n,j} dV_{n,j} \tag{D.5}$$

and

$$\int_0^{V_{n,j}^{\text{policy}}} P_{n,j} dV_{n,j} \tag{D.6}$$

Thus, for the difference in consumer surpluses of the two scenarios we get:

$$\int_{V_{n,j}^{\text{no policy}}}^{V_{n,j}^{\text{policy}}} P_{n,j} dV_{n,j} = \left[\ln \sum_i \frac{e^{\alpha_j + \beta c_{n,j} + \gamma_{1,j} z_{1,n} + \gamma_{2,j} z_{2,n}}}{\beta} \right]_{V_{n,j}^{\text{no policy}}}^{V_{n,j}^{\text{policy}}} \tag{D.7}$$

To compute the compensating variation of household n CV_n, we need to find the amount of money CV_n that compensates the costs caused by the policy measures to keep the utility at the 'without policy' level. Thus, the following equation based on McFadden (1999) must hold for the compensating variation CV_n of household n for each period y:

$$\ln \sum_j \frac{e^{\alpha_j+\beta(c_{n,j}^{\text{policy}}-CV_n)+\gamma_{1,j}z_{1,n}+\gamma_{2,j}z_{2,n}}}{\beta} = \ln \sum_i \frac{e^{\alpha_i+\beta c_{n,j}^{\text{no policy}}+\gamma_{1,j}z_{1,n}+\gamma_{2,j}z_{2,n}}}{\beta} \tag{D.8}$$

We have a constant β over all alternatives, so the formula by Small and Rosen (1981) to compute the compensating variation in our logit model can easily be derived:

$$CV_n = \frac{1}{\beta}\left[ln \sum_j exp(V_{n,j}^{\text{policy}}) - ln \sum_j exp(V_{n,j}^{\text{no policy}})\right] \tag{D.9}$$

The division by β translates the utility into monetary units. This formula by Small and Rosen (1981) depends on certain assumptions: the goods considered are normal goods, the representatives in each group (households with the same dwelling characteristics) are identical with regard to their income, the marginal utility of income β is approximately independent of all costs and other parameters in the model, income effects from changes of the households' characteristics are negligible, i.e. the compensated demand function can adequately be approximated by the Marshallian demand function.

Hausman-McFadden Test

We conduct tests of Hausman and McFadden (1984) to make sure the Independence of Irrelevant Alternatives (IIA) assumption holds. We therefore reestimate the model presented in Table 5.1 by dropping different alternatives i. For instance one could assume that the choice of a heating technology depends rather on fossile versus non-fossile fuels than on the different energy carriers presented. Thus, we first drop the alternative *biomass*, *oil*, and *heatpump* in seperate tests, and then both *biomass* and *oil* and both *oil* and *heatpump*. We compare these estimators with those of our basic model.

Under H0 the difference in the coefficients is not systematic. The test statistic is the following:

$$t = (b-\beta)'(\Omega_b - \Omega_\beta)^{-1}(b-\beta), \text{ with } t \sim \chi^2(1) \tag{D.10}$$

b is the cost coefficient of the reduced estimations dropping alternatives and Ω_b and Ω_β are the respective estimated covariance matrices.

Table D.11 shows the results:

Table D.11: Hausman-McFadden Test of IIA

	b	β	T	Prob(T>t)
cost coeff. drop biomass	-31.97016	-26.76507	0.83	0.3633
cost coeff. drop oil	-26.06515	-26.76507	0.04	0.8399
cost coeff. drop heatpump	-3.358324	-26.76507	0.28	0.5969
cost coeff. drop biomass and oil	-32.64896	-26.76507	0.66	0.4167
cost coeff. drop heatpump and oil	-19.15256	-26.76507	0.03	0.8693

The results show that IIA cannot be rejected.

Bibliography

Abada, I., 2012. Modélisation des marchés du gaz naturel en Europe en concurrence oligopolistique: le modèle GaMMES et quelques applications. Ph.D. thesis, Paris 10.

Allcott, H., Greenstone, M., 2012. Is There an Energy Efficiency Gap? Journal of Economic Perspectives 26 (1), 3–28.

ARGE Kiel, 2010. Wohnungsbau in Deutschland 2011 – Modernisierung oder Bestandsersatz. Arbeitsgemeinschaft für zeitgemäßes Bauen, Kiel.

Auerbach, A., 1985. Handbook of Public Economics. Elsevier, North-Holland, Ch. The Theory of Excess Burden and Optimal Taxation.

Ballard, C., Medema, S., 1993. The marginal efficiency effects of taxes and subsidies in the presence of externalities – A computational general equilibrium approach. Journal of Public Economics 52, 199–216.

Bauer, F., Bremberger, C., Kunz, F., 2011. Implementation of the Hogan, Rosellón, and Vogelsang (HRV) incentive mechanism into the InTraGas model.

Baumol, 1972. On Taxation and the Control of Externalities. American Economic Review 62 (3), 307–322.

BDH, 2010. Trends und Herausforderungen im Wärmemarkt – Marktentwicklung Wärmeerzeuger 1999–2009. available at: `http://bdh-koeln.de/uploads/media/100126_bdh-pm-folien_pk.pdf` (09/23/2014).

Beckmann, M. J., 1972. Spatial cournot oligopoly. Papers in Regional Science 28 (1), 37–48.

Beckmann, M. J., 1973. Spatial oligopoly as a noncooperative game. International Journal of Game Theory 2 (1), 263–268.

Bennear, L. S., Stavins, R. N., 2007. Second-best theory and the use of multiple policy instruments. Environmental and Resource Economics 37 (1), 111–129.

Benquey, R., Lecarpentier, A., 2010. Underground Gas Storage In The World. CEDIGAZ.

Berry, S., 1994. Estimating Discrete-Choice Models of Product Differentiation. The RAND Journal of Economics 25 (2), 242–262.

Berry, S., Levinsohn, J., Pakes, A., 1995. Automobile Prices in Market Equilibrium. Econometrica 63 (4), 841–890.

Bertrand, J., 1883. Révue de la théorie mathématique de la richesse sociale et des recherches sur les principles mathématiques de la théorie des richesses. Journal des Savants (w), 409–508.

Bettzüge, M. O., Lochner, S., 2009. Der russisch-ukrainische Gaskonflikt im Januar 2009 – eine Modell-gestützte Analyse. Energiewirtschaftliche Tagesfragen 59 (7), 26–30.

BGR, 2008-2011. Rohstoffpreismonitor (Monthly resources' price overview). Bundesanstalt für Geowissenschaften und Rohstoffe (Federal Institute for Geoscience and Natural Resources).

Böhringer, C., Koschel, H., Moslener, U., 2008. Efficiency losses from overlapping regulation of EU carbon emissions. Journal of Regulatory Economics 33 (3), 299–317.

Böhringer, C., Rosendahl, K. E., 2011. Greening electricity more than necessary: on the cost implications of overlapping regulation in EU climate policy. Schmollers Jahrbuch 131 (3), 469–492.

Boots, M., Rijkers, F., Hobbs, B., 2004. Trading in the downstream European gas market: a successive oligopoly approach. The Energy Journal 25 (3), 73–102.

Borenstein, S., Bushnell, J., 1999. An empirical analysis of the potential for market power in California's electricity industry. The Journal of Industrial Economics 47 (3), 285–323.

Bovenberg, A. L., de Mooij, R. A., 1994. Environmental Levies and Distortionary Taxation. American Economic Review 84 (4), 1085–1089.

Bovenberg, A. L., Goulder, L., 1996. Optimal Environmental taxation in the Presence of Other Taxes: General-Equilibrium Analyses. The American Economic Review 86, 985–1000.

Braun, F. G., 2010. Determinants of households' space heating type: A discrete choice analysis for German households. Energy Policy 38 (10), 5493–5503.

BREE, 2011. Energy in Australia 2011. Bureau of Resources and Energy Economics, Canberra, Australia.

Buildings Performance Institute Europe (BPIE), 2011. Europe's buildings under the microscope – A country-by-country review of the energy performance of buildings. available at: `http://www.bpie.eu/eu_buildings_under_microscope.html` (09/23/2014).

Bushnell, J. B., Mansur, E. T., Saravia, C., March 2008. Vertical Arrangements, Market Structure, and Competition: An Analysis of Restructured US Electricity Markets. American Economic Review 98 (1), 237–66.

CIEP, 2008. The Geopolitics of EU Gas Supply – The role of LNG in the EU Gas Market. Tech. rep., Clingendael International Energy Programme (CIEP), The Hague, Netherlands.

Cournot, A. A., 1838. Recherches sur les principes mathématiques de la théorie des richesses. L. Hachette.

Cremer, H., Gahvari, F., Ladoux, N., 2003. Environmental taxes with heterogeneous consumers: an application to energy consumption in France. Journal of Public Economics 87, 2791–2815.

del Río González, P., 2007. The interaction between emissions trading and renewable electricity support schemes. An overview of the literature. Mitigation and adaptation strategies for global change 12 (8), 1363–1390.

Destatis, 2008. Bauen und Wohnen – Mikrozensus – Zusatzerhebung 2006. Fachserie 5 Heft 1, Statistisches Bundesamt.

Destatis, 2010a. Bauen und Wohnen – Baugenehmigungen / Baufertigstellungen von Wohn- und Nichtwohngebäuden (Neubau) nach Art der Beheizung und Art der verwendeten Heizenergie. Lange Reihen ab 1980, Statistisches Bundesamt.

Destatis, 2010b. Bauen und Wohnen – Bestand an Wohnungen. Fachserie 5 Reihe 3, Statistisches Bundesamt.

Destatis, 2010c. Gebäude und Wohnungen – Bestand an Wohnungen und Wohngebäuden, Abgang von Wohnungen und Wohngebäuden. Lange Reihen ab 1969 - 2009, Statistisches Bundesamt.

Diamond, P., McFadden, D., 1974. Some uses of the expenditure funtion in public finance. Journal of Public Economics 3, 3–22.

Dieckhöner, C., 2012a. Does subsidizing investments in energy efficiency reduce energy consumption? Evidence from Germany. EWI Working Paper 12/17.

Dieckhöner, C., 2012b. Simulating security of supply effects of the Nabucco and South Stream projects for the European natural gas market. The Energy Journal 33 (3).

Dirkse, S. P., Ferris, M. C., 1995. MCPLIB: A collection of nonlinear mixed complementarity problems. Optimization Methods and Software 5 (4), 319–345.

Egging, R., Gabriel, S., Holz, F., Zhuang, J., 2008. A complementarity model for the European natural gas market. Energy Policy 36 (7), 2385–2414.

Egging, R., Holz, F., Gabriel, S. A., 2010. The World Gas Model: A multi-period mixed complementarity model for the global natural gas market. Energy 35 (10), 4016–4029.

ENTSOG, 2011. Ten-Year Network Development Plan 2011-2020. European Network for Transmission System Operators for Gas (ENTSOG), available at: `http://www.entsog.eu/public/uploads/files/publications/TYNDP/2012/TYNDP_Report_110217_MQ_.pdf` (09/23/2014).

European Commission, 2007. Accompanying document to the Communication from the Commission to the Council and the European Parliament – Renewable Energy Road Map – Renewable energies in the 21st century: building a more sustainable future – Impact Assessment. Commission Staff Working Document SEC(2006) 1719.

Eurostat, 2011. Eurostat Statistics Database: Renewable energy primary production: biomass, hydro, geothermal, wind and solar energy. available at: `http://appsso.eurostat.ec.europa.eu/nui/show.do?dataset=nrg_107a&lang=en` (09/23/2014).

Ferris, M. C., Munson, T. S., 2000. Complementarity problems in GAMS and the PATH solver. Journal of Economic Dynamics and Control 24 (2), 165–188.

FGE, December 2010. China Oil and Gas Monthly: A Monthly Report on the Latest Oil, Gas, and Other Energy Sector Developments in China. Vol. VI, Issue no. 8.

Fischer, C., Preonas, L., et al., 2010. Combining policies for renewable energy: Is the whole less than the sum of its parts. International Review of Environmental and Resource Economics 4 (1), 51–92.

Fiuza, E. P., Tito, F. F., 2010. Post-merger time series analysis: Iron ore mining. Resources Policy 35 (3), 141–155.

Fullerton, D., Metcalf, G., 1998. Environmental Taxes and the Double-Dividend Hypothesis: Did You Really Expect Something for Nothing? Chicago-Kent Law Review 73, 221–256.

Fürsch, M., Lindenberger, D., Malischek, R., Nagl, S., Panke, T., Trüby, J., 2012. German Nuclear Policy Reconsidered: Implications for the Electricity Market. Economics of Energy & Environmental Policy 1 (3).

Gabriel, S., Kiet, S., Zhuang, J., 2005. A mixed complementarity-based equilibrium model of natural gas markets. Operations Research 53 (5), 799.

Geroski, P., 2000. Models of technology diffusion. Research Policy 29, 603–625.

GIIGNL, 2010. The LNG Industry. Tech. rep., Levallois, France.

GIIGNL, 2011. Ex-Ship Master LNG Sale and Purchase Agreement - 2011 Version. available at: `http://www.giignl.org/fileadmin/user_upload/pdf/A_PUBLIC_INFORMATION/Publications/GIIGNL_DES_MSA2011_Final_.doc` (17/02/2013).

Golombek, R., Gjelsvik, E., Rosendahl, K., 1995. Effects of liberalizing the natural gas markets in Western Europe. The Energy Journal 16 (1), 85–112.

Golombek, R., Gjelsvik, E., Rosendahl, K., 1998. Increased competition on the supply side of the Western European natural gas market. The Energy Journal 19 (3), 1–18.

Goulder, L. H., 1995. Environmental taxation and the double dividend: A reader's guide. International Tax and Public Finance 2 (2), 157–183.

Graham, P., Thorpe, S., Hogan, L., 1999. Non-competitive market behaviour in the international coking coal market. Energy Economics 21 (3), 195–212.

Growitsch, C., Hecking, H., Panke, T., 2014. Supply disruptions and regional price effects in a spatial oligopoly – an application to the global gas market. Review of International Economics 22 (5), 944–975.

Häckner, J., 2000. A note on price and quantity competition in differentiated oligopolies. Journal of Economic Theory 93 (2), 233–239.

Haftendorn, C., 2012. Evidence of market power in the Atlantic steam coal market using oligopoly models with a competitive fringe. DIW Berlin discussion paper 1185.

Haftendorn, C., Holz, F., 2010. Modeling and analysis of the international steam coal trade. The Energy Journal 31 (4), 205–229.

Hagspiel, S., Jägemann, C., Lindenberger, D., Brown, T., Cherevatskiy, S., Tröster, E., 2014. Cost-optimal power system extension under flow-based market coupling. Energy 66 (0), 654–666.

Harker, P. T., 1984. A variational inequality approach for the determination of oligopolistic market equilibrium. Mathematical Programming 30 (1), 105–111.

Harker, P. T., 1986. Alternative models of spatial competition. Operations Research 34 (3), 410–425.

Hausman, J., McFadden, D., 1984. Specification tests for the multinomial logit model. Econometrica 52 (5), pp. 1219–1240.

Hecking, H., Panke, T., 2012. COLUMBUS – A Global Gas Market Model. EWI Working Paper 12/06.

Hecking, H., Panke, T., 2014. Quantity-setting Oligopolies in Complementary Input Markets – the Case of Iron Ore and Coking Coal. EWI Working Paper 14/06.

Hitchcock, F. L., 1941. The distribution of a product from several sources to numerous localities. Journal of Mathematics and Physics 20 (2), 224–230.

Höffler, F., Sliwka, D., 2012. Organizational Integration, Conflict, and the Choice of Business Strategies – An Incentive Perspective. EWI Working Paper.

Holz, F., Von Hirschhausen, C., Kemfert, C., 2008. A strategic model of European gas supply (GASMOD). Energy Economics 30 (3), 766–788.

Huntington, H., 2011. The Policy Implications of Energy-Efficiency Cost Curves. The Energy Joumal 32 (Special Issue 1), 7–22.

Huppmann, D., Egging, R., 2014. Market Power, Fuel Substitution and Infrastructure: A Large-Scale Equilibrium Model of Global Energy Markets. DIW Berlin discussion paper 1370.

IE Leipzig, 2009. Vollkostenvergleich Heizsysteme 2009. Informationen für Verbraucher, Leipziger Institut für Energie GmbH, Leipzig.

IEA, 2011a. Energy Balances of OECD Countries 2011. International Energy Agency, Paris.

IEA, 2011b. Medium-Term Oil & Gas Markets 2011. International Energy Agency, Paris.

IEA, 2011c. Natural Gas Information 2011. International Energy Agency, Paris.

IEA, 2011d. World Energy Outlook 2011. International Energy Agency, Paris.

IEA, 2012. Coal Information 2012. International Energy Agency, Paris.

IEA, 2013a. Medium-Term Gas Market Report 2013. International Energy Agency, Paris.

IEA, 2013b. World Energy Outlook 2013. International Energy Agency, Paris.

IGU, 2003. ABCs of Underground Gas Storage. IGU WOC2 group for WGC 2003 in Tokyo.

IPCC, 2007. Climate Change 2007: The Physical Science Basis. The Fourth Assessment Report of the Intergovernmental Panel on Climate Change. IPCC.

IWU / BEI, 2010. Datenbasis Gebäudebestand. Datenerhebung zur energetischen Qualität und zu den Modernisierungstrends im deutschen Wohngebäudebestand, Institut Wohnen und Umwelt (IWU) / Bremer Energie Institut (BEI).

Jägemann, C., Fürsch, M., Hagspiel, S., Nagl, S., 2013. Decarbonizing europe's power sector by 2050 – analyzing the economic implications of alternative decarbonization pathways. Energy Economics 40 (0), 622–636.

Jensen, J. T., 2004. The Development of a Global LNG Market. Alden Press, Oxford.

Kantorovich, L. V., 1942. On the translocation of masses. In: Doklady Akademii Nauk SSSR. Vol. 37. pp. 199–201.

Kavgic, M., Mavrogianni, A., Mumovic, D., Summerfield, A., Stevanovic, Z., Djurovic-Petrovic, M., 2010. A review of bottom-up building stock models for energy consumption in the residential sector. Building and Environment 45 (7), 1683–1697.

Kolstad, C. D., Abbey, D. S., 1984. The effect of market conduct on international steam coal trade. European Economic Review 24 (1), 39–59.

Labson, S. B., 1997. Changing patterns of trade in the world iron ore and steel market: An econometric analysis. Journal of Policy Modeling 19 (3), 237–251.

Lienert, M., Lochner, S., 2012. The importance of market interdependencies in modeling energy systems – the case of the European electricity generation market. International Journal of Electrical Power & Energy Systems 34 (1), 99–113.

Lise, W., Hobbs, B., 2008. Future evolution of the liberalised European gas market: Simulation results with a dynamic model. Energy 33 (7), 989–1004.

Lise, W., Hobbs, B., Van Oostvoorn, F., 2008. Natural gas corridors between the EU and its main suppliers: Simulation results with the dynamic GASTALE model. Energy Policy 36 (6), 1890–1906.

Llavador, H., Roemer, J. E., Silvestre, J., 2011. A dynamic analysis of human welfare in a warming planet. Journal of Public Economics 95, 1607–1620.

Lochner, S., Dieckhöner, C., 2011. Civil unrest in North Africa – Risks for natural gas supply? EWI Working Paper 11/01.

Madlener, R., 1996. Econometric Analysis of Residential Energy Demand: A Survey. The Journal of Energy Literature 2, 3–32.

Mansur, E. T., Mendelsohn, R., Morrison, W., 2008. Climate change adaptation: A study of fuel choice and consumption in the US energy sector. Journal of Environmental Economics and Management 55 (2), 175–193.

Mayshar, J., 1990. On measures of excess burden and their application. Journal of Public Economics 43 (3), 263–289.

McFadden, D., 1976. Quantal choice analysis: A survey. Annals of Economic and Social Measurement 5, 349–368.

McFadden, D., 1999. Trade, Theory and Econometrics. Essays in Honor of John S. Routledge. Chipman, London, Ch. Computing willingness-to-pay in random utility models.

McFadden, D., Train, K., 2000. Mixed MNL Models with Discrete Response. Journal of Applied Econometrics 15 (5), 447–470.

McFadden, D. L., 1974. Conditional logit analysis of qualitative choice behavior. New York: Academic Press, pp. 105–142.

McKinsey & Company, Inc., 2009. Unlocking Energy Efficiency in the U.S. Economy. McKinsey Global Energy and Materials, McKinsey & Company, Inc.

Michelsen, C. C., Madlener, R., 2012. Homeowners' preferences for adopting innovative residential heating systems: A discrete choice analysis for Germany. Energy Economics 34 (5), 1271–1283.

Morris, J., Paltsev, S., Reilly, J., November 2008. Marginal Abatement Costs and Marginal Welfare Costs for Greenhouse Gas Emissions Reductions: Results from the EPPA Model. *Report No* 164, MIT Joint Program on the Science and Policy of Global Change.

Neumann, A., Viehrig, N., Weigt, H., 2009. InTraGas – A Stylized Model of the European Natural Gas Network. Dresden University of Technology WP-RM-16.

Newbery, D. M., 2008. Climate change policy and its effect on market power in the gas market. Journal of the European Economic Association 6 (4), 727–751.

Nordhaus, W. D., 2011. Estimates of the Social Cost of Carbon: Background and Results of the RICE-2011 Model. Cowles Foundation Discussion Paper.

Öko-Institut e.V., 2011. Global Emission Model for Integrated Systems (GEMIS). available at: `http://www.oeko.de/service/gemis/en/index.htm` (08/29/2011).

OME, 2001. Assessment of internal and external gas supply options projects for the EU, Evaluation of the Supply Costs of New Natural Gas Supply Projects to the EU and an Investigation of Related Financial Requirements and Tools. Ch. Assessment of Future Supply Costs to Europe, Observatoire Méditerranéen de l'Energie (OME).

Paulus, M., Trüby, J., 2011. Coal lumps vs. electrons: How do Chinese bulk energy transport decisions affect the global steam coal market? Energy Economics 33 (6), 1127–1137.

Pearce, D., 2003. The social cost of carbon and its policy implications. Oxford Review of Economic Policy 19 (3), 362–384.

Rehdanz, K., 2007. Determinants of residential space heating expenditures in Germany. Energy Economics 29 (2), 167–182.

Rempel, H., 2002. Natural Gas for Europe – Present State and Predictions for a Stable Supply in the Future. Energy Exploration & Exploitation 20 (2&3), 219–237.

Richter, J., 2011. DIMENSION – A Dispatch and Investment Model for European Electricity Markets. EWI Working Paper 11/03.

Salinger, M. A., 1989. The meaning of "upstream" and" downstream" and the implications for modeling vertical mergers. The Journal of Industrial Economics, 373–387.

Samuelson, P., 1952. Spatial price equilibrium and linear programming. The American Economic Review 42 (3), 283–303.

Seeliger, A., 2006. Entwicklung des weltweiten Erdgasangebots bis 2030. No. 61 in Schriften des Energiewirtschaftlichen Instituts. Oldenbourg Industrieverlag, München.

Sijm, J., 2005. The interaction between the EU emissions trading scheme and national energy policies. Climate Policy 5 (1), 79–96.

Singh, N., Vives, X., 1984. Price and quantity competition in a differentiated duopoly. The RAND Journal of Economics, 546–554.

Small, K. A., Rosen, H. S., 1981. Applied welfare economics with discrete choice models. Econometrica 49 (1), pp. 105–130.

Söderbergh, B., Jakobsson, K., Aleklett, K., 2009. European energy security: The future of Norwegian natural gas production. Energy Policy 37 (12), 5037–5055.

Söderbergh, B., Jakobsson, K., Aleklett, K., 2010. European energy security: An analysis of future Russian natural gas production and exports. Energy Policy 38 (12), 7827–7843.

Sonnenschein, H., 1968. The dual of duopoly is complementary monopoly: or, two of Cournot's theories are one. The Journal of Political Economy 76 (2), 316–318.

Sorrell, S., Sijm, J., 2003. Carbon trading in the policy mix. Oxford Review of Economic Policy 19 (3), 420–437.

Stadler, M., Kranzl, L., Huber, C., Haas, R., Tsioliaridou, E., 2007. Policy strategies and paths to promote sustainable energy systems – The dynamic *Invert* simulation tool. Energy policy 35 (1), 597–608.

Stern, N., 2007. The Economics of Climate Change. Cambridge University Press, Cambridge and New York.

Swan, L. G., Ugursal, V. I., 2009. Modeling of end-use energy consumption in the residential sector: A review of modeling techniques. Renewable and Sustainable Energy Reviews 13 (8), 1819–1835.

Takayama, T., Judge, G. G., 1964. Equilibrium among spatially separated markets: A reformulation. Econometrica: Journal of the Econometric Society, 510–524.

Takayama, T., Judge, G. G., 1971. Spatial and temporal price and allocation models. North-Holland, Amsterdam.

Tinbergen, J., 1952. On the theory of economic policy. North-Holland, Amsterdam.

Tirole, J., 1988. The theory of industrial organization. MIT press.

Torres, C., Hanley, N., Riera, A., 2011. How wrong can you be? Implications of incorrect utility function specification for welfare measurement in choice experiments. Journal of Environmental Economics and Management 62, 111–121.

Toweh, S. H., Newcomb, R. T., 1991. A spatial equilibrium analysis of world iron ore trade. Resources Policy 17 (3), 236–248.

Tra, C., 2010. A discrete choice equilibrium approach to valuing large environmental changes. Journal of Public Economics 94, 183–196.

Train, K., 2003. Discrete Choice Methods with Simulation. Cambridge University Press.

Trüby, J., 2013. Strategic behaviour in international metallurgical coal markets. Energy Economics 36, 147–157.

Trüby, J., Paulus, M., 2012. Market structure scenarios in international steam coal trade. Energy Journal 33 (3), 91–123.

Van Oostvoorn, F., et al., 2003. Long-term gas supply security in an enlarged Europe. Tech. rep., Energy Research Centre of the Netherlands (ECN).

World Mine Cost Data Exchange, 2013. Mining Cost Curves for Iron Ore (2008-2010). URL `www.minecost.com`

World Steel Dynamics, 2011. Why have spot iron prices remained so high and what is WSD's outlook for spot iron prices in 2011? Iron & Steel Technology 1, 21–22.

WSA, 2010. World Steel in Figures 2010. World Steel Association, Brussels, Belgium.

WSA, 2011. World Steel in Figures 2011. World Steel Association, Brussels, Belgium.

WSA, 2012. World Steel in Figures 2012. World Steel Association, Brussels, Belgium.

WSA, 2013. World Steel in Figures 2013. World Steel Association, Brussels, Belgium.

Yang, C. W., Hwang, M. J., Sohng, S. N., 2002. The Cournot competition in the spatial equilibrium model. Energy Economics 24 (2), 139–154.

Yoshizaki, K., Sato, N., Fukagawa, H., Sugiyama, H., Takagi, G., Jono, T., 2009. Utilization of Underground Gas Storage (UGS) in Japan. *24th World Gas Conference 2009.*

Yuwen, Z., 2009. Study and Construction of underground gas storage facilities in China: Current status and its future. *24th World Gas Conference 2009.*

Curriculum Vitae

Harald Hecking

Personal Details

Date of Birth	February 16th, 1984
Place of Birth	Vreden, Germany

Education

Ph.D. student	since 2011
University of Cologne	*Cologne, Germany*
Diploma in Geoinformation Science	2011
Westfälische Wilhelms-Universität Münster	*Münster, Germany*
Diploma in Economics	2010
Westfälische Wilhelms-Universität Münster	*Münster, Germany*
Study Abroad	2008
Université Paul Cézanne Aix-Marseille III	*Aix-en-Provence, France*
University Entrance Examination (Abitur)	2003
Gymnasium Vreden	*Vreden, Germany*

Professional Experience

Research Associate	since 2011
Institute of Energy Economics at the University of Cologne (EWI)	*Cologne, Germany*
Secondee	2014
International Energy Agency (IEA)	*Paris, France*
Secondee	2013
International Energy Agency (IEA)	*Paris, France*

Scholarships and Awards

Scholarship	2008-2011
German National Academic Foundation	
Best Diploma in Geoinformation Science	2011
Westfälische Wilhelms-Universität Münster	
Best Diploma in Economics	2010
Westfälische Wilhelms-Universität Münster	

Refereed Journal Publications

Growitsch, C., Hecking, H., Panke, T., 2014. Supply Disruptions and Regional Price Effects in a Spatial Oligopoly – an Application to the Global Gas Market. Review of International Economics 22 (5), 944–975.

Dieckhöner, C., Hecking, H., 2014. Developments of the German Heat Market of Private Households Until 2030: A Simulation Based Analysis. Zeitschrift für Energiewirtschaft, 38 (3), 117-130.

Non-Refereed Publications & Working Papers

International Energy Agency, 2014 (forthcoming). Medium-Term Coal Market Report 2014. IEA Publications, Paris.

Hecking, H., John, C., Weiser, F., 2014. An Embargo of Russian Gas and Security of Supply in Europe. Institute of Energy Economics at the University of Cologne.

Hecking, H., 2014. CO_2 Abatement Policies in the Power Sector under an Oligopolistic Gas Market. EWI Working Paper 14/14.

Hecking, H., Panke, T., 2014. Quantity-setting Oligopolies in Complementary Input Markets – the Case of Iron Ore and Coking Coal. EWI Working Paper 14/06.

International Energy Agency, 2013. Medium-Term Coal Market Report 2013. IEA Publications, Paris.

Dieckhöner, C., Hecking, H., 2012. Greenhouse Gas Abatement Curves of the Residential Heating Market – a Microeconomic Approach. EWI Working Paper 12/16.